

Contents

1. Purpose	1-1
2. Overview	2-1
3. Experiment Materials and Parts	3-1
4. Operation	4-1
5. Evaluation of Installed Materials	5.1-1
6. Evaluation of Flight Articles of the Cosmic Dust Collectors	6-1

1.Purpose

This document covers the result of the material exposure experiment installed on MFD(Manipulator Flight Demonstration).

The purpose of the experiment is as follows;

- (1) to confirm materials durability against the low earth orbit (LEO) environment
- (2) to capture cosmic dusts with a Dust Collectors

2.Overview

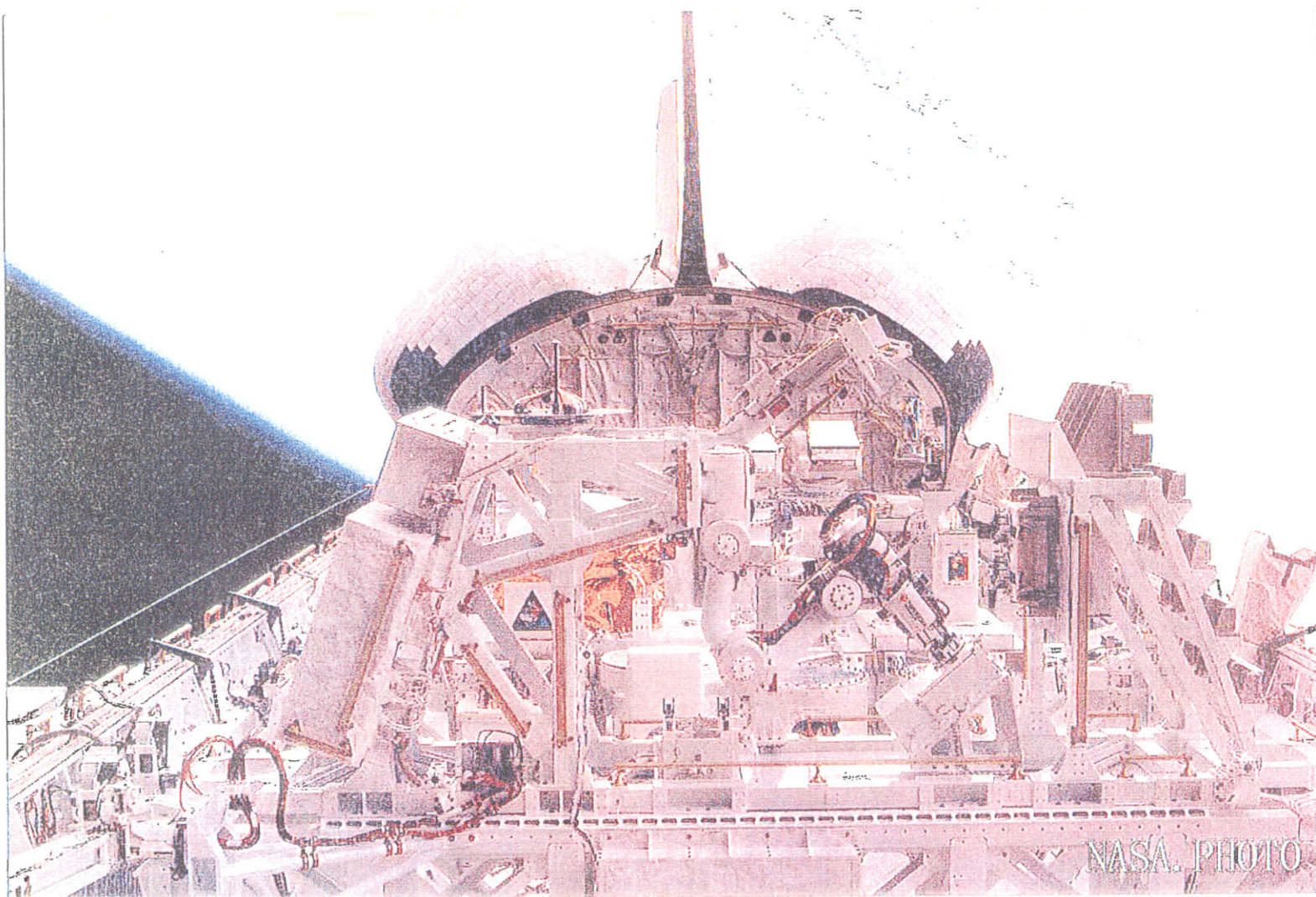
Evaluation of space environment and effects on materials (ESEM) is consists of the evaluation of material durability and the capturing of cosmic dust.

The configuration of MFD/ESEM installed on STS-85 is shown in Fig.2-1.

The configuration of ESEM at Kennedy Space Center is shown in Fig.2-2.

The operation is as follows;

- (1)Mission No. :STS-85
- (2)Term of mission :Aug.7,1997 to Aug.19,1997
- (3)Duration :54 hr
- (4)Altitude :296 km
- (5)Inclination :57 degrees



S85E5030 1997:08:10 16:43:44

Figure 2-1 Photograph of STS-85 & MFD-ESEM

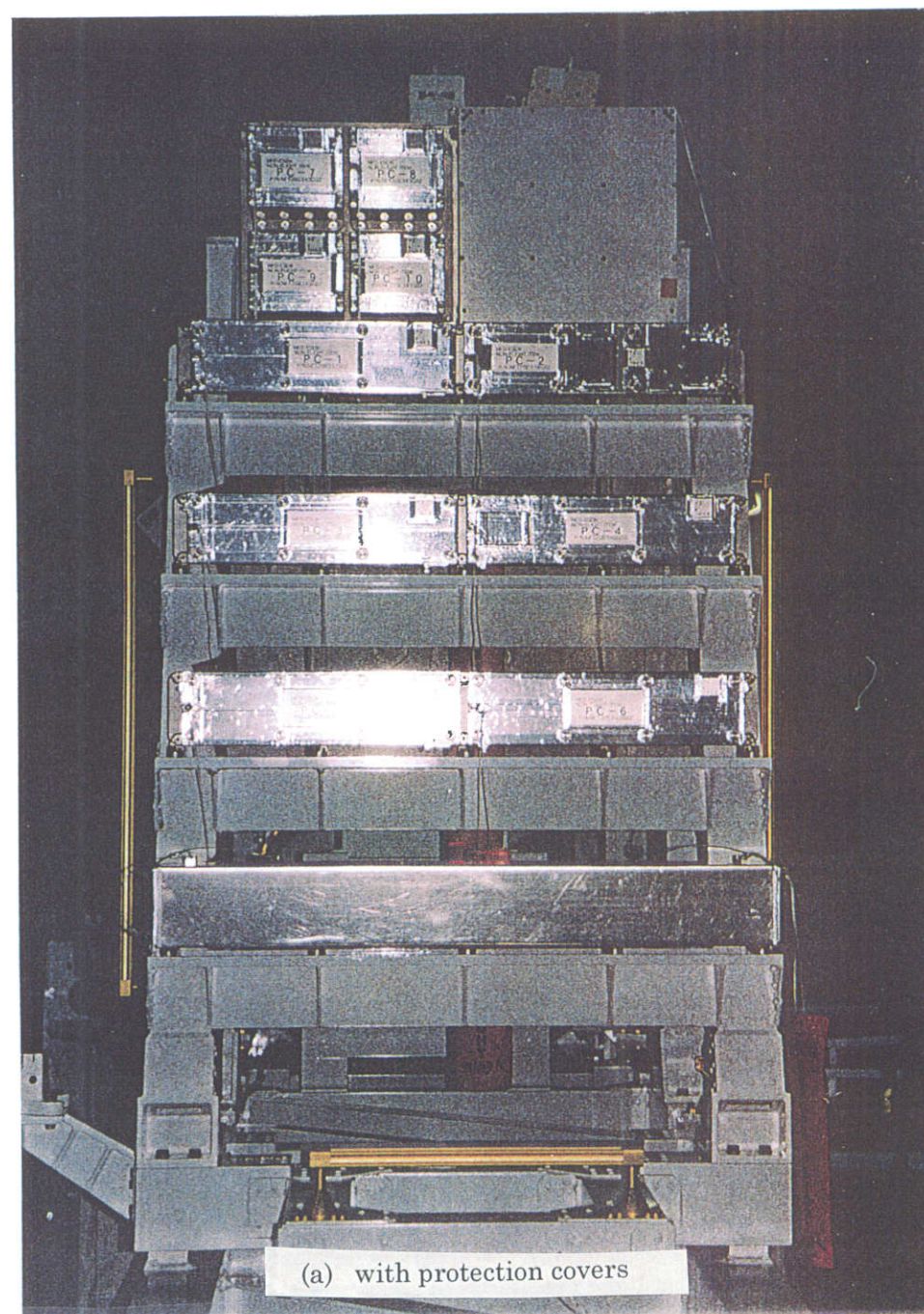
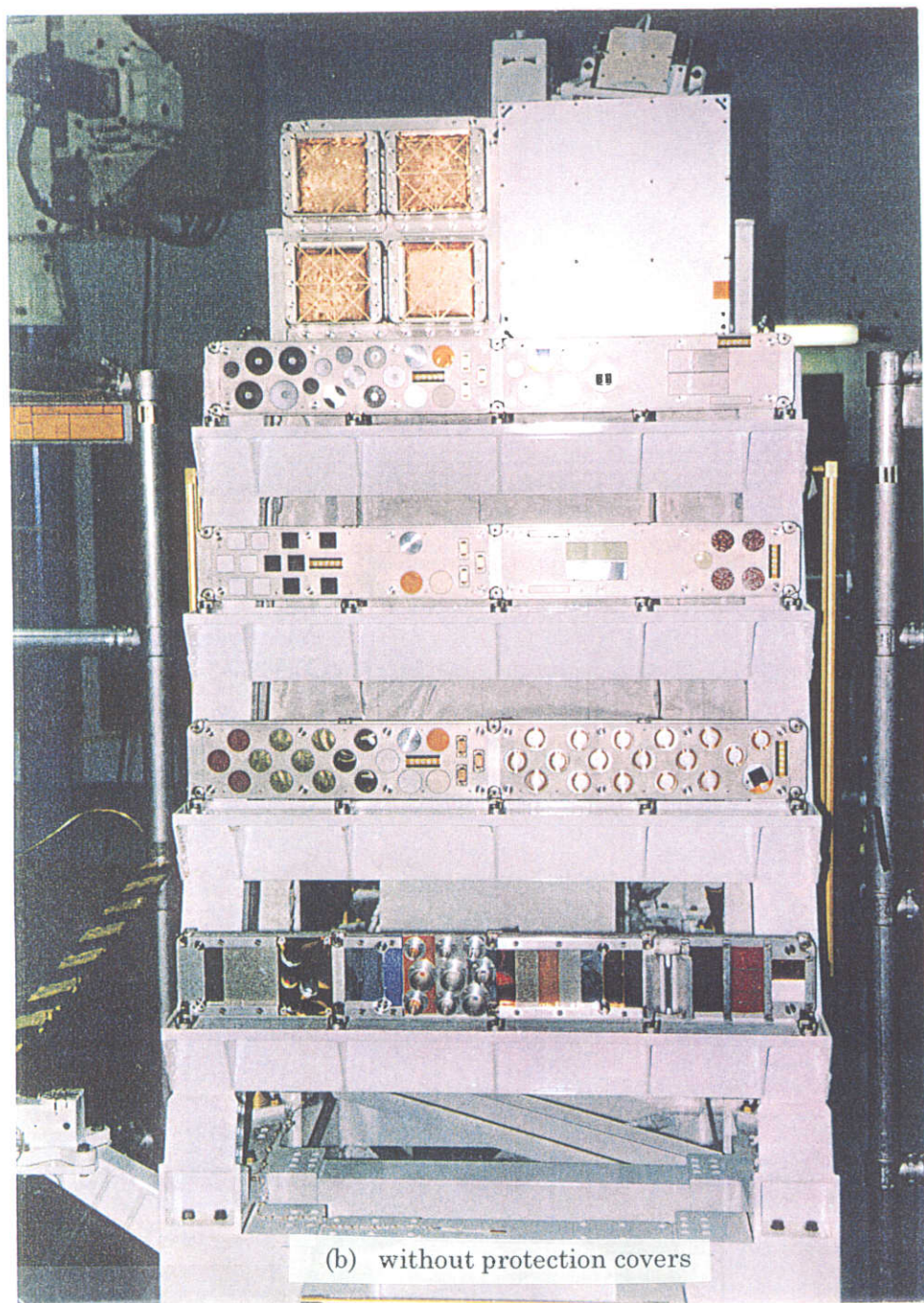


Figure 2-2 Configuration of ESEM

3.Experiment Materials and Parts

The experiment materials and parts installed on MFD-ESEM are shown in Table 3.1-1.

The experiment samples were selected from the candidate materials for the Japanese Experiment Module(JEM) or future space crafts, including NASDA developed and qualified materials.

In order to monitor the space environment conditions, change of mass and surface thermal-optical properties of monitor materials were evaluated after retrieval.

The photographs of the samples are shown in Fig.3.1-1 through 3.1-21.

Table 3.1-1 (1/5) Experiment Material Samples

Name of material or part	Use	Reason for choice	Dimensions of specimen	Quantity	Evaluations and measurements
<u>ID No.: 1</u> Non-flammable electrical wire (Cable conductor/PFA*/TP1**) N1064/101-26 *PFA (perfluoroalcoxy) **TP1 (thermoplastic polyimide) Hitachi Cable, Ltd.	All electrical wire inside and outside JEM	-NASDA developed this wire for space use. -Teflon (PFA), a wire coating material, was exposed also in EFFU, but it did not take the form of wire coating. → After exposed to the space environment, an electrothermal cable will be subjected to a safety test on the ground to check its heat resistance.	The wire is wound into a coil 32 mm in diameter. Wire length: 350 mm	17	-Surface analysis -Fire resistance -Arc tracking -Electrical characteristics tan δ Dielectric strength Insulation resistance -Mass
<u>ID No.: 2</u> Epoxy resin adhesive for securing parts (Base: mixture of bisphenol-F epoxy resin and urethane modified epoxy resin) Sunstar Engineering Co.		-NASDA developed this adhesive for space use. We have already collected exposure test data on the silicone resin adhesive in EOIM-3 but have not yet gathered exposure test data on the epoxy resin adhesive. We have not obtained exposure test data on the adhesive tape for acrylic resin multilayer insulation, either. → The space adhesive and space adhesive tape developed by NASDA will be installed to examine the effects of exposure to the space environment.	The adhesive is applied to an Al plate $\phi 25.4$ mm and 1 mm thickness.	1	-Surface analysis -Mass
			Two Al plates (25.4 mm \times 190.5 mm \times 1.6 mm thickness) bonded together.	2	-Resistance against shearing
<u>ID No.: 3</u> Acrylic resin Adhesive tape for multi-layer insulation (Primary monomer: 2-ethylhexylacrylate) (Liner: white woodfree paper) Sony Chemical Co.	Adhesive in space		The adhesive is applied to an Al plate $\phi 25.4$ mm and 1 mm thickness.	1	-Surface analysis -Mass
			A 20 mm \times 150 mm aluminum foil sheet and a 20 mm \times 230 mm thermal control film bonded each together.	1 for each	-Resistance to peeling-off
<u>ID No.: 4</u> Thermal control film (polyimide/Al) N1048/101-025R-NANN Ube Industries, Ltd.	Thermal control film for satellites, JEM, and launch vehicles.	• NASDA developed and qualified this film. • We have already collected exposure test data on polyimide in EOIM-3 but have not yet gathered exposure test data on the film. → These films developed by NASDA will be installed to examine the effects of exposure to the space environment in various orbits.	$\phi 32$ mm \times 0.025 mm thickness	3	-Surface analysis -Electrical characteristics -Surface resistance -Optical characteristics of the surface
<u>ID No.: 5</u> Thermal control film (ITO/polyimide/Al) N1048/101-025R-TANN Ube Industries, Ltd.			$\phi 32$ mm \times 0.025 mm thickness	3	α_s and ϵ_N -Mass

Table 3.1-1 (2/5) Experiment Material Samples

Name of material or part	Use	Reason for choice	Dimensions of specimen	Quantity	Evaluations and measurements
ID No.: 6 White paint (Resin: silicone resin) (Pigment: mixture of oxidized titanium and oxidized zinc) N1049/101 Nippon Paint Co., Ltd.	Thermal control paint for satellites, JEM, and launch vehicles	-The α and ϵ data on two types of white paint obtained in the EOIM-3 space environment exposure test exhibits converse tendencies. -We must collect more data on the two types of white paint. -Also in EFFU, white paint was installed. → The qualified white paint for space uses, which was developed by NASDA, will be installed into ESEM to collect comparison data for different orbit conditions and exposure times. → Black paint has been hardly installed. It will be installed to compare it with white paint.	A 25 mm × 25 mm base plate coated with white paint Base plate : CFRP, Al	3 for each	-Surface analysis -Surface optical characteristics α_s and ϵ_N -Mass
ID No.: 7 Black paint (Resin: Urethane resin) (Pigment: Carbon black) N1049/201 Nippon Paint Co., Ltd.			A 25 mm × 25 mm base plate coated with white paint Base plate : CFRP, Al	3 for each	
ID No.: 8 & 9 Solar cell (1) N1013/107Y10W22 (Cell type: BSFR 100 μ m AR) (2) N1013/109Y10W22-1 (Cell type: NRS/BSF 100 μ m BRR) Sharp Corp.	Solar cell panel for satellites	-Effects of AO rays on a finished solar cell are checked. -BSFR cell AR-coated cover glass has been installed. -NRS/BSF cell BRR - coated cover glass is a new type of solar cell, called a "high efficiency cell." -The new cell is the same type as the cell installed into ADEOS-II. A major purpose of the test is to compare the two types of glass.	(1) N1013/107Y10710W22 ϕ 40 mm	1	-Output voltage
			(2) N1013/109Y10W22-1 ϕ 40 mm	1	
ID No.: 10,11,12 & 13 Cover glass for solar cell (1) OCLI*0213 AR (2) OCLI 0213 BRR (3) OCLI 0213 CC (4) PPE* CMX AR *: Name of glass manufacturer		-Because Asahi Glass Co., Ltd. discontinued the cover glass qualified by NASDA, we no longer use the cover glass produced by the company. In the oncoming test, four types of cover glass coated with different materials will be installed to examine their characteristic changes due to exposure to the space environment.	(1) OCLI 0213 AR (2) OCLI 0213 BRR ϕ 40 mm	1	-Surface analysis -Surface optical characteristics $(\alpha_s \text{ and } \epsilon_N, \text{ permeability})$ -Mass
			(3) OCLI 0213 CC (4) PPE CMX AR ϕ 40 mm	1	
ID No.: 14,15 & 16 Inter-connector material for solar cell (1) Ag (2) Ag-X (3) Ag (nickel plating)		-Some inter-connectors are plated with gold to protect them against erosion due to silver AO. Three types of silver inter-connectors will be installed to evaluate, especially their deterioration, since the exposure time will be short.	(1) Ag (2) Ag-X (3) Ag (nickel plating)	1	-Surface analysis -Mass
ID No.: 17 & 18 OSR for solar cell (1) OCLI 0213 SSM (2) PPE CMX SSM	To control heat, these materials are used on the surface of a bypass diode for preventing reverse-bias voltage.	-Because the OSR has an SSM (Second Surface Mirror) structure (mirror material is deposited on its back), the mirror material is not expected to deteriorate. However, the reflectivity of the OSR is expected to change due to deterioration of glass on its face. Reflectivity change is evaluated.	(1) OCLI 0213 SSM (2) PPE CMX SSM ϕ 40 mm	1	-Surface analysis -Mass

Table 3.1-1 (3/5) Experiment Material Samples

Name of material or part	Use	Reason for choice	Dimensions of specimen	Quantity	Evaluations and measurements
RADFET(Radiation sensitive field effect transistor) (Accumulated dosage meter) (ceramic package IC) NMRC Co.	Environment monitor for total dose measurement	-To evaluate the effects of atomic oxygen(AO), ultraviolet rays (UV) and radiation during the space exposure test, the space environment data are needed.	16mm× 30mm × 5.9mm thickness The meter is placed in an aluminum case.	9	-Threshold voltage
Thermal luminescence dose meter MSO-S Kasei Optonics Co.	Environment monitor for total dose measurement		32 mm in diameter × 5.5 mm thickness The meter is placed in a container (from IHI) in an aluminum case.	3	-Exposure dose -Surface chemical characteristics
CR-39 plastic glass Nagase Co.	Environment monitor for measuring the amount of energy of high-energy rays and counting				
Thermo-label Nichiyu Giken Co.	Environment monitor for maximum temperature measurement		40 mm × 15 mm	1 for each DC and MSH	-Maximum exposure temperature
Polyimide film (Kapton 100H) Toho Rayon Co., Ltd.	Environment monitor for AO measurement		32.3 mm in diameter × 0.025mm thickness	3	-Surface analysis -Surface optical characteristics (α_s and ϵ_N) -Mass
Polyurethane film DUD601	Environment monitor for ultraviolet ray measurement		Polyurethane film + synthesized quartz 32.3 mm in diameter × 3.3 mm thickness	3	-Surface optical characteristics (α_s and ϵ_N)

Table 3.1-1 (4/5) Experiment Material Samples

Name of material or part	Use	Reason for choice	Dimensions of specimen	Quantity	Evaluations and measurements
ID No.: 19 Aluminum-deposited β cloth (two types) (β cloth/A1) Proposer: Nissan Motor Co., Ltd.	Outermost layer for JEM ELM-ES MLI	-Since the manufacture of the structure on which aluminum is deposited differs from that of the material which IHI installed into EFFU, it is desired that the manufacturer of the structure be confirmed. (The same one manufacturer produces β cloth.)	ϕ 32 mm \times 4 mm thickness	2	-Surface analysis -Surface chemical characteristics α_s and ϵ_N -Mass
ID No.: 20, 21, 22 & 23 Binder for bonded MoS₂ film, Bonded MoS₂ films The following materials were deposited on Ti-6Al-4V bases by heating: (1) Polyamideimide A (2) Polyamideimide B (3) Polyimide (4) HMB 34 film Note: Polyamideimide and polyimide are binders for solid lubricant (mixture of MoS ₂ , an additive, and binders). Proposer: Nissan Motor Co., Ltd.	Solid lubricant for JEM exposed gears (Ti-6Al-4V)	-Because The results of evaluation of the binders (polyimide and polyamideimide) differ between two tests (ground evaluation tests performed at EFFU and Nissan), they need to be checked.	(1) Polyimideamide A ϕ 25mm \times 2.5 mm thickness ϕ 40mm \times 2.5 mm thickness	1 1	-Surface analysis -Mass -Friction characteristics
			(2) Polyimideamide B ϕ 25mm \times 2.5 mm thickness ϕ 40mm \times 2.5 mm thickness	1 1	-Surface analysis -Mass -Friction characteristics
			(3) Polyimide ϕ 25mm \times 2.5 mm thickness ϕ 40mm \times 2.5 mm thickness	1 1	-Surface analysis -Mass -Friction characteristics
			(4) Solid lubricant ϕ 25mm \times 2.5 mm thickness ϕ 40mm \times 2.5 mm thickness	1 1	-Surface analysis -Mass -Friction characteristics
ID No.: 24 Silica FRP (one type) (silica cloth and phenol resin layers bonded together) Proposer: Nissan Motor Co., Ltd.	Outermost layer (heat protection material) of recovered capsule (NASDA is in the process of recovered capsule conceptual design.)	Because no data on exposure of silica FRP to AO rays are available in Japan, it is desired that the effects of AO exposure on silica FRP be examined.	ϕ 32mm \times 1mm thickness ϕ 32mm \times 4mm thickness	2 2	-Surface analysis -Surface chemical characteristics α_s and ϵ_N -Mass -Functional evaluation (Abrasion resistance)

Table 3.1-1 (5/5) Experiment Material Samples

Name of material or part	Use	Reason for choice	Dimensions of specimen	Quantity	Evaluations and measurements
ID No.: 25 Silicone adhesive RTV-S691 WACKER CHEMICAL Co. Proposer: NEC Corp.	Application of solar cells	This material was chosen as a substitute for GE's RTV-566, but no AO exposure data are available for the material. Thus the effects of AO exposure on the material will be checked.	φ 25mm× 4 mm thickness	3	-Surface analysis -Mass
ID No.: 26 Flexible OSR (ITO*/oxidized cerium/PEI*/Ag/Ni) *ITO: Transparent conductive film *PEI: Polyetherimide NASDA-QTS-1048/301 Smitomo Bakelite Co., Ltd. Proposer: NEC Corp.	Thermal control material Second mirror surface	This is a qualified material for space uses. We have gathered data on AO exposure through an space test. The material will be installed into EFFU to practically check the effects of exposure to the space environment in several orbits.	φ 32mm × 0.075mm thickness	3	-Surface analysis -Surface chemical characteristics α_s and ϵ_N -Mass
ID No.: 27 Sputtered MoS₂ film (1)MoS ₂ film/SUS440C (SUS440C is water-cooled and sputtered with MoS ₂ .) Proposer: National Aerospace Laboratory	Lubricant for space use	The characteristics of film used in the space environment are assumed to be like those of material (2) or a material intermediate between materials (1) and (2). The effects of AO exposure on material (1), which has a fine microstructure, is limited to the proximity of its surface. However, AO exposure may dramatically deteriorate material (2), which has a columnar structure and a low density. The effects have been examined of AO exposure only on materials which have fine microstructures as does material (1). Through such examinations only, the friction characteristics of AO may be underestimated. Thus the friction characteristics must be confirmed, using material (2). Basic data on resistance to AO are expected to be obtained because the film of material (3) differs in composition from those of the two materials.	(1) MoS ₂ film/SUS440C (SUS440C is water-cooled.) φ 32 mm × 2.5 mm thickness	2	-Surface analysis -Friction characteristics
ID No.: 28 Sputtered MoS₂ film (2) MoS ₂ film/SUS440C (SUS440C is not water-cooled but spattered with MoS ₂ .) Proposer: National Aerospace Laboratory			(2) MoS ₂ film/SUS440C (SUS440C is not water-cooled.) φ 32 mm × 2.5 mm thickness	2	-Surface analysis -Friction characteristics
ID No.: 29 Sputtered MoS₂ film (3) MoS ₂ film/SUS440C (Using an ECR gun, MoS ₂ is spattered.) Proposer: National Aerospace Laboratory			(3) MoS ₂ film/SUS440C (SUS440C is water-cooled.) φ 32 mm × 2.5 mm thickness	2	-Surface analysis -Friction characteristics



AO(ground test)

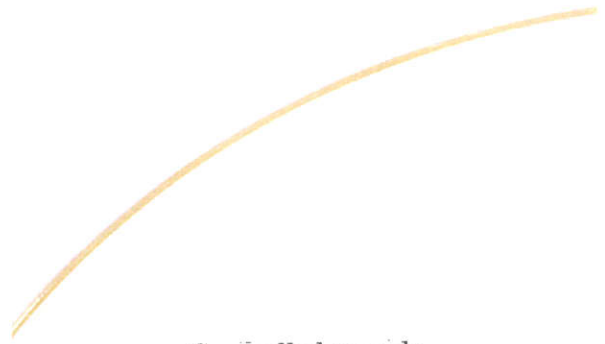


EB(ground test)

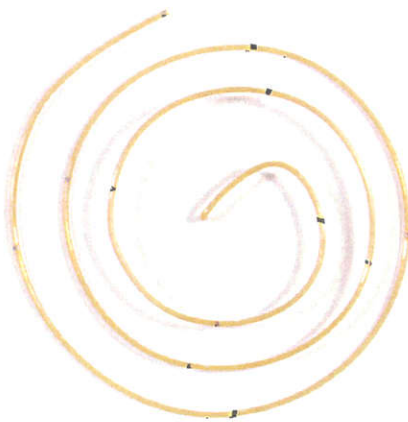
Figure 3.1-1 Photograph of ID No.1
Non-flammable electrical wire (1/2)



UV(ground test)



Controlled sample



Exposed in space

Figure 3.1-1 Photograph of ID No.1 (2/2)
Non-flammable electrical wire



AO(ground test)



EB(ground test)



UV(ground test)



Controlled sample



Exposed in space

Figure 3.1-2 Photograph of ID No.2
Epoxy resin adhesive for securing parts



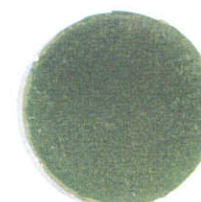
AO(ground test)



EB(ground test)



UV(ground test)



Controlled sample

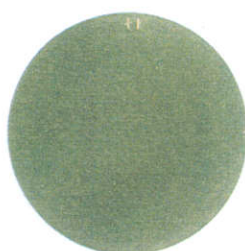


Exposed in space

Figure 3.1-3 Photograph of ID No.3
Acrylic resin Adhesive tape for multi-layer insulation



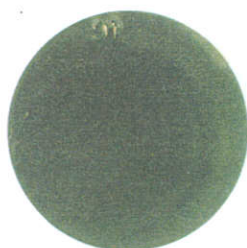
AO(ground test)



EB(ground test)



UV(ground test)



Controlled sample



Exposed in space

Figure 3.1-4 Photograph of ID No.4
Thermal control film without ITO



AO(ground test)



EB(ground test)



UV(ground test)



Controlled sample



Exposed in space

Figure 3.1-5 Photograph of ID No.5
Thermal control film with ITO



Al/O(ground test)



Al/EB(ground test)



Al/UV(ground test)



Al/Controlled sample



Al/Exposed in space



CFRP/AO(ground test)



CFRP/EB(ground test)



CFRP/UV(ground test)



CFRP/Controlled sample



CFRP/Exposed in space

Figure 3.1-6 Photograph of ID No.6
White paint



Al/AO(ground test)



Al/EB(ground test)



Al/UV(ground test)



Al/Controlled sample



Al/Exposed in space



CFRP/AO(ground test)



CFRP/EB(ground test)



CFRP/UV(ground test)



CFRP/Controlled sample



CFRP/Exposed in space

Figure 3.1-7 Photograph of ID No.7
Black paint

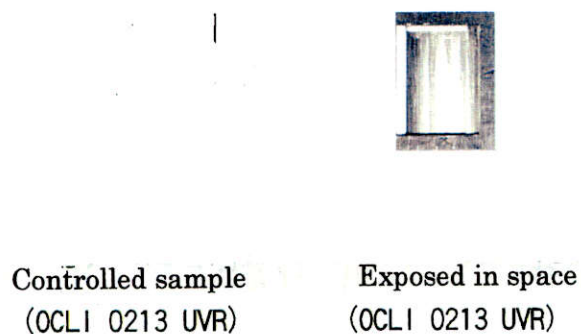
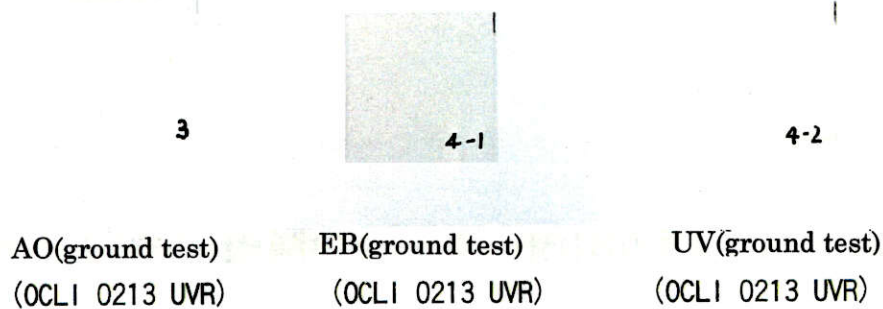
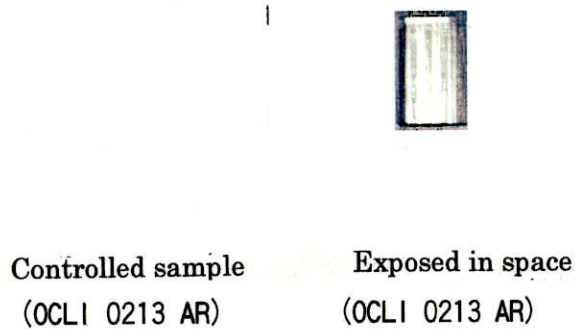
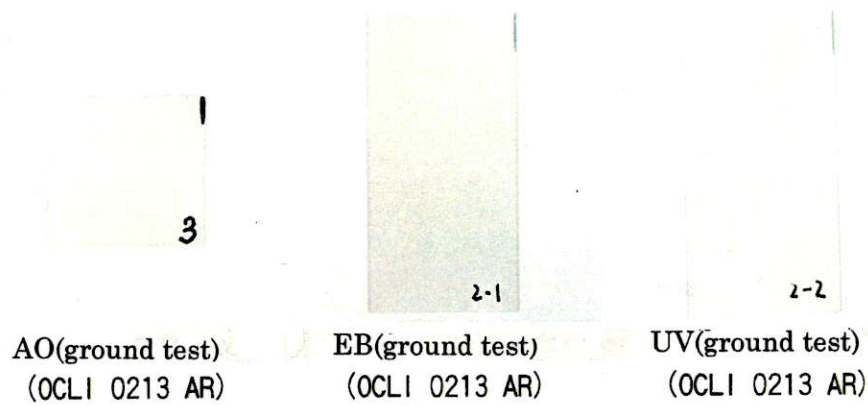
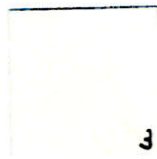
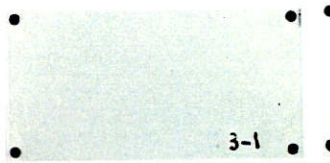


Figure 3.1-9 Photograph of ID No.10,11,12 & 13
Cover glass for solar cell

(1/2)



3



3-1



3-2

AO(ground test)
(OCLI 0213 AR+CC)

EB(ground test)
(OCLI 0213 AR+CC)

UV(ground test)
(OCLI 0213 AR+CC)



Controlled sample
(OCLI 0213 AR+CC)

Exposed in space
(OCLI 0213 AR+CC)



1-4

AO(ground test)
(PRE CMX AR)

EB(ground test)
(PRE CMX AR)

UV(ground test)
(PRE CMX AR)

1-1



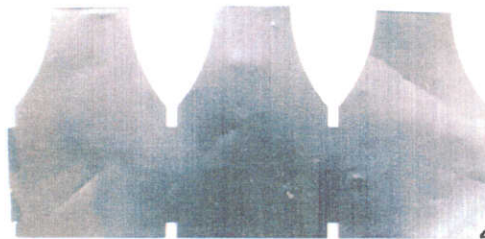
Controlled sample
(PRE CMX AR)

Exposed in space
(PRE CMX AR)

Figure 3.1-9 Photograph of ID No.10, 11, 12 & 13 (2/2)
Cover glass for solar cell



AO(ground test)



Controlled sample



Exposed in space



AO(ground test)



Controlled sample



Exposed in space

Figure 3.1-10 Photograph of ID No.14, 15, & 16 (2/2)
Inter-connector material for solar cell



AO(ground test)



Controlled sample



Exposed in space

Figure 3.1-10 Photograph of ID No.14, 15 & 16
Inter-connector material for solar cell



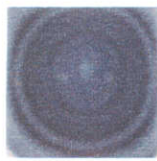
AO(ground test)
(OCLI 0213 SSM)



EB(ground test)
(OCLI 0213 SSM)



UV(ground test)
(OCLI 0213 SSM)



Controlled sample
(OCLI 0213 SSM)



Exposed in space
(OCLI 0213 SSM)



AO(ground test)
(PPE CMX SSM)



EB(ground test)
(PPE CMX SSM)



UV(ground test)
(PPE CMX SSM)



Controlled sample
(PPE CMX SSM)



Exposed in space
(PPE CMX SSM)

Figure 3.1-11 Photograph of ID No.17 & 18
OSR for solar cell

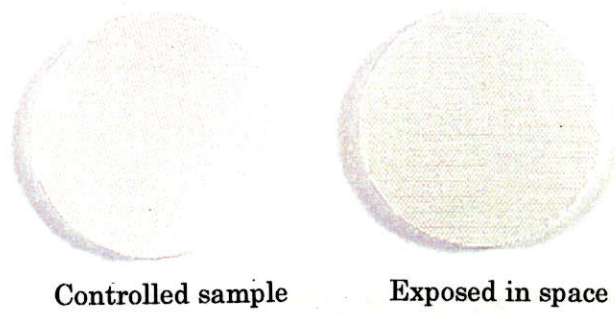
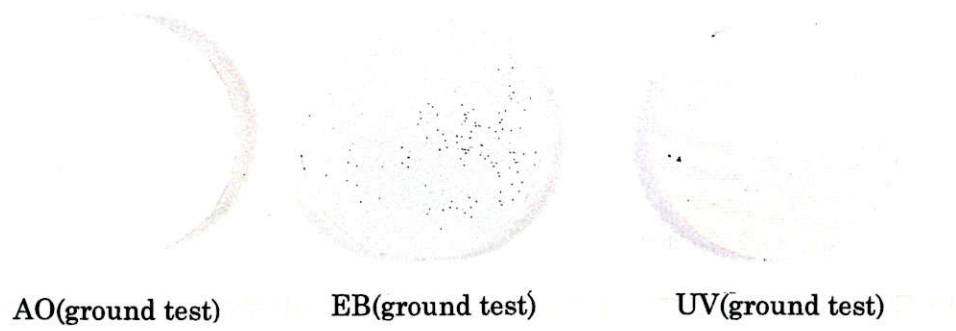


Figure 3.1-12 Photograph of ID No.19
Aluminum-deposited β cloth



HMB34 AO(ground test)



HMB34 Controlled sample HMB34 Exposed in space

Figure 3.1-13 Photograph of ID No.20, 21, 22 & 23
Binder for bonded MoS₂ film, Bonded MoS₂ films

(1/3)



Polyamideimide A
AO(ground test)



Polyamideimide A
EB(ground test)



Polyamideimide A
UV(ground test)



Polyamideimide A
Controlled sample



Polyamideimide A
Exposed in space



Polyamideimide B
AO(ground test)



Polyamideimide B
EB(ground test)



Polyamideimide B
UV(ground test)



Polyamideimide B
Controlled sample



Polyamideimide B
Exposed in space



Figure 3.1-13 Photograph of ID No.20, 21, 22 & 23
Binder for bonded MoS₂ film, Bonded MoS₂ films

(2/3)

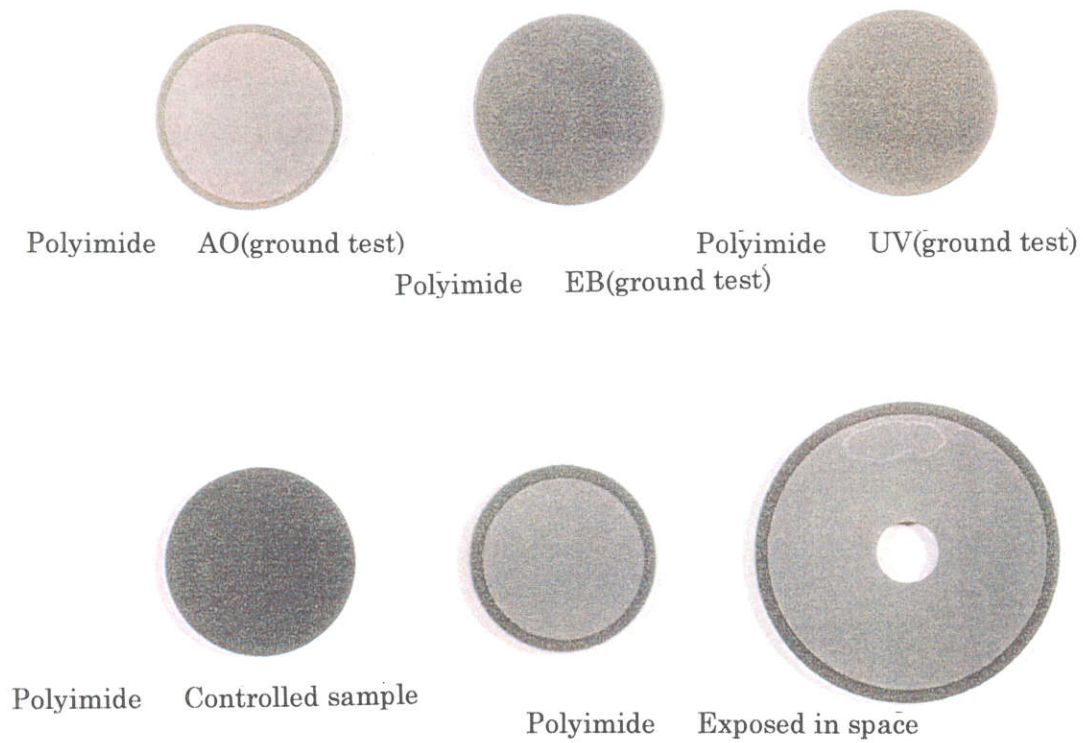


Figure 3.1-13 Photograph of ID No.20, 21, 22 & 23 Binder for bonded MoS₂ film, Bonded MoS₂ films (3/3)

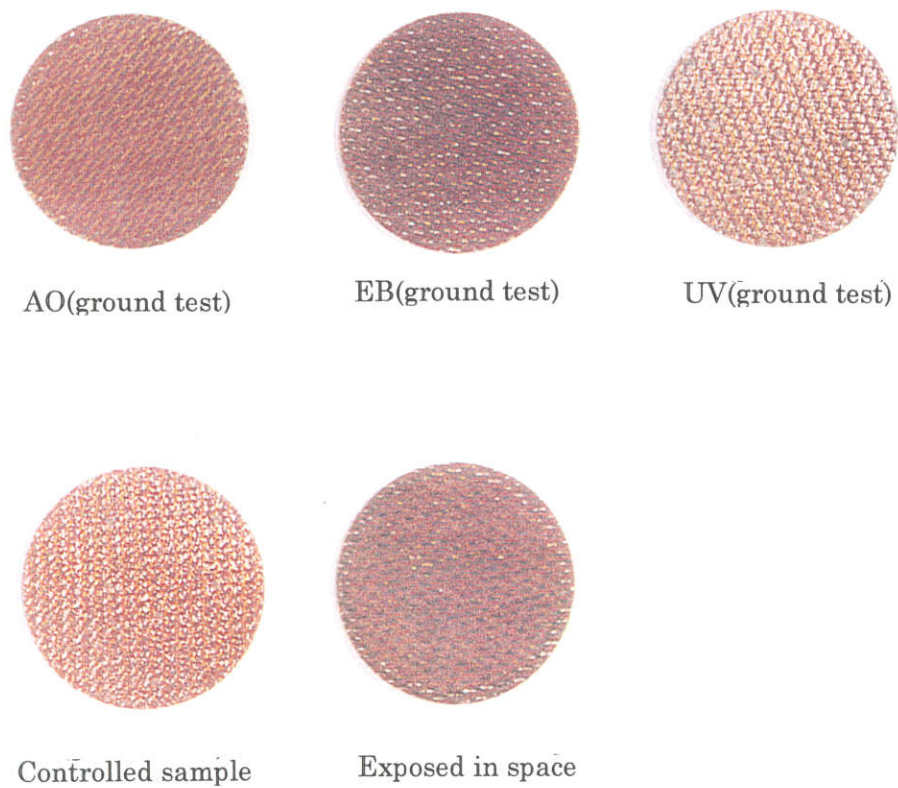


Figure 3.1-14 Photograph of ID No.24 Silica FRP



AO(ground test)



EB(ground test)



UV(ground test)



Controlled sample



Exposed in space

Figure 3.1-15 Photograph of ID No.25
Silicone adhesive(RTV-S691)



AO(ground test)



EB(ground test)



UV(ground test)



Controlled sample



Exposed in space

Figure 3.1-16 Photograph of ID No.26
Flexible OSR



AO(ground test)



UV(ground test)



Controlled sample



Exposed in space

Figure 3.1-17 Photograph of ID No.27
Sputtered MoS2 film



AO(ground test)



UV(ground test)



Controlled sample



Exposed in space

Figure 3.1-18 Photograph of ID No.28
Sputtered MoS2 film



AO(ground test)



UV(ground test)



Controlled sample



Exposed in space

Figure 3.1-19 Photograph of ID No.29
Sputtered MoS2 film



No.27



No.28



No.29 (N side)



No.29 (F side)

Figure 3.1-20 Photograph of ID No.27,28&29
Controlled samples of sputtered MoS2 film



Exposed in space



Controlled sample

Figure 3.1-21 Photograph of shielding plates
for sample ID No.28(Sputtered MoS₂ film)

4.Operation

4.1 Results of Flight Operation

- 1996.12 Assembly for flight
- 1997.1 Transportation of ESEM (from IHI to KSC)
 - Visual inspection and photographing
 - Installation of protection covers
 - Installation of MSH onto MFD
- 1997.2 Installation of CDC onto MFD
- 1997.8 Launched and retrieved by STS-85
- 1997.9 Removal of ESEM form MFD
 - Visual inspection and photographing
 - Installation of protection covers
- 1997.9 Transportation of ESEM (from KSC to IHI)

4.2 Analysis of Space Environment

Results of space environment monitors and analysis are shown in Table 4.1-1.

4.3 Ground Simulation Test

The ground simulation tests were performed to predict any possible characteristic degradation in the space environment to which the samples were exposed.

The following tests were performed.

- (1)Irradiation of Atomic oxygen (AO irradiation test)
 - at Physical Science Inc.(USA)
- (2)Irradiation of Electron beam(EB irradiation test)
 - at Takasaki Radiation Chemistry Research Establishment, Japan Atomic Energy Research Institute
- (3)Irradiation of Ultraviolet rays(UV irradiation test)
 - at NASDA Tsukuba Space Center

5. Evaluation of Installed Materials

5.1 Summary

5.1.1 Purpose of Experiment

All materials installed on the surface of spacecraft are affected by the space environment for example of atomic oxygen, ultra-violet ray and radiation.

The purpose of the experiment are as follows;

- (1) To acquire characteristics degradation data of parts and materials installed on MFD.
- (2) To contribute to improvement of parts and materials installed on MFD.

5.1.2 Evaluation Flow

The evaluation flow is shown in Fig.5.1-1.

5.1.3 Materials

The materials supplied for this experiment are shown in Table 5.1-1.

5.1.4 Location of Materials

The location of each material is shown in Table 5.1-1 and Fig.5.1-2.

5.2 Evaluation Items

Evaluation items for supplied materials are shown in Table 5.2-1.

Table 5.1-1 (1/3) Location of Material Samples and Result of Post-flight Visual Inspection

Materials	Dimension (mm)	Sample No.	Serial No.	Holder No.	Location No. See Fig. 5.1-1	ID No. on Case	Packing		Result of Post-flight Visual Inspection
							Cace	Category	
Non-flammable Electrical Wire	Electrical Wire wound into a coil 32mm in diameter	1	1	3-2	2b	PC6/ID2b	Wafer tray	1	○
			2	3-2	2a	PC6/ID2a		1	○
			3	3-2	2c	PC6/ID2c		1	○
			4	3-2	2d	PC6/ID2d		1	○
			5	3-2	2e	PC6/ID2e		1	○
			6	3-2	2f	PC6/ID2f		1	○
			7	3-2	2g	PC6/ID2g		2	○
			8	3-2	2h	PC6/ID2h		2	○
			9	3-2	2i	PC6/ID2i		2	○
			10	3-2	2j	PC6/ID2j		2	○
			11	3-2	2k	PC6/ID2k		2	○
			12	3-2	2l	PC6/ID2l		2	○
			13	3-2	2m	PC6/ID2m		3	○
			14	3-2	2n	PC6/ID2n		3	○
			15	3-2	2p	PC6/ID2p		3	○
			16	3-2	2q	PC6/ID2q		3	○
			17	3-2	2r	PC6/ID2r		3	○
Epoxy Resin Adhesive	Adhesive on Al plate	2-1	26	1-2	2	PC2/ID2	▼	15	○
	Adhesive 2 Al plate	2-2	A25	1-2	3a	PC2/ID3a	Venil bag	16	○
			A26	1-2	3b	PC2/ID3b	▼	16	○
Acrylic Resin Adhesive Tape	Adhesive on Al plate	3-1	39	2-2	2	PC4/ID2	Wafer tray	15	○
	Adhesive 2 thermal control film	3-2	A35	2-2	6	PC4/ID6	Venil bag	17	○
		3-3	T35	2-2	3	PC4/ID3	▼	17	○
Thermal Control Film without ITO	Film(Polyimide/Al/Ni)	4	49	3-1	2b	PC5/ID2b	Wafer tray	4	○
			410	3-1	2a	PC5/ID2a		4	○
			411	3-1	2c	PC5/ID2c		4	○
Thermal Control Film with ITO	Film(Polyimide/Al/Ni /ITO)	5	59	3-1	3b	PC5/ID3b		4	○
			510	3-1	3a	PC5/ID3a		4	○
			511	3-1	3c	PC5/ID3c		4	○
White Paint	Paint on Al plate □25	6-1	26	2-1	7c	PC3/ID7c		5	○
			27	2-1	7b	PC3/ID7b		5	○
			28	2-1	7a	PC3/ID7a		5	○
	Paint on CFRP plate □25	6-2	9	2-1	1c	PC3/ID1c		5	○
			10	2-1	1b	PC3/ID1b		5	○
			11	2-1	1a	PC3/ID1a		5	○
Black Paint	Paint on Al plate □25	7-1	67	2-1	8c	PC3/ID8c		6	○
			71	2-1	8b	PC3/ID8b		6	○
			97	2-1	8a	PC3/ID8a		6	○
	Paint on CFRP plate □25	7-2	77	2-1	2c	PC3/ID2c		6	○
			78	2-1	2b	PC3/ID2b		6	○
			79	2-1	2a	PC3/ID2a	▼	6	○

Table 5.1-1 (2/3) Location of Material Samples and Result of Post-flight Visual Inspection

Materials	Dimension (mm)	Sample No.	Serial No.	Holder No.	Location No. See Fig. 5.1-1	ID No. on Case	Packing		Result of Post-flight Visual Inspection	
							Cace	Category		
									○ : Not changed △ : Changed	
Solar Cell	φ 39×3t	8	A-I	1-2	1	PC2/ID1	Wafer tray	7	△ Colared.	
Solar Cell	φ 39×3t	9	A-II	3-2	1	PC6/ID1		7	△ Colared.	
Inter-connector material for solar cell	Whole φ 39×3t 5×15 5×15 5×15	14	C-1	1-2	6	PC2/ID6		7	△ Colared.	
		15								
		16								
OSR for solar cell	Whole φ 39×3t 5×15 5×15	17	B-3	1-2	7	PC2/ID7		7	○	
		18								
Cover glass for solar cell	Whole φ 39×3t 5×15 5×15	10	B-1	1-2	5a	PC2/ID5a		7	○	
		11								
Cover glass for solar cell	Whole φ 39×3t 5×15 5×15	12	B-2	1-2	5b	PC2/ID5b		7	○	
		13								
Al deposited β cloth	adhesive on al plate	19	1910	3-1	5a	PC5/ID5a		8	○	
			1911	3-1	5b	PC5/ID5b		8	○	
Bonded MoS2 film (HMB34 film)	coated on Ti plate φ 25	20-1	205	1-1	8	PC1/ID8		8	△ Contamination.	
	coated on Ti plate φ 40	20-2	L201	1-1	4	PC1/ID4		13	△ Contamination.	
Binder for bonded MoS2 film (Polyamideimide A)	coated on Ti plate φ 25	21-1	S216	1-1	5	PC1/ID5		8	△ Colared.	
	coated on Ti plate φ 40	21-2	215	1-1	1	PC1/ID1		13	○	
Binder for bonded MoS2 film (Polyamideimide B)	coated on Ti plate φ 25	22-1	S226	1-1	6	PC1/ID6		8	○	
	coated on Ti plate φ 40	22-2	225	1-1	2	PC1/ID2		13	△ Colared.	
Binder for bonded MoS2 film (Polyimide)	coated on Ti plate φ 25	23-1	S236	1-1	7	PC1/ID7		8	○	
	coated on Ti plate φ 40	23-2	235	1-1	3	PC1/ID3		13	△ Colared.	
Silica FRP	coated on SUS plate φ 40 φ 40×tl	24-1	S247	2-2	8	PC4/ID8		14	○	
			S248	2-2	7	PC4/ID7		14	○	
	coated on SUS plate φ 40 φ 40×tl	24-2	247	2-2	9	PC4/ID9		14	○	
			248	2-2	5	PC4/ID5		14	○	
Silicone adhesive (RTV-S691)	adhesive on al plate	25	255	3-1	1b	PC5/ID1b		9	○	
			256	3-1	1a	PC5/ID1a		9	○	
			257	3-1	1c	PC5/ID1c		9	○	
Flexible OSR	Thin film	26	265	3-1	4b	PC5/ID4b		9	○	
			266	3-1	4a	PC5/ID4a		9	○	
			267	3-1	4c	PC5/ID4c		9	○	
Sputtered MoS2 film	Exposed all surface	27-1	0016	1-1	9	PC1/ID9		10	△ Contamination.	
	Exposed partial surface	27-2	0010	1-1	17	PC1/ID17		10	△ Colared.	
Sputtered MoS2 film	Exposed all surface	28-1	0013	1-1	18	PC1/ID18		10	○	
	Exposed partial surface	28-2	0003	1-1	10	PC1/ID10		10	○	
Sputtered MoS2 film	Exposed all surface	29-1	0042	1-1	19	PC1/ID19		10	○	
	Exposed partial surface	29-2	0039	1-1	11	PC1/ID11		10	○	

Table 5.1-1 (3/3) Location of Material Samples and Result of Post-flight Visual Inspection

Materials	Dimension (mm)	Sample No.	Serial No.	Holder No.	Location No. See Fig. 5.1-1	ID No. on Case	Packing		Result of Post-flight Visual Inspection ○ : Not changed △ : Changed	
							Cace	Category		
continued from (2/3) Sputtered MoS2 film										
	Shielding plate			1-1	17	PC1/ID9	Wafer tray	11	○	
	Shielding plate			1-1	10	PC1/ID18	↓	11	○	
	Shielding plate			1-1	11	PC1/ID19	↓	11	○	
Sample for Environment Monitoring										
Polyimide film for AO monitor	Kapton-100H film φ 32.3mm×0.025mm	1	1-1	13	PC1/ID13	Wafer tray	12	○		
		2	2-1	4	PC3/ID4		12	○		
		3	3-1	7	PC5/ID7		12	○		
Polyurethane film for UV monitor	Ulethane film covered with quartz glass φ 32.3mm×3.3mm	1	1-1	14	PC1/ID14		12	△	Glass, Ulethane and Al plate were sticked.	
		2	2-1	5	PC3/ID5		12	△	Glass, Ulethane and Al plate were sticked.	
		3	3-1	8	PC5/ID8		12	△	Glass, Ulethane and Al plate were sticked.	
Thermal luminescence dose meter (TLD) (MSO-S)	TLD contained in Al case φ 32mm×5.5mm	002	1-1	12	PC1/ID12		19	△	Little liquid on side.	
		003	2-1	3	PC3/ID3		19			
		005	3-1	6	PC5/ID6	↓	19			
RADFET (Radiation sensitive field effect transistor)	Ceramic package IC 16mm×30mm×5.9mm thickness	P172-W3	177	1-1	15a	1-1-1	Venil bag ↓	18	△	P/N marking disappeared.
		P456-W5	047	1-1	15b	1-1-2		18	△	P/N marking disappeared.
		P210/W2	004	1-1	15c	1-1-3		18	△	P/N marking disappeared.
		P172-W3	178	2-1	6a	2-1-1		18	△	P/N marking disappeared.
		P456-W5	048	2-1	6b	2-1-2		18	△	P/N marking disappeared.
		P210/W2	005	2-1	6c	2-1-3		18	△	P/N marking disappeared.
		P172-W3	179	3-1	9a	3-1-1		18	△	P/N marking disappeared.
		P456-W5	049	3-1	9b	3-1-2		18	△	P/N marking disappeared.
		P210/W2	008	3-1	9c	3-1-3		18	△	P/N marking disappeared.
Thermo-Label (Temperature Indicator)	5E-50 40mm×15mm			1-1					○	Thermal indicator did not indicated.
	5E-75			1-2					○	Thermal indicator did not indicated.
	5E-50			2-1					○	Thermal indicator did not indicated.
	5E-75			2-2					○	Thermal indicator did not indicated.
	5E-50			3-1					○	Thermal indicator did not indicated.
	5E-75	↓		3-2					○	Thermal indicator did not indicated.

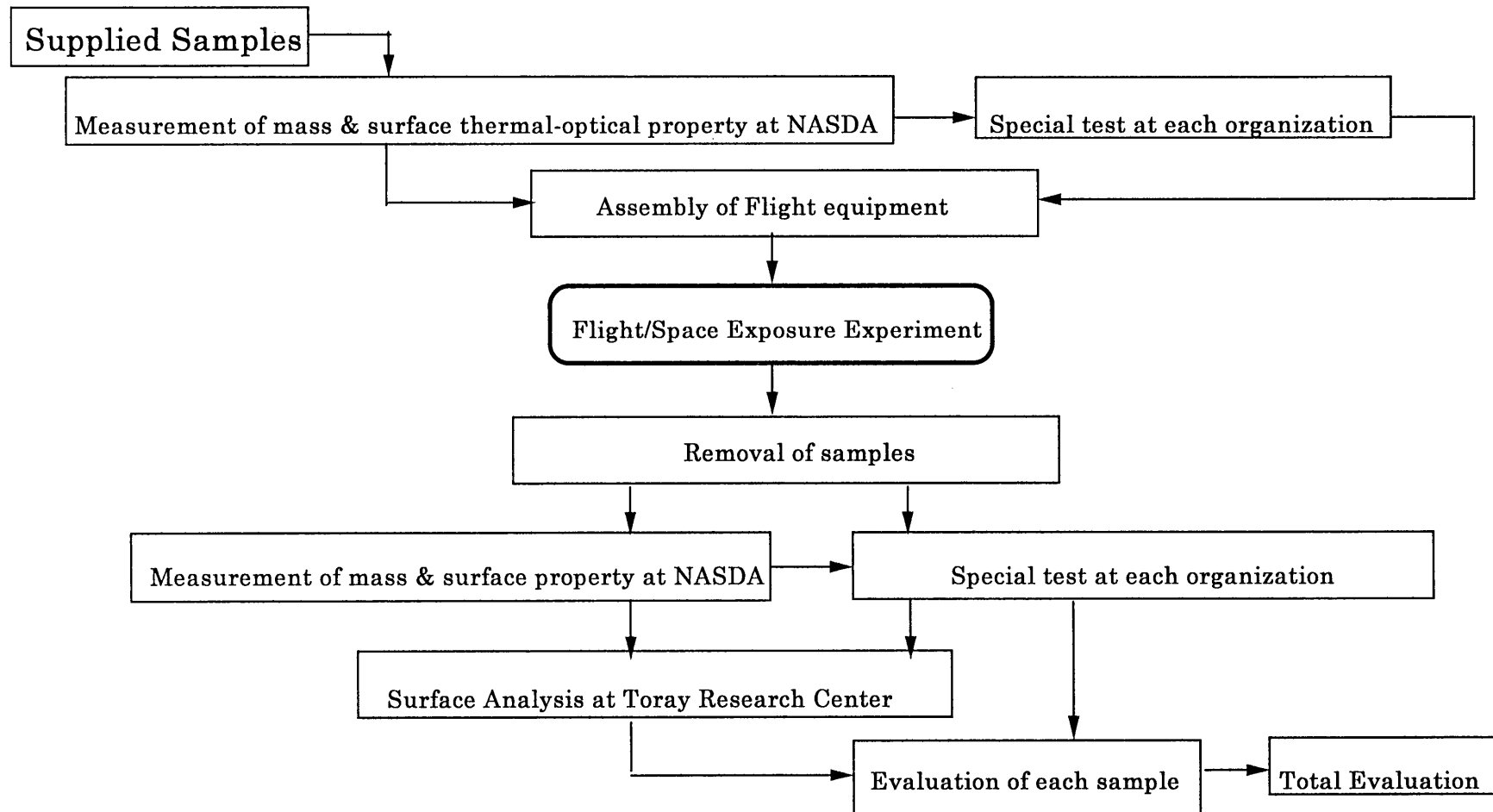


Figure 5.1-1 Evaluation Flow of Post-flight Analysis

5.2 Evaluation Items

Evaluation items for supplied materials are shown in Table 5.2-1.

Table 5.2-1 (1/2) Analysis & Test Item List of Exposed Material Samles

Materials	Dimension (mm)	Sample No.	Serial No.	Holder No.	TKSC*7		Surface Analysis at TRC *1											Special	Remarks
					Mass *2	α, ϵ	Photo	OM *3	Cut	FE-SEM *4	ESCA		FTIR	AES			EPMA	Test at supplier *8	
											Surface	Depth Profile		OSR	Cover Glass	solid Lubricant			
Non-flammable electrical wire	Electrical Wire	1	1	3-2	○		○	○	○	○	○		○						Arc-tracking test
			2~17		○														
Epoxy resin adhesive	Adhesive on Al plate	2-1	26	1-2	○		○	○	○	○	○		○					Tensile test	
	Adhesive 2 Al plate	2-2	A25	1-2													Tensile test		
Acrylic resin adhesive tape	Adhesive on Al plate	3-1	39	2-2	○		○	○	○	○	○		○					Peeling test	
	Adhesive 2 thermal	3-2	A35	2-2													Peeling test		
	control film	3-3	T35	2-2													Peeling test		
Thermal control film without ITO	Film(Polyimide/Al/Ni)	4	49	3-1	○	○	○	○	○	○	○		○						
			410	3-1	○	○													
			411	3-1	○	○													
Thermal control film with ITO	Film(Polyimide/Al/Ni /ITO)	5	59	3-1	○	○	○	○	○	○	○		○						
			510	3-1	○	○													
			511	3-1	○	○													
White paint	Paint on Al plate □25	6-1	26	2-1	○	○	○	○	○	○	○		○						
			27	2-1	○	○													
			28	2-1	○	○													
	Paint on CFRP plate □25	6-2	9	2-1	○	○	○	○	○	○	○		○						
		10	2-1	○	○														
		11	2-1	○	○														
Black paint	Paint on Al plate □25	7-1	67	2-1	○	○	○	○	○	○	○		○						
			71	2-1	○	○													
			97	2-1	○	○													
	Paint on CFRP plate □25	7-2	77	2-1	○	○	○	○	○	○	○		○						
			78	2-1	○	○													
			79	2-1	○	○													
Solar Cell	φ 39×3t	8	A-I	1-2	○													Output Voltage	
Solar Cell	φ 39×3t	9	A-II	3-2	○													Output Voltage	
Inter-connector material for solar cell	Whole φ 39×3t 5×15	14	C-1-1	1-2	○	○	○	○	○	○						○			
		15	C-1-2		○	○		○					○						
		16	C-1-3		○	○		○	○					○					
OSR for solar cell	Whole φ 39×3t 5×15	17	B-3-1	1-2	○	○	○	○	○	○	○			○			Transparency		
		18	B-3-2		○	○		○	○			○			Transparency				
Cover glass for solar cell	Whole φ 39×3t 5×15	10	B-1-1	1-2	○	○	○		○	○	○				○		Transparency		
		11	B-1-2		○	○			○	○	○			○		Transparency			
Cover glass for solar cell	Whole φ 39×3t 5×15	12	B-2-1	1-2	○	○	○		○	○	○				○		Transparency		
		13	B-2-2		○	○			○	○	○			○		Transparency			
Al deposited β cloth	adhesive on al plate	19-1	1910	3-1	○	○	○	○	○	○	○		○						
		19-2	1911	3-1	○	○													

* 1 : After surface observation with OM, cut sample and analyzed with another methods.

* 2 : accuracy $\pm 1 \times 10^{-5}$ g

* 3 : Two fields

* 4 : Three magnitudes

* 5 : 0.2 μm depth

* 6 : 29-1 : One is several hundred nm depth, the other is 1 μm depth.

27-1, 28-1 : several hundred nm depth.

* 7 : measured by NASDA at Tukuba Spade Center(TKSC)

* 8 : performed by each sample supplier

* 9 : FTIR, micro-FTIR, microscope-FTIR or TOF-SIMS

* 10 : for comparison of contaminated sample and control sample.

Table 5.2-1 (2/2) Analysis & Test Item List of Exposed Material Samles

Materials	Dimension (mm)	Sample No.	Serial No.	Holder No.	TKSC*7		Surface Analysis at TRC *1											Special Test at supplier *8	Remarks
					Mass *2	α, ϵ	Photo	OM *3	Cut	FE-SEM *4	ESCA		FTIR	AES			EPMA		
											Surface	Depth Profile		OSR	Cover Glass	solid lubricant			
Bonded MoS2 film	coated on Ti plate ϕ 25	20-1	205	1-1	○		○	○	○	○	○		○						
(HMB34 film)	coated on Ti plate ϕ 40	20-2	L201	1-1	○													Property	
Binder for bonded MoS2 film	coated on Ti plate ϕ 25	21-1	S216	1-1	○		○	○	○	○	○		○						
(Polyamideimide A)	coated on Ti plate ϕ 40	21-2	215	1-1														Property	
Binder for bonded MoS2 film	coated on Ti plate ϕ 25	22-1	S226	1-1	○		○	○	○	○	○	□	○ □*9						
(Polyamideimide B)	coated on Ti plate ϕ 40																		22-2
Binder for bonded MoS2 film	coated on Ti plate ϕ 25	23-1	S236	1-1	○		○	○	○	○	○	□	○ □*9						
(Polyimide)	coated on Ti plate ϕ 40	23-2	235	1-1														Property	
Silica FRP	ϕ 40×t1	24-1	247	2-2	○	○	○	○	○	○			○*5	○					
	248		2-2	○	○												Property		
	ϕ 40×t4	24-2	247	2-2	○	○													
			248	2-2	○	○												Property	
Silicone adhesive (RTV-S691)	ϕ 32	25	255	3-1	○		○	○	○	○	○		○						
			256	3-1	○														
			257	3-1	○														
			265	3-1	○	○	○	○	○	○	○	○		○					
Flexible OSR	Thin film ϕ 32	26	266	3-1	○	○													
			267	3-1	○	○													
Sputtered MoS2 film	Exposed all surface	27-1	0010	1-1	○		○	○	○	○	○	□×2	*10	*13				Property	
	Exposed partial surface	27-2	0016	1-1	○		○	○	○	○			□×2	*9			○*6	□×2	
Sputtered MoS2 film	Exposed all surface	28-1	0003	1-1	○		○	○	○	○	○	□×2	*10	*13				Property	
	Exposed partial surface	28-2	0013	1-1	○		○	○	○	○							○*6		
Sputtered MoS2 film	Exposed all surface	29-1	0039	1-1	○		○	○	○	○	○	□×2	*10	*13				Property	
	Exposed partial surface	29-2	0042	1-1	○		○	○×2	○	○×2							○×2	*6	
Sputtered MoS2 film	Control sample for 27-2 ϕ 32	27-3					○			○									
	Control sample for 28-2 ϕ 32	28-3					○			○									
	Control sample for 29-2 ϕ 32	29-3					○			○×2									
Sputtered MoS2 film	Shielding plate	注15		1-1			○		○		○		○*9						
Shielding plate	Shielding plate	未照射					○		○		○		○*9						
	Shielding plate for 28-1	28-10		1-1			○*13		○*13				□×2	*9	*13		□×2	*9	

* 1 : After surface observation with OM, cut sample and analyzed with another methods.

* 2 : accuracy $\pm 1 \times 10^{-5}$ g

* 3 : Two fields

* 4 : Three magnitudes

* 5 : 0.2 μ m depth* 6 : 29-1 : One is several hundred nm depth, the other is 1 μ m depth.

27-1, 28-1 : several hundred nm depth.

* 7 : measured by NASDA at Tukuba Spade Center(TKSC)

* 8 : performed by each sample supplier

* 9 : FTIR, micro-FTIR, microscope-FTIR or TOF-SIMS

* 10 : for comparison of contaminated sample and control sample.

5.3 Space Environment Monitor

5.3.1 Summary

(1) Monitor Materials

- a) Polyimide film (KAPTON-100H) for atomic oxygen monitor
- b) Urethane based film for ultraviolet monitor
- c) Thermal Luminescence Dosimeter(MSO-S) & CR-39 plastic glass for radiation monitor

(2) MFD Mission Orbit & Period

- a) Flight number STS-85
- b) Altitude 296 km
- c) Inclination 57 degree
- d) Period '97.8.7~'97.8.19 (exposed 278hr)

(3) Space environment

The space environment evaluated with the monitor materials is shown in Table 5.3-1

Table 5.3-1 MFD/ESEM Summary of space environment evaluation

Space environment		Location		
		MSH1	MSH2	MSH3
Total fluence of atomic oxygen [atoms/cm ²]		8.14E+19~ 9.69E+19	4.36E+19~ 5.18E+19	3.01E+19~ 3.58E+19
Total doze of radiation [mSv]	Inside Al container (1mm thickness)* ¹	4.3	4.1	4.2
	Exposed environment* ²	210		
Total fluence of ultraviolet[ESD* ³]		2.0~2.6	2.2~3.0	1.8~2.7

Remarks *1:Thermal Luminescence Dose-meter(TLD),

*2:Evaluation with measurement result and space environment analysis,

*3:Equivalent Solar Day

5.3.2 Atomic Oxygen Environment

Total fluence of atomic oxygen (AO) is evaluated with the following equations.

The mass decrease of the AO monitor (KAPTON-100H) measured at pre-flight and post-flight analysis is used as the weight variation.

$$\text{AO Fluence}[\text{atoms}/\text{cm}^2] = \Delta W / (\text{Re} \cdot \rho \cdot A)$$

where

ΔW : weight variation

ρ : Kapton density [=1.42 g/cm³]

A : Kapton exposed surface area[=6.16 cm²]

Re: Kapton reactivity [cm³/atom]

$$\text{Re}=4.62\text{E-}24*\text{EXP}(-1041/(\text{R}*T)) \leftarrow \text{Test result}$$

R: Gas constant

T: Temperature of Kapton [K]

The temperature of monitor materials are predicted from -50 to +50 [degree C].

- The result of the thermo-labels : less than +50 [degree C]
- The result of thermal analysis of MFD by Toshiba in accordance with the technical letter No.SS21-K96169 : more than -50 [degree C]

The evaluation result including the monitor materials' temperature is shown in Table 5.3-2.

Table 5.3-2 MFD/ESEM Evaluation Result of Atomic Oxygen Monitor

Monitor Material	S/N	Location	Mass[mg]			Re [cm ³ /atom]	AO Fluence [atoms/cm ²]
			Pre-flight	Post-flight	Degradation		
KAPTON-100H	1	M S H 1	27.873	25.640	-2.233	2.64E-24~ 3.14E-24	8.14E+19~ 9.69E+19
	2	M S H 2	29.828	28.633	-1.195	2.64E-24~ 3.14E-24	4.36E+19~ 5.18E+19
	3	M S H 3	29.083	28.257	-0.826	2.64E-24~ 3.14E-24	3.01E+19~ 3.58E+19

Result of EFFU : 4.68E+19[atoms/cm²]

The monitor in MSH1 shows the least fluence among MSH1,2,3. MSH1 is located in the outmost position in the space shuttle cargo-bay.

Appendix

(1) Rough estimation

ESEM experiment term : RAM exposure time = 54hr

No ESEM experiment term : Solar-viewing = 224hr

In according to the atmospheric model shown in Fig.5.3-1, AO fluence is as follows;

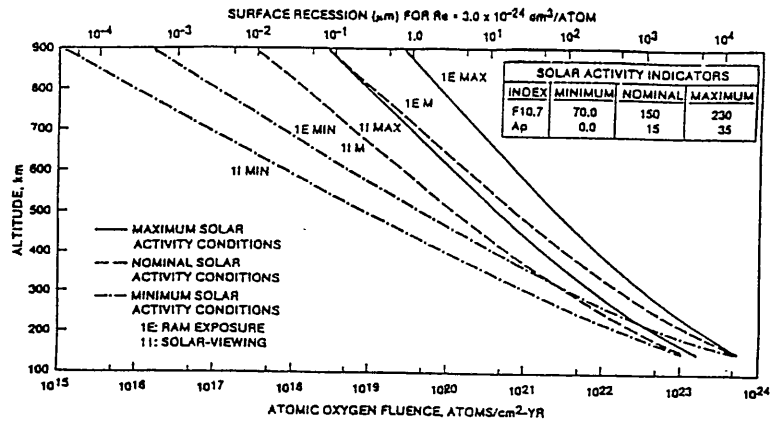
$$\begin{aligned}
 \text{AO fluence} &= \frac{2\text{E}+14[\text{atoms}/\text{cm}^2 \cdot \text{sec}] \cdot 3600[\text{sec}/\text{hr}] \cdot 54[\text{hr}]}{\text{At RAM exposure (Fig. 5. 3-1 (b))}} \\
 &+ \frac{1\text{E}+21[\text{atoms}/\text{cm}^2 \cdot \text{year}] \cdot 224[\text{hr}]/24[\text{hr}]/365[\text{day}/\text{year}]}{\text{At Solar viewing (Fig. 5. 3-1 (a))}} \\
 &= 3.89\text{E}+19 + 2.56\text{E}+19 \\
 &= 6.45\text{E}+19 [\text{atoms}/\text{cm}^2]
 \end{aligned}$$

(2) Detail estimation

In according to the result of the space environment analysis conducted by NASDA(Doc.No.GDA-98003), the AO fluence on RAM face of ESEM is $4.39\text{E}+19[\text{atoms}/\text{cm}^2]$.

The evaluation result of the AO monitors fits to the analytical result.
Therefore the result of the monitors is

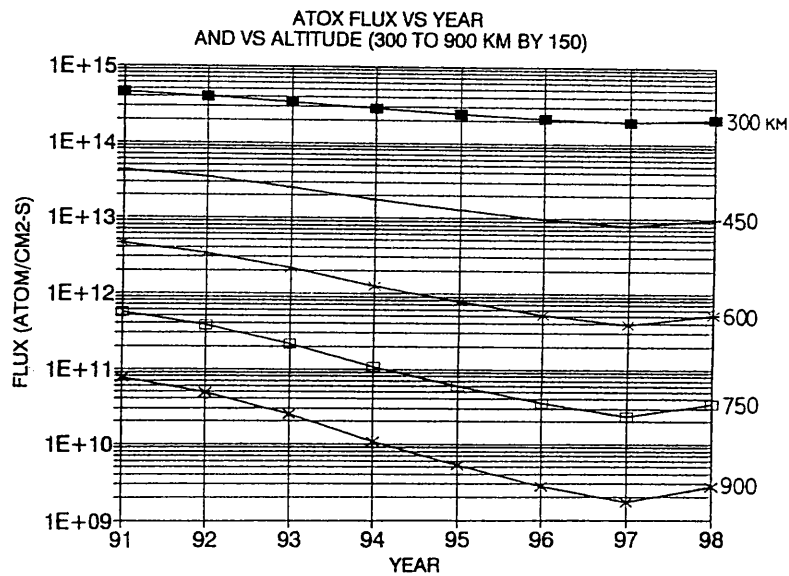
The AO fluence at the ground simulation test is $1.54\text{E}+20$ through $2.0\text{E}+20[\text{atoms}/\text{cm}^2]$.



J.SPACECRAFT, Vol.23

No.5 Sept.-Oct. 1986

Fig.5.3-1(a)



Supplied from
Physical Science Inc.

Fig.5.3-1(b)

Fig.5.3-1 Atomic oxygen atmospheric model

5.3.3 Radiation Environment

The radiation environment is shown in Fig.5.3-2.

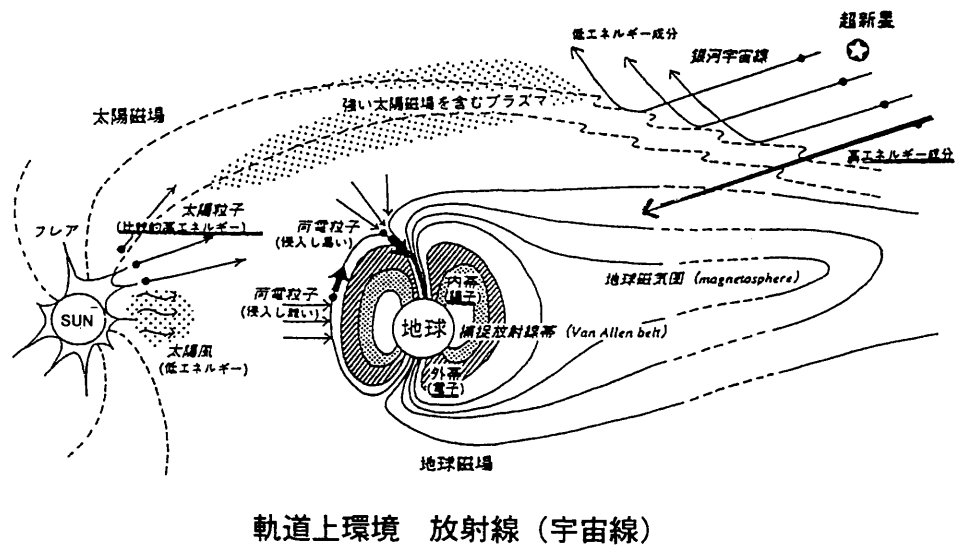


Fig.5.3-2 Radiation Environment

(1) General

Thermal Luminescence Dosimeter (TLD/MSO-S)) and CR-39 plastic glass are were installed on MFD-ESEM as radiation environment monitors.

We plan that the radiation environment is basically measured by TLD and corrected by CR-39 plastic glass.

Total dose of radiation was evaluated with the following equations by the measurement data of TLD and CR-39.

$$\begin{aligned} D_{\text{total}} &= D_{\text{TLD}} - \kappa \cdot D_{>3.5\text{KeV}/\mu\text{ m}} + D_{>3.5\text{KeV}/\mu\text{ m}} \\ &= D_{\text{TLD}} + (1 - \kappa) \cdot D_{\text{CR-39}} \end{aligned}$$

$$\begin{aligned} H_{<3.5\text{keV}/\mu\text{ m}} &= D_{\text{TLD}} - \kappa \cdot D_{>3.5\text{keV}/\mu\text{ m}} \\ &= D_{\text{TLD}} - \kappa \cdot D_{\text{CR-39}} \end{aligned}$$

$$\begin{aligned} H_{\text{total}} &= H_{<3.5\text{keV}/\mu\text{ m}} + H_{>3.5\text{keV}/\mu\text{ m}} \\ &= D_{\text{TLD}} - \kappa \cdot D_{\text{CR-39}} + H_{\text{CR-39}} \end{aligned}$$

D_{total}	: Total absorbed dose
H_{total}	: Total dose equivalent
D_{TLD}	: Absorbed dose of TLD
$D_{>3.5\text{KeV}/\mu\text{ m}}$: Absorbed dose of radiation ($\text{LET} \geq 3.5\text{KeV}/\mu\text{ m}$)
$H_{>3.5\text{KeV}/\mu\text{ m}}$: Dose equivalent of radiation ($\text{LET} \geq 3.5\text{KeV}/\mu\text{ m}$)
$H_{<3.5\text{KeV}/\mu\text{ m}}$: Dose equivalent of radiation ($\text{LET} \leq 3.5\text{KeV}/\mu\text{ m}$)
$D_{\text{CR-39}}$: Absorbed dose of CR-39
$H_{\text{CR-39}}$: Dose equivalent of CR-39
κ	: Sensitivity coefficient of TLD for radiation more than $3.5\text{KeV}/\mu\text{ m}$

*5 : T.Doke, T.Hayashi, S.Nagaoka, K.Ogura, and R.Takeuchi

"Estimation of dose equivalent in STS-47 by a combination of TLDs and CR-39", Radiat.Meas., 24(1995)75-82.

(2) Measurement Result of Thermal Luminescence Dosimeter

The measurement result of Thermal Luminescence Dosimeter is shown in Table 5.3-4.

Table 5.3-4 Measurement result of Thermal Luminescence Dosimeter

Monitor Material	S/N	Location	Measured value a [mSv]	Corrected value [mSv] (a-1.724)	Corrected value [mSv/day]
MSO-S	002A	MSH1	6.077	4.353	0.38
	002B	MSH1	6.016	4.292	0.37
	003A	MSH2	5.941	4.217	0.36
	003B	MSH2	5.671	3.947	0.34
	005A	MSH3	5.995	4.271	0.37
	005B	MSH3	5.914	4.190	0.36
	004A	Controlled sample	1.701	avg.1.724	—
	004B	Controlled sample	1.724		
	006A	Controlled sample	1.757		
	006B	Controlled sample	1.712		

(3) Analysis result of CR-39 plastic glass

The CR-39 installed on MFD-ESEM was treated with etching and the tracks of particles were evaluated.

· Etching condition : 70°C、7.04N NaOH、30[HR]

The photograph of CR-39 after etching is shown in Photo 5.3-1.

The diagram of particle tracks is shown in Fig.5.3-3.

The etching velocity of track(V_T) and the etching velocity of surface of CR-39 are evaluated with the following equation. Then REL and LET are evaluated by the data of the calibration test(see Fig.5.3-4).

$$V_T/V_B = (16 \cdot D_A^2 \cdot B^2 / (4 \cdot B^2 \cdot D_B^2 + 1))^{1/2}$$

$$LET(\text{kev}/\mu \text{ m-water}) = 0.19 \cdot REL$$

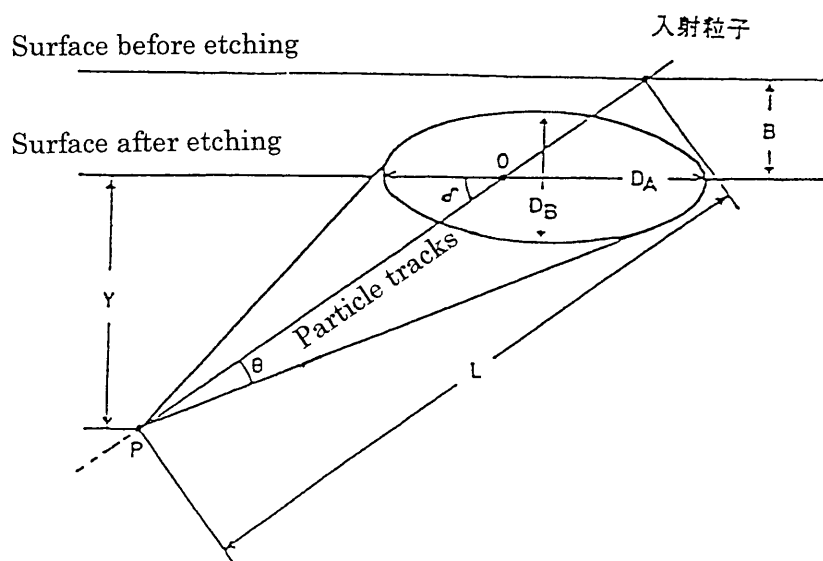


Fig.5.3-3 Diagram of particle tracks of CR-39 after etching

The LET distribution acquired by inspection with optical microscope is shown in Fig.5.3-5.

(4) Evaluation of Total Dose

The total dose of the monitor materials inside aluminum container (1mm thickness) is shown in Table 5.3-5.

Table 5.3-5 MFD-ESEM Measurement Result of Radiation Monitor

Location	DCR-39		HCR-39		D _{total}		H _{total}	
	[mGy]	[mGy/day]	[mSv]	[mSv/day]	[mGy]	[mGy/day]	[mSv]	[mSv/day]
M S H 1	0.476	0.041	2.418	0.209	4.514	0.390	6.455	0.557
M S H 2	0.447	0.039	2.674	0.231	4.261	0.368	6.488	0.560
M S H 3	0.455	0.039	1.948	0.168	4.413	0.381	5.906	0.510

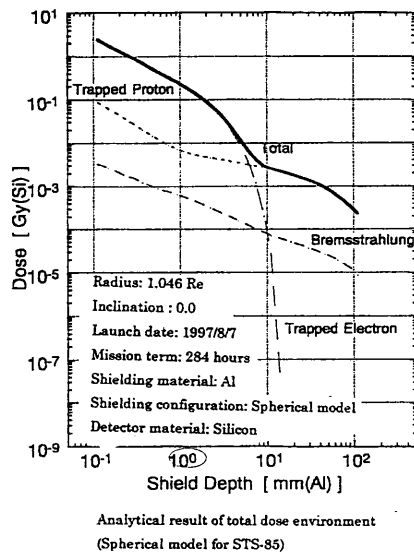
The analytical result conducted by NASDA is shown in the right figure.

In case of 1mm thickness shielding(Al), the dose is about 0.2[Gy](\approx 200[mSv]).

The analytical result is different from the measurement result of TLD.

The reason is supported that the analytical model is the complete spherical model, is not considered any bodies to shield the radiation.

The dose without shielding is 50 times as much as the dose with shielding in according to the analytical result in the right figure. Therefore, the dose without shielding is about 210[mSv] in according to the measurement result of TLD (avg.4.2[mSv]).



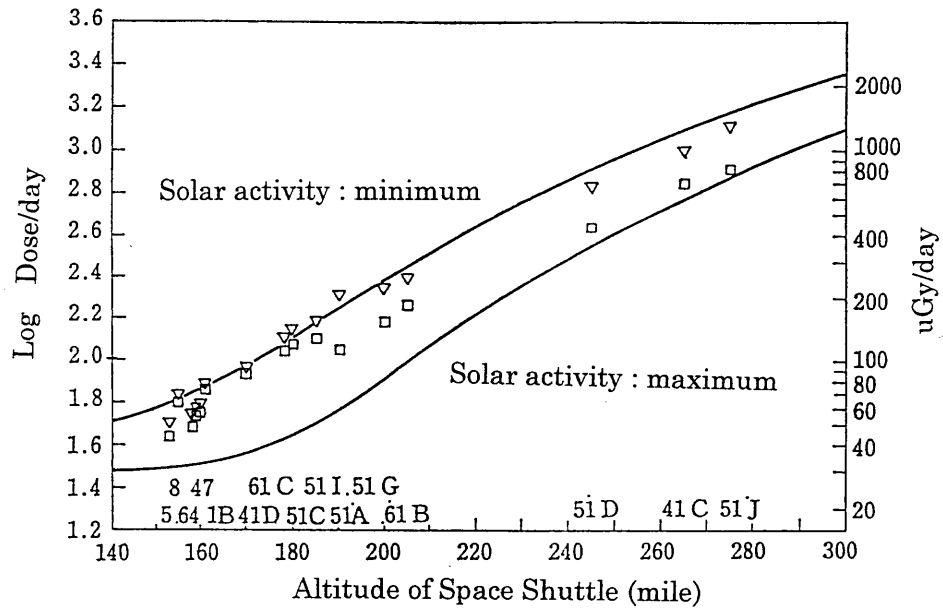
The same monitor materials were installed on SFU-EFFU program. The dose H_{total} at EFFU is 3[mSv/day], that is 6 times as MFD-ESEM.

	Altitude H[km]	Inclination i [degree]
• SFU	482	28.5
• MFD (STS-85)	296	57

The measurement result in the space shuttle is shown in the figure below.

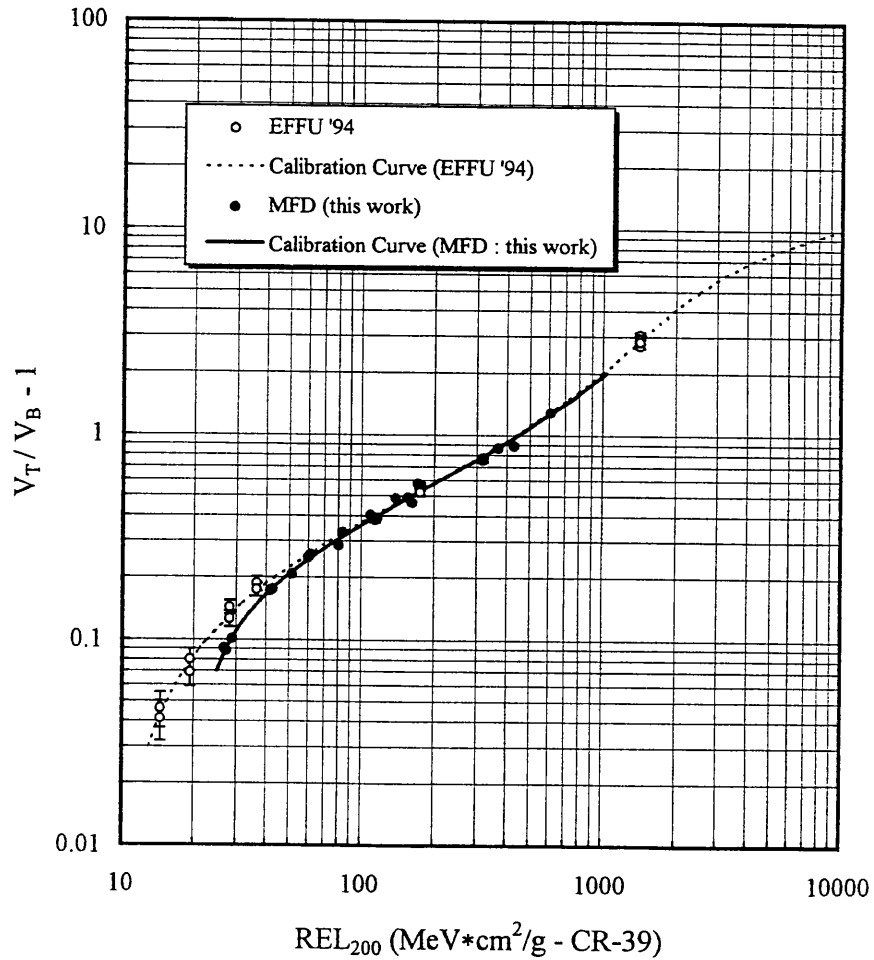
In according to the figure, it is obviously that the dose in attitude 482km is more than 10 times as in 296km from the figure.

The dose of the ground simulation test is 8212[R], that is much greater than the dose of the flight environment.



Prediction and measurement result of radiation

Calibration Curve



$$REL_{200} = 10^Y + 20$$

$$Y = -0.3189X^3 - 0.5651X^2 + 1.4474X + 2.6308$$

$$X = \log_{10} (V_T/V_B - 1)$$

Fig.5.3-4 MFD/ESEM Calibration Data of CR-39 installed on MFD

5.3.4 Ultraviolet ray environment

The ultraviolet fluence was evaluated by solar absorption(α s) data with the calibration data (Fig.5.3-6) acquired in the ground simulation test.

The evaluation result is shown in Table 5.3-6.

Table5.3-6 MFD/ESEM Evaluation Result of Ultraviolet Monitor Material

Monitor Material	S/N	Location	Solar Absorption α s			Ultraviolet Fluence [ESD]
			Pre-flight	Post-flight	Degradation	
Urethane Film (Head)	1	MSH1	0.163	0.185	0.022	2.0
	2	MSH2	0.176	0.188	0.012	2.2
	3	MSH3	0.169	0.181	0.012	1.8
Urethane Film (Tale)	1	MSH1	—	0.184	—	2.6
	2	MSH2	—	0.189	—	3.0
	3	MSH3	—	0.186	—	2.7

The analytical result conducted by NASDA is 3.2[ESD]. The measurement result is slightly less than the analytical result.

The fluence in the ground simulation test is 10[ESD]. The fluence is greater than the flight environment.

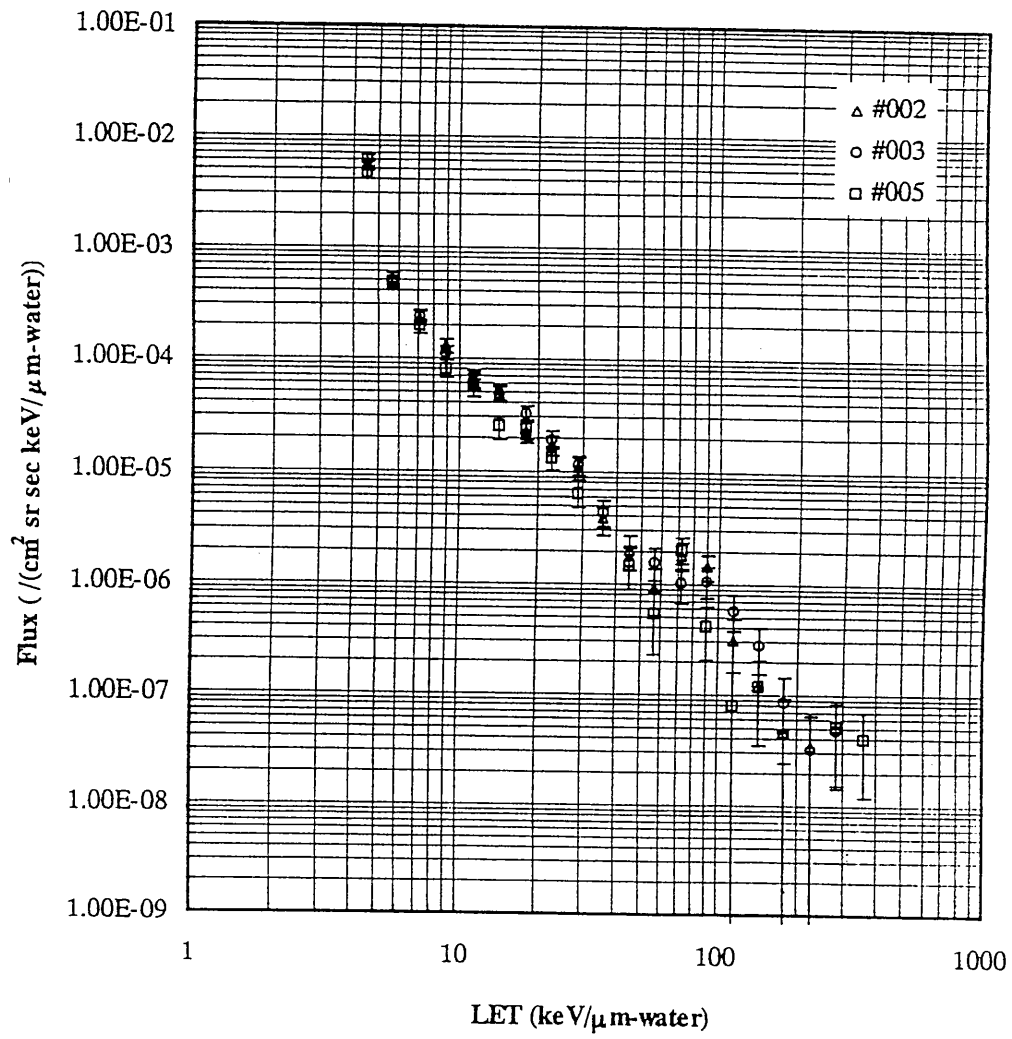


Fig. 5. 3 - 5 Distribution Data acquired in MFD/ESEM

Urethane based Film Calibration Curve

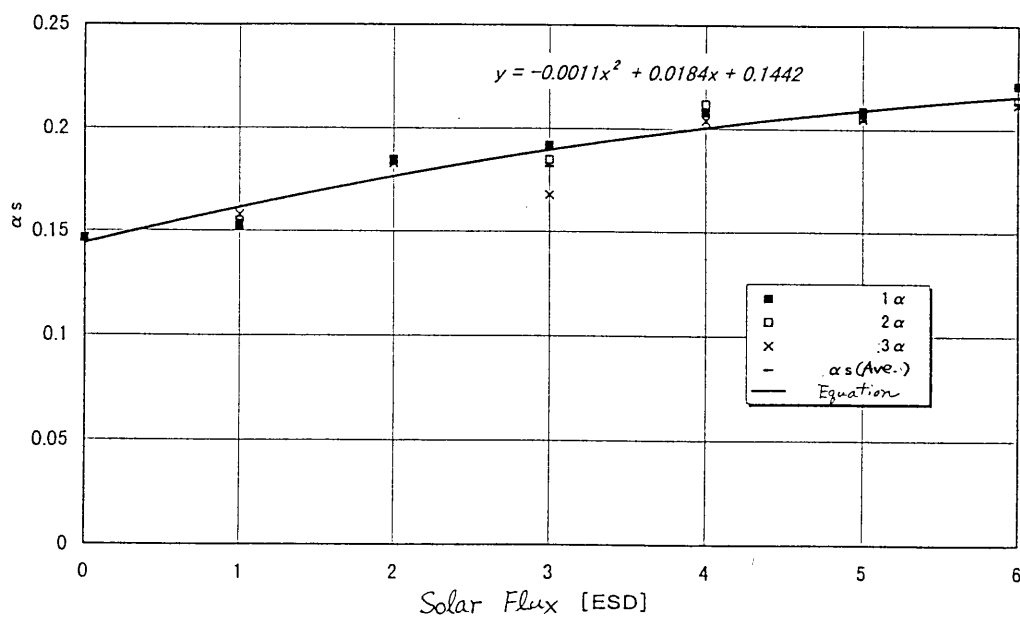
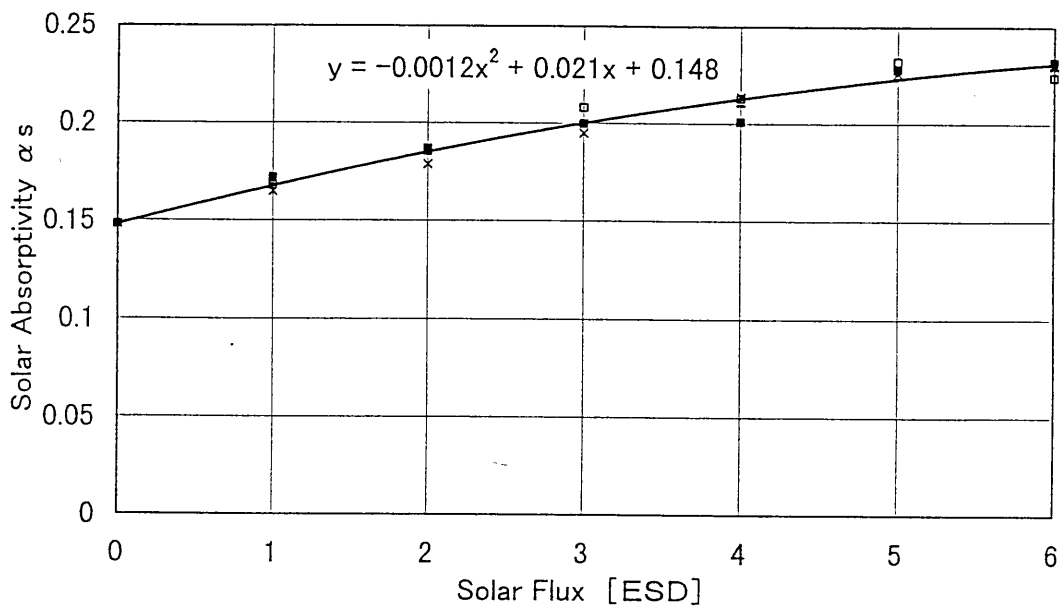


Fig5.3-6 MFD/ESEM Calibration Curve of Ultraviolet Monitor Material

5.4 Common Evaluation & Analysis of Installed Materials

5.4.1 Measurement of mass and surface thermal-optical properties

5.4.1.1 Measurement of mass

The mass of each sample was measured at Tsukuba Space Center.

(1) Samples

Samples are shown in Table 5.4-1.

(2) Equipment

(a) Vacuum Thermo - Micro-balance (3-3-245)

- Capacity : 1 g
- Accuracy : 1 ug

(b) Electrical Micro-balance (3-5-1227)

- Capacity : 3050 mg
- Accuracy : 1 ug

(c) Balance(3-3-349-24)

- Capacity : 160 g
- Accuracy : 0.1 mg

(3) Method

Each sample is exposed in the measuring room in more than 24 hours before measuring mass.

5.4.1.2 Surface thermal-optical properties

The surface thermal-optical properties of each sample was measured at Tsukuba Space Center.

(1) Samples

Samples are shown in Table 5.4-1.

(2) Equipment

(a) Solar Absorption(α s) Measuring equipment (3-3-262)

- Scanning wave-length : 250 through 2500 nm

- Measuring system : single beam system
- Scanning width : 1nm
- Accuracy of wave-length : +/- 0.5nm

(b) Vertical Infrared Emittance(ϵ_N) Measuring Equipment (3-5-1808)

- Measuring range : 0 through 100 %
- Accuracy : +/- 1 % (F.S.)
- Dimension of sample : more than 0.9 inch in diameter

(3) Method

Solar absorption and vertical infrared emittance of each sample are measured with (2)(a) and (b). respectively.

5.4.1.3 Result of Mass Measurement

Result of mass measurement is shown in Table 5.4-1.

5.4.1.4 Result of Surface Thermal-optical Properties Measurement

Result of surface thermal-optical properties measurement is shown in Table 5.4-1.

5.4.2 Summary of Surface Analysis Results

Surface analysis for the exposure samples was performed by Toray Research Center, Inc..

In this section, (#) means sample ID No. defined in Table 3.1-1.

5.4.2.1 Non-flammable Electrical Wire [TPI/PFA/cable conductor]

a) Sample

1: Non-flammable electrical wire

b) Appearance

OM

As is the case with the sample exposed to AO rays in the ground simulation test, the surface of the sample exposed to the space environment is found to be roughened. The sample exposed to EB and UV rays in the ground simulation test are found to be unchanged.

FE-SEM

The same is true as in the case of the observation under an OM.

c) Composition and bonding (ESCA)

The sample exposed to the space environment had an increased O/C value. The amount of groups, C-O, C=O, and COO, in C1s increased significantly. The sample exposed to AO and UV rays were more oxidized than the sample exposed to EB rays but less oxidized than the sample exposed to the space environment. Silicon compounds, such as SiO₂, were detected in the sample.

d) Chemical structure change (FT-IR)

In the sample exposed to the space environment, the amount of hydrocarbons decreased, and resin diffused. SiO₂ was detected in the sample.

e) Summary

The appearance and chemical composition significantly changed of the sample exposed to the space environment. In a ground comparison test, the sample exposed to AO rays deteriorated in nearly the same manner as the sample exposed to the space environment.

5.4.2.2 Epoxy Resin Adhesive

a) Sample

2-1: Epoxy resin adhesive for securing parts

b) Appearance

OM

As is the case with the sample exposed to AO rays in the ground simulation test, the sample exposed to the space environment is found to be roughened. The sample exposed to the EB and UV rays are found to be unchanged.

FE-SEM

The same is true as in the case of the observation under an OM.

c) Composition and bonding (ESCA)

The amount of groups, C-O, C=O, and COO, in C1s increased significantly. Similarly, oxidation had progressed in the sample exposed to AO and UV rays in the ground simulation test. The progress, however, was more slight, compared with the sample exposed to the space environment. Silicon compounds, such as SiO₂, were detected in the sample, especially the sample exposed to AO rays and the space environment. Besides surface contamination, the filler of the epoxy resin may have exposed.

d) Chemical structure change (FT-IR)

The sample exposed to the space environment deteriorated in nearly the same manner as the sample exposed to AO rays in the ground simulation test. Hydroxyl groups are found to have formed in all the sample exposed to AO, UV, and EB rays in the ground simulation test. We assume that hydrolysis, oxidation, and molecule chain cutting caused resin to deteriorate and diffuse and silica to expose.

e) Summary

The appearance and chemical composition significantly changed of the sample exposed to the space environment and AO rays in the ground simulation test. The appearance of the sample exposed to EB and UV rays changed slightly, but their chemical composition varied considerably.

5.4.2.3 Thermal Control Film [PI: Polyimide] and [ITO: Transparent electrodes/PI]

a) Sample

- 3-1: Thermal control film on acrylic adhesive tape for multilayer insulation
[PI (25 μm)/adhesive tape/Al plate]
- 4: Thermal control film without ITO [PI (25 μm)/Al (70 nm)/Ni]
- 5: Thermal control film with ITO [ITO (100 nm)/PI (25 μm)/Al (70 nm)]

b) Appearance

OM

PI surface (3-1, 4)

The PI surfaces of the sample exposed to the space environment and AO rays in the ground simulation test are found to be rougher than before exposure. The PI surfaces of the sample exposed to UV and EB rays in the ground simulation test, on the other hand, are not found to have changed.

ITO surface (5)

No difference is found between the exposed and controlled sample.

FE-SEM

PI surface (3-1, 4)

The PI surfaces of the sample exposed to the space environment and AO rays are found to be rougher than before exposure. The PI surface of the sample exposed to EB rays, on the other hand, is not found to have changed.

ITO surface (5)

No difference is found between the exposed and controlled sample.

c) Composition and bonding (ESCA)

PI surface (3-1, 4)

The composition of the sample 3-1 and 4 changed similarly.

That is, the surfaces of the sample exposed to the space environment and AO rays were oxidized markedly, and the amount of groups, COO (ester and carboxyl groups), C=O (carbonyl groups), and C-O (ether and hydroxyl groups), was found to have increased.

In the sample exposed to UV rays, the amount of groups, CON, COO, C=O, and C-O, including oxygen slightly decreased.

The sample exposed to EB rays was not found to significantly differ from the controlled sample.

ITO surface (5)

Irrespective of the type of rays which the sample 5 were exposed to, they were not found to significantly differ from each other in terms of the ratio of the amount of indium to that of tin and the chemical condition of indium and tin. The controlled sample and sample exposed to UV, AO, and EB rays in the ground simulation test and the space environment are arranged as follows in the order of increasing percentage of organic contaminants (composed mainly of hydrocarbons) in the surface:

Controlled < exposed to UV rays < exposed to AO rays < exposed to EB rays < exposed to the space environment

d) Chemical structure change (FT-IR) PI (3-1, 4)

The PI surfaces slightly deteriorated. No significant difference was found between the types of rays which the sample were exposed to. Amide bonds which formed due to imide ring cleavage, oxidized constituents such as carbonyl groups, and hydrocarbon and SiO₂ deposits were found in the surfaces of the sample.

ITO (5)

Deterioration due to oxidation (carbonyl group formation) and SiO₂ deposits were found in the ITO surface of the sample exposed to the space environment. In a ground comparison test, the chemical structures of the sample unnoticeably changed no matter what type of rays which the sample were exposed to.

e) Summary PI (3-1, 4)

The sample exposed to the space environment and AO rays markedly changed in appearance. The sample exposed to UV and EB rays, on the other hand, were not found to have changed in appearance.

A change in composition occurred only in the topmost layer. The sample exposed to the space environment and AO, UV, and EB rays were found to have more significantly changed in composition in that order.

ITO (5)

From the IR spectrum of the sample exposed to the space environment, carbonyl groups were found to have formed, and SiO₂ deposits were found using ESCA and IR. Except these findings, no change in appearance or composition was found irrespective of the type of rays which the sample were exposed to.

5.4.2.4 Paint

a) Sample

6-1 White paint [white paint/Al plate]

6-2 White paint [white paint/CFRP plate]

7-1 Black paint [black paint/Al plate]

7-2 Black paint [black paint/CFRP plate]

b) Appearance

OM

White paint (6-1, 6-2)

The surfaces of the sample exposed to the space environment and AO and UV rays are found to be rougher than before exposure. The sample exposed to EB rays is not found to have changed.

Black paint (7-1, 7-2)

The surfaces of the sample exposed to the space environment and AO rays are found to be rougher than before exposure. The sample exposed to EB and UV rays are not found to have changed.

FE-SEM

White paint (6-1, 6-2)

The sample exposed to the space environment and AO, UV, and EB rays are not found to have more significantly changed than the controlled sample.

Black paint (7-1, 7-2)

Particles are exposed on the surfaces of the sample exposed to the space environment and AO rays. Resin (urethane) appears to have disappeared. The sample exposed to EB and UV rays are not found to have changed.

c) Composition and bonding (ESCA)

White paint (6-1, 6-2)

The topmost surfaces of the sample exposed to the space environment and AO rays were found to have oxidized, thus producing functional siloxane (SiO_2). The percentage of carbon in the topmost surfaces of the sample exposed to the space environment and AO rays is assumed to have decreased. The surface composition and chemical condition of the sample exposed to EB and UV rays were almost the same as in the case of the controlled sample. The sample 6-1 (Al plates) and 6-2 (CFRP plates) changed in surface composition in the same manner.

Black paint (7-1, 7-2)

The amount of groups, COO and COON (ester, carboxyl groups, and urethane), were

found to have markedly decrease in the sample 7-1 (Al plates) exposed to the space environment and AO and UV rays. The surface composition and chemical condition of the sample exposed to EB rays were almost the same as in the case of the controlled sample. The controlled sample 7-2 (CFRP plate) greatly differed in terms of surface composition and chemical condition from the controlled sample 7-1. Much hydrocarbon as well as fluorine and chlorine was detected in the surface of the controlled sample 7-2. A higher concentration of oxygen was found in the sample 7-2 exposed to the space environment and AO rays, compared with the controlled sample 7-2. This is due to silicon oxide formation. The sample exposed to EB rays have a high concentration of fluorine, and the sample exposed to UV rays have a low concentration of silicon.

d) Chemical structure change (FT-IR)
White paint (6-1, 6-2)

In the sample 6-1 exposed to the space environment, the amount of silanol groups increased and carbonyl groups formed. However, the sample 6-1 slightly deteriorated (this is exceptional, but the reason is unknown). The sample 6-2 exposed to the space environment and the sample exposed to AO rays deteriorated most significantly. The sample exposed to UV and EB rays deteriorated to the same extent. In the sample exposed to the space environment and AO rays, molecules cross-linked, resin diffused, the amount of SiO₂ increased due to silicon resin deterioration, silanol groups formed, and oxidation and dehydrogenation reactions occurred. In the sample exposed to UV rays, oxidation reactions occurred. In the sample exposed to EB rays, resin diffused, the amount of SiO₂ increased due to silicon resin deterioration, and oxidation reactions occurred.

Black paint (7-1, 7-2)

The sample exposed to UV rays deteriorated most significantly of all the sample. The sample exposed to the space environment and AO rays deteriorated the second most significantly. The sample exposed to EB rays deteriorated slightly. In the sample exposed to UV and AO rays, the amount of SiO₂ increased due to resin diffusion, urethane bonds were cut, and oxidation and dehydrogenation reactions occurred. In the sample exposed to EB rays, oxidation and dehydrogenation reactions occurred.

e) Summary

Exposure to the space environment and AO rays caused white paint to deteriorate markedly. On the other hand, exposure to the space environment and UV and AO rays caused black paint to deteriorate significantly. How deterioration behavior varies with the type of rays may depend on the characteristics of silicone resin contained in white paint and those of

urethane resin contained in black paint. When exposed to EB rays, both white and black paint deteriorate slightly.

5.4.2.5 Cover Glass

a) Sample

10: Cover glass OCLI 0213 AR [MgF₂/glass]

11: Cover glass OCLI 0213 BRR [(SiO₂/Ta₂O₅)/glass]

12: Cover glass OCLI 0213 AR+CC [ITO/MgF₂/glass]

13: Cover glass PPE CMX AR [MgF₂/glass]

b) Appearance

FE-SEM

AR (10, 13)

The sample exposed to the space environment and AO, UV, and EB rays are not found to differ noticeably from the controlled sample.

BRR (11)

The sample exposed to the space environment and AO, UV, and EB rays are not found to differ noticeably from the controlled sample.

AR+CC (12)

The sample exposed to the space environment and AO, UV, and EB rays are not found to differ noticeably from the controlled sample.

c) Composition and bonding (ECSA)

The sample exposed to the space environment was found to have SiO₂ deposited on it.

AR (10, 13)

Like the sample exposed to UV and EB rays, the sample exposed to the space environment was found to have magnesium-fluorine bonds in MgFx (x < 2) cut. The number of cuts in the sample 10 exposed to the space environment was almost equal to that of cuts in the sample 10 exposed to UV rays and larger than that of cuts in the sample 10 exposed to EB rays. The number of cuts in the sample 13 exposed to the space environment was larger than that of cuts in the sample 13 exposed to UV rays, and the latter number was larger than that of cuts in the sample 13 exposed to EB rays. Although MgFx molecules in the sample exposed to AO rays were not found to have significantly changed, the concentration of oxygen in the surfaces of the sample were higher, compared with the other sample.

BRR (11)

The sample exposed to the space environment and AO, UV, and EB rays are not found to differ noticeably from the controlled sample.

AR+CC (12)

Magnesium and fluorine, the constituents of MgF_x ($x < 2$), were detected in the sample exposed to the space environment and the controlled sample. On the other hand, indium, tin, and oxygen, the constituents of ITO, were detected in the sample exposed to EB and UV rays.

d) Element analysis in the direction of depth (AES)
AR (10, 13)

Oxygen was detected in the MgF_2 film of all the sample 10 including the controlled sample. The amount of oxygen in the MgF_2 film of the sample 10 exposed to AO, EB, and UV rays and the controlled sample was less than the lower limit of detection.

Oxygen was detected in the sample exposed to the space environment.

BRR (11)

A comparison did not find any difference between the SiO_2 films, the first layers, of the sample exposed to the space environment and AO, UV, and EB rays and the controlled sample.

AR+CC (12)

An ITO layer was found in the MgF_x film, the outermost layer, of the controlled sample and the sample exposed to AO rays. Although an ITO film was detected in the outermost layer of the sample exposed to EB and UV rays, no MgF_x film was found between the topmost layer and glass substrate. The sample exposed to the space environment consists of MgF_x film and glass. No ITO constituents were detected in the sample exposed to the space environment.

e) Summary

No sample were found to have changed due to exposure to the space environment and AO, UV, and EB rays.

The chemical composition may differ from sample to sample.

AR (10, 13)

The concentration increased of oxygen in the topmost surface of the sample exposed to AO rays. The concentration decreased of oxygen in the surface of MgF_x [$x < 2$] film of the sample exposed to UV and EB rays. Oxygen was detected in the MgF_x film of all the four sample 10 including the controlled sample. Oxygen was detected in the MgF_x film of the sample 13 exposed to the space environment. The amount of oxygen in the MgF_x film of the sample 10 exposed to AO, EB, and UV rays and the controlled sample was less than the lower limit of detection.

BRR (11)

The sample exposed to the space environment and AO, UV, and EB rays were not found to differ noticeably from the controlled sample.

AR+CC (12)

We found that the controlled sample and the sample exposed to AO rays consist of MgFx [$x < 2$], ITO, and glass, that the sample exposed to EB and UV rays consist of ITO and glass, and that the sample exposed to the space environment consists of MgFx [$x < 2$] and glass.

5.4.2.6 Inter-connector Materials

a) Sample

14: Inter-connector material Ag

15: Inter-connector material Ag-X

16: Inter-connector material Ag/

b) Appearance

OM

Brown or black film is found on the exposed surface and its opposite surface of the sample exposed to the space environment and AO rays.

FE-SEM

Film produced by exposure to AO rays was in various forms, including a complex fine structure and a conglomeration of needle-like particles. Some surfaces which exposed due to film flaking have a grain boundary structure (sample 14 and 16); the others have a rough texture as if they were eroded (sample 15). The sample exposed to the space environment also had a similar texture.

c) Detection of elements in surface layer (XMA)

Only silver and carbon were detected in portions of the controlled sample and sample exposed to AO rays, portions from which film flaked off. Silver, oxygen, and carbon were detected in the film of the sample exposed to AO rays. There is no significant difference in level of detection of silver and carbon between the sample exposed to AO rays and the controlled sample. Thus the film detected in the sample exposed to AO rays is assumed to be a silver oxide.

Silver, oxygen, sulfur, and carbon were detected in the sample exposed to the space environment. We consider that a silver oxide or a silver sulfide formed.

e) Summary

Brown or black film found in the sample exposed to AO rays is a silver oxide.

A discolored substance found in the sample exposed to the space environment is a silver oxide or a silver sulfide.

5.4.2.7 OSR

a) Sample

17: OSR OCLI 0213 SSM [(SiO₂/Ta₂O₅)/Ag (50 nm)]

18: OSR PPE CMX SSM [glass (0.1 mm)/Ag (50 nm)]

b) Appearance
FE-SEM

No change is found which is due to exposure to the space environment or rays.

c) Composition and bonding (ESCA)

The topmost surface of a sample 17 is composed of SiOx. The concentration of oxygen in the sample exposed to AO rays increased more than that of oxygen in the controlled sample. No significant difference in oxygen concentration was found between the sample exposed to the space environment and EB and UV rays and the controlled sample. A small amount of potassium and nitrogen was detected only in the sample exposed to the space environment.

Ten or more elements, including silicon, oxygen, sodium, and cerium, were found in the surface of a sample 18. The sample exposed to the space environment has a high concentration of SiO₂ probably because SiO₂ deposited or SiO₂ contained in the base exposed. In a ground comparison test, no noticeable change was found except that fluorine was detected only in the controlled sample and that the sample exposed to AO rays had a high concentration of nickel.

d) Element analysis in the direction of depth (AES)

The sample 17 exposed to different types of rays had different layer arrangements. The sample exposed to the space environment and AO rays and the controlled sample had laminated film consisting of (Si+O) and (Ta+O) layers while the sample exposed to EB and UV rays had film consisting of only one (Si+O) layer 1 μm or more thick. The (Si+O) layer was not found to have changed due to exposure to the space environment or rays.

The constituents of a sample 18 were silicon, oxygen, boron, and cerium. The sample 18 were not found to have changed due to exposure to the space environment or rays. Nickel and copper were detected in the surfaces of the sample exposed to AO and EB rays. Fluorine was detected only in the controlled sample.

e) Summary

We found no change due to exposure to rays.

5.4.2.8 Aluminum Deposited β Cloth

a) Sample

19: Aluminum deposited β cloth [β cloth/Al plate]

b) Appearance

OM

No change is found which is due to exposure to the space environment.

FE-SEM

Fibers are exposed on the surface of the sample exposed to AO rays. The surface of the sample exposed to the space environment is somewhat rough. The sample exposed to EB and UV rays are not found to have changed.

c) Composition and bonding (ESCA)

Organic contaminants composed mainly of hydrocarbons are assumed to be on the surface of the controlled sample. For the sample exposed to AO rays, carbon-fluorine bonds in Teflon constituents are found to be cut. Fluorine produced by decomposition may have partly combined with calcium to form calcium fluoride. Some of the carbon-fluorine bonds contained in the sample exposed to the space environment have been cut. This change is intermediate between the change in the controlled sample and the change in the sample exposed to the AO rays. For the sample exposed to UV rays, Teflon is exposed. Based on this finding, organic contaminants appear to have been removed from the topmost surface. The surface composition and chemical condition of the sample exposed to EB rays were almost the same as in the case of the controlled sample.

d) Chemical structure change (FT-IR)

Exposure to rays caused Teflon resin to diffuse. The sample exposed to AO rays underwent the highest degree of Teflon resin diffusion of all the samples. The degree of Teflon resin diffusion was nearly the same for the sample exposed to EB and UV rays. The sample exposed to the space environment deteriorated slightly. When the parameter of deterioration is defined as the ratio of the absorption of Teflon resin (1147 cm^{-1}) to that of glass (875 cm^{-1}), the parameters for the controlled sample and the sample exposed to the space environment and EB, UV, and AO rays become progressively smaller in that order. The degrees of deterioration for the sample become smaller in the reverse order.

e) Summary

Exposure to AO rays caused the most serious deterioration. Exposure to the space environment and EB and UV rays caused deterioration to some extent.

5.4.2.9 Bonded MoS₂ film, Binder for bonded MoS₂ film

a) Sample

- 20-1: Bonded MoS₂ film HBM34 film [MoS₂, additive, binder]
21-1: Binder for bonded MoS₂ film Polyamideimide film A (1) [thermoplastic]
22-1: Binder for bonded MoS₂ film Polyamideimide film B (2) [thermoset]
23-1: Binder for bonded MoS₂ film Polyimide (3) [amide, containing PTFE]

b) Appearance

OM

20 HMB 34 film

No effects are found of exposure to the space environment or rays (AO rays only).

21-1: Polyamideimide film A (1), 22-1: Polyamideimide film B (2), and 23-1: Polyimide (3)

The surfaces of the sample exposed to the space environment and AO rays became rougher. EB and UV rays are not found to have affected the sample.

FE-SEM

The same is true as in the case of the observation under an OM.

c) Composition and bonding (ECSA)

20: HBM34 film

The surfaces of the sample exposed to the space environment and AO rays are oxidized more, compared with the controlled sample. This is partly because the amount of groups, C-O, C=O, and COO, increased. In the sample exposed to the space environment and the controlled sample, sulfur is mainly in the form of MoS₂. Sulfur contained in the sample exposed to AO rays was partly oxidized, so that SO₄²⁻ ions formed.

21-1: Polyamideimide film A (1) and 22-1: Polyamideimide film B (2)

In addition to carbon, nitrogen, and oxygen, fluorine was detected in the sample including the controlled sample but excluding the sample exposed to UV rays. Fluorine was in the form of a combination with carbon, but it is unknown how the combination formed. Impurities, such as sulfur and silicon, were detected in some of the sample. Inorganic elements, including titanium, iron, copper, and calcium, were also detected in the samples exposed to the space environment and AO rays. Organic contaminants composed mainly of hydrocarbons may have been removed from the surface of the sample exposed to EB rays, so that its inside exposed. In the sample exposed to UV rays, organic fluorine is assumed to have separated from it. Fluorine, which should not be contained in the sample, was really detected in them, so it is difficult to determine how the structures of the sample changed.

23-1: Polyimide (3)

Because much deposit was on the sample exposed to the space environment and AO rays, they were difficult to compare with other sample. The surface composition and chemical condition of the sample exposed to EB rays was the same as in the case of the controlled sample. In the sample exposed to UV rays, organic fluorine on the surface is assumed to have partially separated from it.

d) Chemical structure change (FT-IR) 20: HMB34 film

HMB34 film did not deteriorate severely due to exposure to the space environment or AO rays. In the film, amide group molecular chains broke, imide rings cleaved, and carbonyl groups formed.

21-1: Polyamideimide film A (1) and 22-1: Polyamideimide film B (2)

No imide rings or amide groups were not particularly found to have deteriorated.

23-1: Polyimide (3)

No imide rings or amide groups were not found to have markedly deteriorated. The amount of carbonyl groups and that of organic fluorine compounds were found to have increased.

e) Summary

No change was found in the appearance of the sample 20 exposed to the space environment or AO rays. Findings from the sample 20 are advanced surface oxidation (formation of groups, C-O, C=O, and COO), broken molecular chains in amide groups, imide ring cleavage, and carbonyl formation. In the sample exposed to AO rays, sulfur oxidation progressed (SO_4^{2-} ions formed).

The 21-1 polyamideimide film A (1), 22-1 polyamideimide film B (2), and 23-1 polyimide (3) sample exposed to the space environment and AO rays were found to be rougher than before exposure. The composition of the sample exposed to AO, EB, or UV rays was not found to have markedly changed; that is, no amide groups or imide rings were found to have deteriorated (because the 21-1, 22-2, and 23-1 sample contained many contaminant elements, it was difficult to determine from their surfaces whether or not their chemical structure changed).

5.4.2.10 Silica FRP

a) Sample

24-1: Silica FPR [silica cloth, phenol resin]

b) Appearance

OM

Fibers are exposed on the surface of the sample exposed to the space environment and AO rays. The sample exposed to EB and UV rays are not found to have noticeably changed.

FE-SEM

The same is true as in the case of the observation under an OM.

c) Surface composition, bonding, and depth composition (ESCA)

In addition to carbon, oxygen, silicon, and nitrogen, fluorine was detected in the sample. The amount of fluorine in the sample exposed to the space environment is smaller, compared with the other sample. The composition of the sample exposed to the space environment somewhat differs from that of the controlled sample and the sample exposed to AO, UV, and EV rays. The sample exposed to AO and EB rays contain a little larger amount of C-O (ether and hydroxyl groups) and C-N (organic nitrogen) constituents than the controlled sample. The sample exposed to UV rays was found to have slightly changed.

For depth composition, the amount of silicon and oxygen in the sample exposed to the space environment was larger, compared with the controlled sample and the sample exposed to AO, UV, and EB rays.

d) Chemical structure change (FT-IR)

SiO₂ exposed noticeably on the surfaces of the sample exposed to the space environment and AO rays because resin diffused. In the sample exposed to EB and UV rays, it was found that the amount of amide groups had slightly decreased and that some carbonyl groups had formed.

e) Summary

The sample exposed to the space environment and AO rays were found to have deteriorated most significantly of all the sample.

5.4.2.11 Silicone adhesive

a) Sample

25: RTV-S691 [silicone resin]

b) Appearance

OM

No change was found which is due to exposure to the space environment or rays.

FE-SEM

No change was found which is due to exposure to the space environment or rays.

c) Composition and bonding (ESCA)

The topmost surfaces of the sample exposed to the space environment and AO rays oxidized and functional siloxane (SiO_2) formed. The percentage of carbon in the surfaces of the sample decreased which were exposed to the space environment and AO rays. Oxidation, SiO_2 formation, and carbon percentage reduction were more noticeable for the sample exposed to the space environment than for the sample exposed to AO rays. The surface composition and chemical condition of the sample exposed to EB and UV rays were almost the same as in the case of the controlled sample.

d) Chemical structure change (FT-IR)

Deterioration due to exposure to rays went to a small extent. For sample exposed to the space environment and AO rays, signs of deterioration include crosslinkage between molecules, resin diffusion, an increase in the amount of SiO_2 due to silicone resin deterioration, silanol group formation, and oxidation and dehydrogenation reactions. For a sample exposed to EB rays, signs of deterioration include resin diffusion, an increase in the amount of SiO_2 , and oxidation reactions. For a sample exposed to UV rays, signs of deterioration include oxidation reactions.

e) Summary

No noticeable change was found which is due to exposure to rays. In the sample exposed to the space environment and AO rays, which changed most significantly, silicone resin deterioration probably caused the amount of SiO_2 to increase.

5.4.2.12 Flexible OSR

a) Sample

26: Flexible OSR [ITO/CeO_x/PEL/Ag/Ni]

b) Appearance

FE-SEM

No change was found which is due to exposure to the space environment or rays.

c) Composition and bonding (ESCA)

No significant difference in the ratio of the amount of indium to that of tin was found between the sample, no matter what type of rays they were exposed to.

Organic contaminants composed mainly of hydrocarbons were found on the surfaces of the sample. Nitrogen and silicon (in the form of SiO₂) were detected in the sample exposed to the space environment.

d) Chemical structure change (FT-IR)

Deterioration was minor which is due to exposure to the space environment and rays. No significant difference was found between the types of rays which the sample were exposed to. The amount of carbonyl groups in the sample exposed to the space environment was found to have increased.

e) Summary

Little deterioration was found which is due to exposure to the space environment or rays.

5.4.2.13 Sputtered MoS₂ film

a) Sample

27-1: Sputtered MoS₂ film [MoS₂/SUS440C, RF sputtering, water-cooling], exposed completely

27-2: Sputtered MoS₂ film [MoS₂/SUS440C, RF sputtering, water-cooling], exposed partially

27-3: Controlled sample

28-1: Sputtered MoS₂ film [MoS₂/SUS440C, RF sputtering], exposed completely

28-2: Sputtered MoS₂ film [MoS₂/SUS440C, RF sputtering], exposed partially

28-3: Controlled sample

29-1: Sputtered MoS₂ film [MoS₂/SUS440C, ECR], exposed completely

29-2: Sputtered MoS₂ film [MoS₂/SUS440C, ECR], exposed partially

29-3: Controlled sample

b) Appearance
OM

No change was found which is due to exposure to the space environment.

FE-SEM

No change was found which is due to exposure to the space environment.

c) Element analysis in the direction of depth (AES)

Composition of the topmost layer of film (a few nanometers thick)

Besides molybdenum, sulfur, carbon, and oxygen, silicon was detected in sample 27-2, 28-2, and 29-2 exposed to the space environment. The concentration of oxygen in the topmost surfaces of the sample 27-1, 28-1, and 29-1 exposed to AO rays and the sample 29-2 exposed to the space environment was found to have increased.

The concentration of sulfur in the topmost surfaces of the sample 27-1 and 29-1 exposed to AO rays decreased significantly.

Composition of surface layer (tens of nanometers thick) through inside layer (hundreds of nanometers thick)

In the surface layer (tens of nanometers thick) of the sample 27-2 exposed to the space environment, the concentration of oxygen increased as in the surface layer of the sample 27-1 (with a close-knit film structure) exposed to AO rays. No noticeable difference was found between the sample 27-1 exposed to AO and UV rays and the controlled sample.

The concentration of oxygen in the surface layer (tens of nanometers thick) of the sample 28-2 increased which was exposed to the space environment. The concentration of

oxygen in the sample 28-1 exposed to AO and UV rays was higher, compared with the controlled sample. The concentration of oxygen in the controlled sample 28-1 was lower than that of oxygen in the controlled sample 27-1.

The MoS layer thickness at point 2 on the sample 29-2 exposed to the space environment was found to be equivalent to an SiO₂ thickness of 800 nm. The [Mo+S] layers of the sample 29-1 exposed to AO and UV rays and the controlled sample 29-1 were found to be thinner at point 2 (on the marked side) than at point 1 (opposite to the marked side).

No noticeable difference was found between the sample 29-1 exposed to AO and UV rays and the controlled sample 29-1.

d) Summary

In addition to molybdenum, sulfur, carbon, and oxygen, silicon was detected in the sample exposed to the space environment.

As is the case with the sample 27-1 and 28-1 exposed to AO rays, the concentration of oxygen increased in the surface layers of the sample 27-2 and 28-2 exposed to the space environment.

The concentration of oxygen in the inside layer of the controlled sample 27-1 (with a close-knit structure) was a little higher, compared with the controlled sample 28-1 (having a little lower layer density than the controlled sample 27-1). The concentration of oxygen in the films of the sample 27-1 did not change through exposure to rays, while the concentration of oxygen in the films of the sample 28-1 increased.

The concentration of oxygen in the controlled sample 29-1 was equal to that of oxygen in the controlled sample 28-1. The concentration of oxygen in the sample 29-1 was not found to have changed due exposure to rays.

The MoS layer thickness at point 2 on the sample 29-2 exposed to the space environment was equivalent to an SiO₂ thickness of 800 nm.

5.4.2.14 Action of atomic oxygen (O^3p electron at ground state) on materials

We are attaching this clause as a reference in determining the mechanism on the deterioration.

We have to notice you that this contents are summary of a few papers selected from the papers that NASA researchers have reported⁸⁻¹²⁾, and do not cover all the information in this field.

As a result of discussing the collected data at EOIM-III, the reaction efficiency of polyimide, Kapton, was calculated, and as a result, the value of $3.1 \times 10^{-24} \text{ cm}^3/\text{atom}$ was derived, from the weight loss and profilemetry when an oxygen fluence was $3 \times 10^{30} \text{ atoms/cm}^2$. Gas released from the reaction between Kapton labeled with C^{13} and atomic oxygen was subjected to mass spectrometry, and as a result, CO, CO₂, H₂O, NO and NO₂ were identified.

Aromatic polymers showed lower reaction efficiency than linear hydrocarbon polymers (Polyethylene $Re = 4.4 \times 10^{-24} \text{ cm}^3/\text{atom}$, Polypropylene $Re = 5.5 \times 10^{-24} \text{ cm}^3/\text{atom}$). Fluorine-substituted linear hydrocarbon polymers showed low reaction efficiency (TFE Teflon $Re = 0.06 \times 10^{-24} \text{ cm}^3/\text{atom}$, FEP Teflon $Re = 0.05 \times 10^{-24} \text{ cm}^3/\text{atom}$). The difference in the reaction efficiency is interpreted by that the rate-determining stage for atomic oxygen in the reaction is in hydrogen abstraction (Lower probability for abstracting fluorine atom). However, the reaction efficiency of fluorine-based polymers would be slightly increased when ultraviolet rays as well as atomic oxygen is applied. An aromatic polymer that exceptionally shows a higher reaction efficiency is CR 39 Polycarbonate ($Re = 6.1 \times 10^{-24} \text{ cm}^3/\text{atom}$). Eypel-F Poly (bistrifluoropropyl-phosphazene) showed a very low reaction efficiency ($Re < 0.03 \times 10^{-24} \text{ cm}^3/\text{atom}$).

The effect of the collision velocity of atomic oxygen was investigated. In the reactions of atomic oxygen having various average kinetic energies (0.04 eV, 0.1 eV, 1.5 eV, 2.8 eV, 5.2 eV) with Kapton, actual measurements of the reaction efficiency of the atomic oxygen were analyzed, and an excitation barrier of the atomic oxygen in Kapton is approximately 0.3 eV. The following is reported¹⁰⁾: The reaction efficiency of Kapton to the atomic oxygen having a kinetic energy of 0.3 eV or more is increased, compared with to the atomic oxygen having a kinetic energy less than 0.3 eV, while the reaction efficiency of Kapton is constant to the atomic oxygen having a kinetic energy of 0.3 eV or more. As the source of atomic oxygen, Flowing discharge gas [average kinetic energy = 0.065 eV], HVAB [high-velocity neutral-atom beam: average kinetic energy = 0.44, 0.72, 0.79, 2.1 eV] and LEO [Low Earth Orbit: average kinetic energy = 5.6 eV] of LANL HVAB [Los Alamos National Laboratory] were selected, and the actual measurements of the reaction efficiency of each AO source and Kapton were obtained^{8,9)}.

Two models for calculating the reaction efficiency were discussed, and Bekerle-Ceyer Model has been proved to be compatible with actual measurements.

Beckerle-Ceyer Model is expressed by the following equation,

$$Re = \int A \cdot f(Et) \cdot \{1 + \exp[-n(Et - Ea)]\}^{-1} d(Et)$$

where,

- Re: reaction efficiency,
- A: the limiting reaction efficiency at high kinetic energies,
- f(Et): the normalized kinetic energy distribution function,
- Et: kinetic energy, and
- Ea: the magnitude of the energetic barrier to reaction.

First, Re's at the four HVAB energies, [Et = 0.44, 0.72, 0.79, 2.1 eV] were actually measured severally, and the following values were determined through the curve fitting from the measurements of Re; $A = 3.7 \times 10^{-24}$ cm³/atom, n = 10, Ea = 0.98 eV, and $\Delta = 0.008$.

The small residual sum of squares, Δ , means a good focusing, and the values of A and Ea are proper.

Reaction efficiencies, Re, in the energy zone of the flowing discharge gas [average kinetic energy = 0.065 eV], and LEO [average kinetic energy = 5.6 eV] were calculated by the use of the above parameters severally, and as a result, Beckerle-Ceyer Model reproduced the measurements.

As described above, in NASA, various organic materials have been analyzed minutely revolving around the analysis of the effects of atomic oxygen on Kapton polyimide.

Other materials, however, should be studied in the same manner that Kapton was analyzed. Furthermore, the following unsolved subject would be an important theme in future; the effects of various functional groups bonded to a main chain in aromatic polymers including Kapton, linear hydrocarbon polymers, or fluorine-substituted polymers in the process that the polymers are deteriorated under atomic oxygen, ultraviolet rays, or electron beam.

It may be meaningful to discriminate the effects of each excitation source in the complex environment comprised of atomic oxygen, ultraviolet rays and electron beam.

It will be require in studying above described items to select clean test samples that their chemical structures have been already identified, and to develop such irradiation equipment that permits an excitation source to be used as a monochromatized energy. In addition, it is desirable to combine irradiation equipment with various physical testing machines and various analytical instruments for evaluating samples in situ.

Table 5. 4-1 (1/2) Result of Mass and Surface Thermal Properties

No.	Material	S/N	Solar Absorption				Vertical Infrared Emissivity				Mass			
			Pre-flight (A)	Post-flight (B)	(B)-(A)	(B)-(A) (A)	Pre-flight (A)	Post-flight (B)	(B)-(A)	(B)-(A) (A)	Pre-flight (A)	Post-flight (B)	(B)-(A)	(B)-(A) (A)
1	Non-flammable Electrical Wire	1									0.9231	0.9235	0.0004	0.04%
		2									0.9244	0.9231	-0.0013	-0.14%
		3									0.9235	0.9234	-0.0001	-0.01%
		4									0.9242	0.9241	-0.0001	-0.01%
		5									0.9253	0.9250	-0.0003	-0.03%
		6									0.9238	0.9238	0.0000	0.00%
		7									0.9192	0.9200	0.0008	0.09%
		8									0.9267	0.9267	0.0000	0.00%
		9									0.9164	0.9164	0.0000	0.00%
		10									0.9271	0.9275	0.0004	0.04%
		11									0.9210	0.9210	0.0000	0.00%
		12									0.9250	0.9248	-0.0002	-0.02%
		13									0.9220	0.9219	-0.0001	-0.01%
		14									0.9203	0.9196	-0.0007	-0.08%
		15									0.9192	0.9204	0.0012	0.13%
		16									0.9261	0.9256	-0.0005	-0.05%
		17									0.9211	0.9211	0.0000	0.00%
2	Epoxy Resin adhesive	26									1532.692	1532.088	-0.604	-0.04%
3	Acrylic Resin adhesive tape	39	0.342	0.370	0.028	8.19%	0.659	0.633	-0.026	-3.95%	1395.633	1394.935	-0.698	-0.05%
4	Thermal Control Film without ITO (Polyimide/Al/Ni)	49	0.334	0.382	0.048	14.37%	0.649	0.627	-0.022	-3.39%	28.383	27.123	-1.260	-4.44%
		410	0.329	0.383	0.054	16.41%	0.652	0.625	-0.027	-4.14%	28.820	27.629	-1.191	-4.13%
		411	0.332	0.381	0.049	14.76%	0.646	0.626	-0.020	-3.10%	28.269	26.825	-1.444	-5.11%
5	Thermal Control Film with ITO (Polyimide/Al/Ni/ITO)	59	0.350	0.349	-0.001	-0.29%	0.472	0.428	-0.044	-9.32%	29.488	29.089	-0.399	-1.35%
		510	0.350	0.350	0.000	0.00%	0.475	0.481	0.006	1.26%	29.358	29.351	-0.007	-0.02%
		511	0.354	0.353	-0.001	-0.28%	0.466	0.476	0.010	2.15%	28.785	28.784	-0.001	0.00%
6	White Paint	27	0.270	0.278	0.008	2.96%	0.873	0.872	-0.001	-0.11%	1902.348	1902.305	-0.043	0.00%
		28	0.271	0.278	0.007	2.58%	0.872	0.874	0.002	0.23%	1887.231	1887.182	-0.049	0.00%
	(White Paint/Al)	26	0.311	0.320	0.009	2.89%	0.854	0.852	-0.002	-0.23%	1855.262	1855.221	-0.041	0.00%
		9	0.329	0.338	0.009	2.74%	0.884	0.882	-0.002	-0.23%	1372.681	1373.072	0.391	0.03%
	White Paint	10	0.326	0.337	0.011	3.37%	0.883	0.882	-0.001	-0.11%	1365.992	1366.495	0.503	0.04%
		11	0.334	0.342	0.008	2.40%	0.884	0.884	0.000	0.00%	1336.611	1333.884	-2.727	-0.20%
7	Black Paint	67	0.946	0.970	0.024	2.54%	0.893	0.902	0.009	1.01%	1787.780	1787.402	-0.378	-0.02%
		71	0.945	0.969	0.024	2.54%	0.893	0.902	0.009	1.01%	1801.438	1801.101	-0.337	-0.02%
	(Black Paint/Al)	97	0.944	0.984	0.040	4.24%	0.880	0.897	0.017	1.93%	1765.492	1765.126	-0.366	-0.02%
		77	0.945	0.968	0.023	2.43%	0.895	0.905	0.010	1.12%	1286.813	1286.578	-0.235	-0.02%
	Black Paint	78	0.945	0.968	0.023	2.43%	0.896	0.905	0.009	1.00%	1328.342	1327.919	-0.423	-0.03%
		79	0.945	0.971	0.026	2.75%	0.897	0.906	0.009	1.00%	1325.699	1325.613	-0.086	-0.01%
10	Cover Glass OCLI 0213 AR	B-1-1									59.992	59.992	0.000	0.00%
11	Cover Glass OCLI 0213 UVR	B-1-2									60.209	60.209	0.000	0.00%
12	Cover Glass OCLI 0213 AR+CC	B-2-1									56.357	56.349	-0.008	-0.01%
13	Cover Glass PPE CMX AR	B-2-2									55.594	55.587	-0.007	-0.01%
14	Interconnector Ag	C-1-1									29.595	29.688	0.093	0.31%
15	Interconnector Ag-X	C-1-2									26.156	26.233	0.077	0.29%
16	Interconnector Ag(Au coating)	C-1-3									25.577	25.663	0.086	0.34%
17	OSR OCLI 0213 SSM	B-3-1									42.680	42.683	0.003	0.01%
18	OSR PPE CMX SSM	B-3-2									52.541	52.541	0.000	0.00%

Remarks	Unit	
		:g
		:mg

Table 5. 4-1 (2/2) Result of Mass and Surface Thermal Properties

Material		Solar Absorption				Vertical Infrared Emissivity				Mass				
		Pre-flight (A)	Post-flight (B)	(B)-(A)	(B)-(A) (A)	Pre-flight (A)	Post-flight (B)	(B)-(A)	(B)-(A) (A)	Pre-flight (A)	Post-flight (B)	(B)-(A)	(B)-(A) (A)	
19	Al deposited β-cloth	1910	0.360	0.361	0.001	0.28%	0.907	0.907	0.000	0.00%	14.1852	14.1852	0.0000	0.00%
		1911	0.354	0.361	0.007	1.98%	0.906	0.907	0.001	0.11%	14.1759	14.1758	-0.0001	0.00%
20	Bonded MoS2 film (HMB34 Coat) φ25	205									5.2427	5.2431	0.0004	0.01%
		206									5.2730		-5.2730	-100.00%
		L201									13.0934	13.0939	0.0005	0.00%
		L202									13.0400		-13.0400	-100.00%
		L203									13.1060		-13.1060	-100.00%
21	Binder for bonded MoS2 film Polyamideimide A φ40	S216									5.1356	5.1348	-0.0008	-0.02%
		S217									5.1184		-5.1184	-100.00%
		S218									5.1200		-5.1200	-100.00%
		S219									5.1011		-5.1011	-100.00%
		S2110									5.1215		-5.1215	-100.00%
		215									13.0835	13.0805	-0.0030	-0.02%
		216									12.7869		-12.7869	-100.00%
		217									12.9903		-12.9903	-100.00%
22	Binder for bonded MoS2 film Polyamideimide B φ25	S226									5.1311	5.1300	-0.0011	-0.02%
		S227									5.1111		-5.1111	-100.00%
		S228									5.1127		-5.1127	-100.00%
		S229									5.1154		-5.1154	-100.00%
		S2210									5.1118		-5.1118	-100.00%
		225									13.0807	13.0773	-0.0034	-0.03%
		226									13.0327		-13.0327	-100.00%
		227									13.0872		-13.0872	-100.00%
23	Binder for bonded MoS2 film Polyimide φ25	S236									5.1294	5.1288	-0.0006	-0.01%
		S237									5.1308		-5.1308	-100.00%
		S238									5.1477		-5.1477	-100.00%
		S239									5.1403		-5.1403	-100.00%
		S2310									5.1233		-5.1233	-100.00%
		235									13.1527	13.151	-0.0017	-0.01%
		236									13.1252		-13.1252	-100.00%
		237									13.1135		-13.1135	-100.00%
24	SiFRP φ32 1t	S247	0.665	0.68	0.015	2.26%	0.892	0.899	0.007	0.78%	1422.204	1418.616	-3.588	
		S248	0.665	0.687	0.022	3.31%	0.892	0.900	0.008	0.90%	1444.839	1440.716	-4.123	
		247	0.653	0.671	0.018	2.76%	0.891	0.897	0.006	0.67%	5.7069	5.6927	-0.0142	-0.25%
		248	0.657	0.675	0.018	2.74%	0.893	0.899	0.006	0.67%	5.7369	5.7216	-0.0153	-0.27%
25	Silicone adhesive (RTV-S691)	255									1277.639	1277.847	0.208	0.02%
		256									1278.272	1273.882	-4.390	-0.34%
		257									1271.992	1270.504	-1.488	-0.12%
26	Flexible OSR	265	0.166	0.165	-0.001	-0.60%	0.815	0.812	-0.003	-0.37%	80.708	80.801	0.093	0.12%
		266	0.166	0.167	0.001	0.60%	0.814	0.814	0.000	0.00%	80.903	80.993	0.090	0.11%
		267	0.165	0.163	-0.002	-1.21%	0.809	0.810	0.001	0.12%	75.904	75.990	0.086	0.11%
27	Sputtered MoS2 film (RF sputtering, Cooling method))	0010									14.3622	14.3627	0.0005	0.00%
		0016									14.3413	14.4081	0.0668	0.47%
28	Sputtered MoS2 film (RF sputtering, No cooling method))	0003									14.3588	14.3591	0.0003	0.00%
		0013									14.4074	14.3411	-0.0663	-0.46%
29	Sputtered MoS2 film (ECR ion beam sputtering)	0039									14.3481	14.3482	0.0001	0.00%
		0042									14.3753	14.3758	0.0005	0.00%
UV Monitor	Ulethane film (Top)	1	0.163	0.185	0.022	13.50%	0.918	0.919	0.001	0.11%	923.137	923.211	0.074	0.01%
		2	0.176	0.188	0.012	6.82%	0.919	0.919	0.000	0.00%	935.545	935.767	0.222	0.02%
		3	0.169	0.181	0.012	7.10%	0.918	0.919	0.001	0.11%	925.687	925.702	0.015	0.00%
Ulethane film (Tale)		1		0.184				0.919						
		2		0.189				0.919						
		3		0.186				0.919						

Material		Mass			
		Pre-flight (A)	Post-flight (B)	(B)-(A)	(B)-(A) (A)
AO Monitor (Kapton film)	1	27.873	25.640	-2.233	-8.01%
	2	29.828	28.633	-1.195	-4.01%
	3	29.083	28.257	-0.826	-2.84%
	4	29.560	29.257	-0.303	-1.03%
	5	28.647	30.257	1.610	5.62%
	6	28.100	31.257	3.157	11.23%

Remarks :Unit	
	:g
	:mg

5.5 Individual Evaluation & Analysis of Installed Materials

5.5.1 Summary

The results of evaluation of each material are shown in Table 5.5-1.

5.5.2 Non-flammable electrical wire

5.5.2.1 Evaluation

- (1) The exposed samples have almost the same dielectric loss tangent and permittivity as the controlled sample.
- (2) The AC breakdown voltage of the exposed samples is 8% lower than that of the controlled sample.
- (3) The exposed samples have almost the same tensile strength as the controlled sample. The tensile strength of the exposed samples meets the following specifications:
 1. Tensile strength: 20 MPa or more
 2. Elongation: 50% or more
- (4) In a winding test, the samples exposed to rays were not found to be defective. Based on this and the finding described in item (3), we consider that the configuration of a sample (with a minimum radius of 4) does not cause the tensile strength of coating to decrease.
- (5) The arc tracking resistance of the samples exposed to rays was not found to be abnormal.
- (6) Based on the findings described items (1) through (5), we consider that exposure to the outer space environment has little detrimental effect on coating material of the wire.

5.5.3 Epoxy resin adhesive

5.5.3.1 Evaluation

The shearing adhesive strength of the flight sample is about 10% higher at a maximum in the range of dispersion than that of the sample without irradiation. Data at the time when the adhesive was developed show that even though test samples were prepared at the same time, there was dispersion in shearing adhesive strength, so that the data shown in Item 6 can be in the range of a variation. Therefore, any significant change in the shearing strength of the flight sample exposed to the space environment could be observed.

5.5.3.2 Discussion

This test resulted in a natural consequence, because the flight sample was made as a structure to prevent its adhered portions from being exposed to the space environment (See Fig. 3-2).

The adhesive strengths of the samples exposed in the ground simulation test are higher than that of the flight sample. This is because, as described in the report on the ground simulation test, temperature around the samples was increased to 53.1°C during the UV irradiation, and thereby the curing of the adhesive was accelerated. On the other hand, a maximum temperature, measured at MFD/ORU, around the flight sample during the space flight was 18.87°C, so that the adhesive could not be affected by the temperature.

5.5.4 Acrylic resin adhesive tapes for multilayer thermal insulator

5.5.4.1 Results

The following table shows the adhesive strengths of the samples before and after the space flight and of the samples in the ground test. The irradiations in the ground test were carried out in order of EB, UV rays and AO.

		With irradiation (After flight)		Without irradiation		Change (%)
Aluminum foil	Flight sample	2.95		(3.18)		-7.23
	Samples in ground test	(1)	3.37	(1)	3.22	4.66
		(2)	3.45	(2)	3.15	9.56
Thermal control film	Flight sample	1.45		(1.22)		18.9
	Samples in ground test	(1)	1.50	(1)	1.17	28.2
		(2)	1.57	(2)	1.27	23.6

Unit: kgf/cm² For flight samples, figures in brackets indicate average values in the ground test.

A flight sample with aluminum foil showed a reduction of about 7% in the adhesive strength required to peel the foil, whereas another sample with thermal control film showed an increase of about 19% in that required to peel the film.

Although the flight sample with the aluminum foil showed a negative change in the adhesive strength required to peel the foil, compared to the adhesive strength of the sample in the ground test, the adhesive strength of the flight sample was sufficient for practical use.

For samples with the thermal control film, both flight sample and exposed ground test sample showed positive changes in the adhesive strength, compared to the adhesive strength of the samples without irradiation, and especially the adhesive strengths of the exposed ground test samples were higher than that of the flight sample.

The peeling adhesion test usually provides a dispersion of about 10%, so that it is impossible to judge a proper adhesive strength from that obtained from only one sample.

Acrylic resins are more easily degraded with EB than polyimides used as a thermal control film. The acrylic resin used with the thermal control film is, however, likely to be affected with the beam because the film is thinner than the aluminum foil. This means that the adhesive strength of the thermal control film was increased with an irradiation dosage used in the test, and would be possibly reduced with further increase in dosage.

Difference in the change of the adhesive strength in the aluminum foil and thermal control film would be due to the difference in stiffness between them.

5.5.4.2 Evaluation

Though the acrylic resin adhesive tapes for multilayer thermal insulator are used to adhere the thermal control film, and are not directly exposed to the outer space, tape samples for the flight were prepared under the specifications, under which samples for the ground test were prepared, and actually exposed to the outer space, and then subjected to the peeling adhesion test.

After the space flight, no trace of indicating deterioration in the adhesive strengths of the acrylic resin tapes for multilayer thermal insulator was observed, and on the contrary, the adhesive strengths of the samples with the thermal control film were increased, so that the acrylic resin has a resistance to the space environment.

5.5.4.3 Discussion

(1) Mass change

The mass changes of the samples were observed because the surface of the thermal control film was corroded by AO, and the mass change of the adhesive was not observed.

(2) Optical characteristics

For the flight samples, no change in optical characteristics was observed.

The surfaces of the flight samples were optically observed to found that they were corroded with AO and rughened into needle-shape. It is expected that the corroded surface will increase the solar absorptance of the sun light and reduce the emittance of the vertical infrared rays. This expectation is proved to be compatible with the test results.

The surface thermal-optical properties of the sample is determined by the surface of the sample, and as a result, the adhesive will not affect on the characteristics.

(3) Peeling adhesive strength

The adhesive strength of the acrylic resin adhesive tape for multilayer thermal insulator is prescribed to be 0.69 kgf/cm^2 (340 N/m) or more, and the adhesive strengths of all tested samples exceed the minimum standard. In the adhesion testing prescribed in JIS, polyester film having a nominal thickness of No. 25 must be used as a substrate. However, the thermal control film has the same properties as the polyester film, so that the adhesive strength of the thermal control film can be regarded as that of the polyester film.

In future, the component analysis of the adhesive should be carried out after the thermal control film is peeled.

5.5.5 Thermal control film without ITO

5.5.5.1 Evaluation

The thermal control film after the space flight showed less deterioration than that in the ground test.

The surface thermal-optical properties have been proved to be changeless under the latest flight environment.

However, the thermal control film was unquestionably affected by AO during the flight, though the effect was not so big as in case of the ground test, so that close attention must be taken to apply the film to spacecrafts.

5.5.5.2 Discussion

(1) Mass change

The mass change of the film was caused by AO. The ratio of the irradiation dosage in the flight environment to that in the ground test was 1:3-4. The reaction of polyimide film with AO is considered to proceed efficiently in proportion to the increase of the dosage, but the ratio of the mass change of the flight film to that of the ground test film is 1:11.

(2) Surface Thermal-optical properties

No change in the surface thermal-optical characteristics of the film was not observed under the latest flight environment. On the other hand, in the ground test, the film corroded by AO as in case of the mass change, showed a considerable increase in the solar absorptance.

From the results of (1) and (2), an evaluation and simulation test technique similar to the space environment must be established space environment

5.5.6 Thermal control film with ITO

5.5.6.1 Evaluation

No significant change in the mass, surface thermal-optical properties, surface observation and surface analysis of the film was not observed. The film will be used practically without causing any trouble.

5.5.6.2 Discussion

(1) Mass change

The aluminum-evaporated film with conductive membrane showed no change in mass, and a high resistance to AO. This is attributed to the conductive membrane coated on the surface of the film.

(2) Surface thermal-optical properties

The surface thermal-optical properties of the film were proved to be not affected by the flight environment.

However, the surface thermal-optical properties of the film was significantly affected by UV rays in the ground test, so that if the film is exposed to the space environment in a long term it may be deteriorated. In future, the creation of a complex environment similar to the space environment must be studied, and the evaluation technique must be improved.

5.5.7 White paint

5.5.7.1 Evaluation

- (1) The surface thermal-optical properties in the surface of samples coated on aluminum plates are changed in the same manner as those of samples coated on CFRP plates. This means that the change of the characteristics is independent of the substrates.
- (2) The solar absorptance of the flight sample and the samples exposed separately with EB, UV rays and AO in the ground simulation test are increased, but the change in the solar absorptance of the flight sample is smaller than those of the samples in the ground test. Thus, the solar absorptance of the white paint would be increased by the space environment. For the flight sample, any significant change in the emittance of vertical infrared rays is not observed as in case of for the ground simulation test samples. Thus, for the white paint, the emittance of vertical infrared rays would not be affected by the space environment.
- (3) The surface of the flight sample was roughened and oxidized. Such changes of the surface were observed in the samples exposed with AO and with UV rays in the ground simulation test. This means that the surface of the flight sample was changed by AO and UV rays in the space environment.

5.5.8 Black paint

5.5.8.1 Evaluation

- (1) The surface thermal-optical properties in the surface of samples coated on aluminum plates (except No. 97) change in the same manner as those of samples coated on CFRP plates. This means that the change of the characteristics is independent of the substrates.
- (2) The solar absorptance of the flight sample (except No. 97) showed a change similar to that of the sample exposed with AO in the ground simulation test. From the fact that the changes in the optical surface characteristics of the samples exposed separately with UV rays and EB in the ground simulation test were small, the change in the surface of the flight sample would be caused only by AO.
- (3) A significant change was observed in the surface of the flight sample; the surface was roughened and the urethane resin used in the paint was lost. Similar change also was observed with the sample exposed with AO in the ground simulation test. Thus, the change in the surface of the flight sample is considered to be caused by AO. It is considered that the roughened surface and the loss of the urethane resin -- exposure of carbon black, led to the change in the optical surface characteristics.
- (4) Composition and chemical changes observed in the samples exposed separately with AO and UV rays in the ground simulation test were observed in the flight sample, too.

This means that the flight sample was affected by AO and UV rays.

5.5.8.2 Remarks

Among the samples coated on the aluminum plates, No. 97 sample showed bigger change in optical surface characteristics than the others. This may be because, As Table 3-1 shows, the sample was prepared by the use of paint belonging to a different lot, and applied a different coating, and is a problem to study in future.

5.5.9 Aluminum deposited β -cloth

5.5.9.1 Evaluation

No significant deterioration of the sample was not observed both from the change in optical surface characteristics and from the surface-analyzed data. Though aluminum-evaporated β -cloth, which was made by Dunmore Company and used in the space flight, can not be simply compared with aluminum-evaporated β -cloth, which was made by Sheldahl Company and used at SFU/EFFU, because the exposure conditions at MFD are different from those at EFFU --- different altitude, different exposure time and different exposure direction. In the deteriorated amount, the Dunmore's product used in the latest flight, can easily stand comparison with the Sheldahl's product, judging from the change in the optical surface characteristics, the change in the mass, and FE-SEM photographs after the irradiation of AO. The deterioration of the Dunmore's product is smaller than expected from the deterioration data at SFU.

5.5.9.2 Discussion

The data obtained from the latest space flight mean that the Dunmore's aluminum-evaporated β -cloth is as resistant to the space environment as the Sheldahl's aluminum-evaporated β -cloth. No significant difference between them is not observed. At SFU/EFFU, a sample to be exposed --- Sheldahl's aluminum-evaporated β -cloth, was partially scratched artificially before being carried, and after the flight, Teflon, used as matrix, at the scratched portion was significantly deteriorated. At MFD/ESHM, when artificially scratched portion was not provided, any significant deterioration on the full surface of the aluminum-evaporated β -cloth was not observed, and no deterioration of Teflon used as matrix also was observed differently than at SFU, so that the traditional theory that Teflon was resistant to AO it was endorsed. Some reports claim that Teflon is resistant to AO, and not resistant to UV rays, though the exposure time in each case is different. From above information, it is considered that exposure time was so long at SFU that UV rays much affected on the sample, whereas at MFD exposure time was so short that the rays less affected on the sample. Though the Exposed Experiment Section of Logistics Module of JEM requires a service life as long as 3 years on the orbit, the latest exposure test was carried out in a period less than 3 years, namely only through the period of NSTS flight. . The Exposed Experiment section of Logistics Module are planning to launch a specific satellite, in which β -cloth is to be used, in February 2002 for the first time and to repair it after recovering it. The deterioration of the β -cloth should be checked after the recovery.

5.5.10 Bonded MoS₂ film (HMB 34 film)

5.5.10.1 Evaluation

Samples of this lubricant have been subjected to an exposure test at SFU/EFFU. The purpose of the latest test was to compare the environment at SFU with that at MFD on the basis of the lubricant. In the latest test, samples without irradiation, samples exposed with AO and samples carried/exposed were primarily subjected to surface analysis, and samples without irradiation and samples carried/exposed were subjected to the friction and abrasion test for confirming the characteristics of the material. Both the surface analysis and friction/abrasion test were carried out to obtain a minimum data necessary for utilizing the data obtained at SFU/EFFU as the data to be obtained at MFD/ESEM.

When the samples at SFU/EFFU were subjected to surface analysis after the recovery, they showed the same results --- oxidized surface, as the samples exposed with AO in the ground simulation test, and when the samples at SFU/EFFU were subjected to friction/abrasion test, they showed a remarkably improved abrasion life. As a mechanism that the abrasion life of the samples exposed to the space environment in a low-altitude orbit was improved, the hardening of the skin of the solid lubricant was considered; the skin was hardened through a cross-linking reaction of the binder by the irradiation of UV rays and space rays. However, the surface analysis provided no positive evidence to prove that the mechanism was right.

The latest surface analysis only provided the same results as those obtained at SFU/EFFU. The oxidative deterioration of polyamide-imide used as a binder --- scission of polymer chain by the elimination of amide groups, cleavage of imide groups, and formation of carbonyl groups---, was confirmed by the use of FT-IR, and the oxidation of MOS₂ used as a pigment was confirmed by the use of ESCA. At both SFU and MFD, the samples exposed with AO in the ground simulation test were oxidized most markedly, and the samples carried/exposed were oxidized to a medium level between the oxidative levels of the samples without irradiation and of the samples exposed with AO. The samples at SFU and at MFD provided the same results as described above. The amount of adhered contamination --- SiO_x, at MFD was less than that at SFU, which was a big difference between at SFU and at MFD.

This would be due to the difference in the exposure time. Logically, the deoxidized surface can increase the initial coefficient of friction, but at SFU/EFFU, the samples recovered and the samples in ground simulation test did not show any significant change in the initial coefficient of friction. The samples at MFD/ESEM provided the

same results as those at SFU/EFFU. Thus, it is considered that scale-shaped particles of MoS₂, pigment, oriented in parallel with the surface of the base material, solid lubricant, will restrict the deterioration of the lubricant exposed to the space environment to only its top surface, and as a result, the properties and functions of the lubricant can be maintained.

5.5.10.2 Discussion

As in the case of SFU, the samples at MFD--- baked MoS₂ membrane bonded with organic binder, DEFRIC COAT HMB 34 film, was not deteriorated. The improvement in the lubricating life was observed in both samples at SFU and ones at MFD. Although mechanical engineers involved in the space apparatuses have entertained some apprehensions about the environmental deterioration of such baked MoS₂ membrane bonded with organic binder like samples described above, there would be nothing to worry about the deterioration judging from the results at SFU and at MFD.

5.5.11 Binder for bonded MoS₂ film (Polyamideimide A)

5.5.11.1 Evaluation

The samples in this test were used to analyze the mechanism, which the samples were deteriorated in the space environment in a low altitude orbit, and primarily used for surface analysis. The samples were coated only with the binder for HMB 34 membrane used with the solid lubricant, as shown in No. 10 appendix to this clause.

The samples subjected to the surface analysis did not show so drastic change in deterioration as expected. At SFU and at MFD, the binder inside HMB showed the deterioration including the formation of carbonyl groups, but the samples coated only with the binder did not show any oxidative deterioration after they were exposed with AO or carried/exposed to the space environment. It was considered that if the binder alone was used, the mechanism of deterioration, or the progress of cross-linking reaction to be caused by AO or UV rays would be determined by the use of FT-IR, but the results were disappointing. The following conclusion derived from this test results must be regarded as important in future; "when the binder alone is used, the deteriorated portion of the binder is lost in turn, and as a result, the binder does not show any oxidative deterioration". However, the SEM photographs of the surface of the binder exposed with AO or those of the surface of the binder carried/exposed to the space environment, show that polyamideimide resin is as resistant to AO as Teflon.

The binder samples exposed with AO showed a sharp decrease in abrasion life in the friction/abrasion test. This is considered because the thickness of the binder coat was reduced by the roughened surface of the binder as the SEM photographs show. The binder samples carried/exposed to the space environment showed a sharp decrease in abrasion life, too. The binder samples exposed with UV rays or EB showed an improvement in abrasion life, but the level of the improved abrasion life is not so high, and it is included in the range of the dispersion taking previous data into consideration. In conclusion, the mechanism that the characteristics of HMB 34 membrane are improved, should be re-studied under the space environment in a low altitude orbit; the mechanism that the sliding characteristics are improved as a result of the cross-linking reaction of the binder, accompanying the hardening of the binder.

5.5.11.2 Discussion

The sample used in this test is what was used as a binder for the solid lubricant, DEFRIC Coat HMB 34 membrane, made by Kawamura Laboratories, Ltd.

It showed the marked improvement in the characteristics at SFU/EFFU as described in

the previous clause. In this test, the pigment was considered a hindrance factor in surface analysis from the results at SFU/EFFU and eliminated in preparing the sample at MFD. However, no conclusion was derived from the analysis data. Though it would be considered that the pigment acted as a catalyst for the chemical reaction of the binder used in the solid lubricant in the space environment in a low altitude orbit, there is no evidence. The test results that "when the binder was used alone, it is partially lost without showing any oxidative deterioration" must be regarded as important.

5.5.12 Binder for bonded MoS₂ film (Polyamidimide B)

5.5.12.1 Evaluation

This binder sample, as a material comparative to polyamidimide A, was used to analyze the mechanism that the sample was deteriorated in the space environment in a low altitude orbit, and primarily was used for surface analysis.

In the surface analysis, the samples do not show any drastic change as expected, except that the flight exposed sample was slightly oxidized to form carbonyl groups. The SEM surface photographs of the AO-exposed sample show that this polyamidimide B is as resistant to AO as polyamidimide A is.

In the friction/abrasion test, the AO-exposed sample and the flight exposed sample show sharp a decrease in abrasion life. This is considered because the roughened surface shown in the SEM surface photographs caused the reduction in the thickness of the skin. Although the UV-exposed sample and the EB-exposed sample show an improvement in abrasion life, the level of the improvement is not significant, and is included in the range of the dispersion that the previous data showed. No significant difference is observed between A and B.

5.5.12.2 Discussion

As described above, this membrane is a new material to substitute for polyamidimide A which was used as a binder for the solid lubricant (DEFRIC Coat HMB 34 membrane made by Kawamura Laboratories, Ltd.) that showed the marked performance at SFU/EFFU.

Compared to polyamidimide A, no significant difference in the surface analysis is observed between the sample exposed in the space environments, and also no significant difference in the surface analysis and the friction/abrasion test was observed between the various environmental elements-exposed samples in the ground simulation test.

In conclusion, no significant difference between polyamidimide A and polyamidimide B is observed, so that, even though A is replaced with B to improve HMB 34 membrane, there is no reason to expect some improvement.

5.5.12.3 Remarks

Among the samples of this binder, some contaminants adhered to the sample exposed in the space environment, SN 225 for the friction/abrasion test, though the sample, SN:S 226, was free from the contaminant. The adhesion of the contaminants was not uniform, differently from common vapor deposition formed from out-gas, namely they adhered partially to the sample, just like fallen drops of water. Thus, the contaminants are called stains. The contaminants did not affect substantially on the initial frictional properties, though some influence was expected.

The sample with stains was subjected to ESCA for surface analysis, avoiding any effect on the friction/abrasion test, because the sample is analyzed by ESCA without any damage on its surface. The analysis data suggest that the stains are comprised of ZnO-SiO₂. As a source of the ZnO-SiO₂, white paint Z93 is considered a candidate, because the white paint contained ZnO as a pigment, and silanol as a binder component, and has been coated on various components at MFD, and as well, it was confirmed that Z93 coated on the tool- fixture for the manipulator test was partially peeled. However, the contaminants do not look like solid but sank liquid, and as well, they do not adhere uniformly to the sample differently from the vapor deposition from out-gas. Therefore, it is indefinable that the white paint Z93 adhered to the sample. The cause that the sample is contaminated has not been determined yet as of January 1998. Additionally, such contaminants were observed in the exposed polyimide sample.

5.5.13 Binder for bonded MoS₂ film (Polyimide)

5.5.13.1 Evaluation

This material has not been used in the outer space as described above.

In the surface analysis, the deterioration of this material is proved to be smaller than expected, and the small deterioration also is shown from the SEM surface photographs of the AO-exposed sample and of the flight- exposed sample, namely, that this polyimide provides less deterioration than other polyimide such as Kapton. Expectations placed on FT-IR were that both the mechanism of deterioration and the degree of cross-linking in the UV-exposed sample and the EB-exposed sample would be determined, but the two problems could not be solved by FT-IR.

In the friction/abrasion test, the abrasion life of the AO-exposed sample or the sample exposed in the space environment is sharply decreased, and the initial coefficient of friction is smaller than that of polyamidimide. This is understood as follows; by the presence of particles formed on the surface as SEM surface photograph show, the tensile strength and the shear strength of the top surface are reduced, thereby the coefficient of friction is reduced. The abrasion life of the UV-exposed sample or the EB-exposed sample are reduced.

5.5.13.2 Discussion

This binder was tested to use for the space apparatuses as a resin solid lubricant free from pigment, as described above. Judging from the surface analysis data and the friction/abrasion test data, however, this binder is so behind the baked MoS₂ membrane that it can not be used under the exposure to the space environment.

Thus, the binder, as toughram, will be used in a limited range, and at best, it could be used in such a space apparatus as one-shot members, which is subjected to only one friction and used under low surface pressure.

5.5.13.3 Remarks

In the test of this material, the adhesion of the contaminants was observed on the sample exposed in the space environment, SN 235 for the friction/abrasion test, while no contaminant was observed on the SN:S 236 sample. The contaminants did not adhere to the sample uniformly differently from vapor deposition from common out-gas, and was in a form of partially fallen drops of water in appearance. The spots of the contaminants are called stains. No significant influence by the stains on the initial friction properties of the sample was observed, though some influence was expected before the test. To avoid any influence on the friction/abrasion test, namely to avoid damaging the surface and breaking the test sample, the surface analysis by the use of ESCA was carried out. The analysis data of the contaminants suggest the presence of SiO_2 . Sources containing such substance are either potting material used in each component at MFD, or white paint Z93, which contained ZnO as a pigment and silanol as binder, and was used in coating the surface of each component at MFD. However, as described above, the contaminants, which are not solid, are in the form of sank liquid, and do not adhere to the sample uniformly differently from the vapor deposition from out-gas. Thus, neither the potting material or peeled white paint Z93 is defined as the source of the contaminants. Questions about the contaminants have not been solved yet as of January 1998, additionally, such contaminants were observed on the sample exposed in the space environment of polyamidimide B.

5.5.14 Silica FRP

5.5.14.1 Evaluation

The sample exposed to each environmental element shows better abrasion resistance than the controlled sample. This is beyond expectation, and various reasons are considered.

- In case of the AO-exposed sample, a reduction in the initial thermal conductivity is caused by the loss of resin in the surface and consequently the exposed glass fiber, and a reduction in the rate of recession is caused by the melting of the glass fiber.
- In case of the UV-exposed sample, the EB-exposed sample, and the sample exposed in the space environment, the reason why the abrasion resistance was improved must be explained in future study. It would be impossible to draw a conclusion from this test data. There would be two ways of thinking about the improvement; the level of the improvement is included in the range of error, and the abrasion resistance is improved by the hardening of resin exposed with UV rays or EB.
- In case of the sample exposed in the space environment, the improvement in abrasion resistance is observed from the test data, as observed in the AO-exposed sample. Judging from these results, a drawn conclusion is that the feedback of this data to re-design this material for design margin is unnecessary. The improvement in abrasion resistance would be caused by that a reduction in the initial thermal conductivity is caused by the loss of resin in the surface, and consequently the exposed glass fiber, and the reduction rate in the recession is caused by the melting of the glass fiber.
-

5.5.14.2 Discussion

As far as judgement is made only from the data in this test, the reduction in the abrasion resistance of the sample exposed in the space environment of Si-FRP would not need to be taken into account. Namely, the material is able to designed well on the basis of the current ground simulation test data on the controlled sample, so that the design margin for the exposure to the outer space would not be needed to be taken into account. However, there are not sufficient data yet to draw a final conclusion.

5.5.15 Flexible OSR

5.5.15.1 Evaluation

This flexible OSR is a material which has been qualified and authorized already for satellites under NASDA-QTS-1048/301, and has been tested through the irradiation of UV rays and EB.

The analysis data on this material by ESCA and FTIR-ATR after the latest flight do not show any significant change in the chemical structure except slight reduction of aliphatics component, and also do not show any significant change in the surface thermal-optical properties. These data are included in the range of tolerance.

A slight increase in the weight is observed after the flight by possible adhesion of contaminants.

5.5.15.2 Discussion

In the comparison between the ground test data and the flight test data, the change in the surface thermal-optical properties after the flight is small compared to that of the ground simulation test. This is because the shorter flight time provided mild environmental conditions.

The deterioration level in the surface of the sample in the flight test was the same as that in the ground test, but an organic oxygen was observed by ESCA. The source of the organic oxygen could not be identified from the latest test data, though contamination from other materials is guessed.

5.5.16 Silicone adhesive (RTV-S691)

5.5.16.1 Evaluation

In the analysis of the sample exposed in the space environment by OM and FE-SEM, any significant change in the appearance was not observed. A molecule level change was observed only in the top skin by ESCA and FTIR-ATR, but the change is too small to affect on the properties of the resin. As a whole, the deterioration of RTV-S691 under the latest exposure environment is not observed.

5.5.16.2 Discussion

Although no significant change in the appearance was not observed, a change in the weight after the flight was observed.

The following factors can be imagined.

Although the specifications define that, as a rule, organic materials used for satellites shall be applied a 1.0% TML as an outgas, the specifications approve that the concentration of the outgas can be varied according to the curing conditions or manufacturing lot of the material, so that, in case of RTV-S691, a 0.4% TML is used in general.

About 0.3% of the weight reduction caused in the latest flight exposure test was lower than that observed in the ground test sample exposed with AO.

5.5.17 Solar Cell and materials for solar cell

5.5.17.1 Solar cell

(1) Evaluation

In case of comparison of the change in the I-V characteristics of solar cell (Si BSFR type) A-1 before and after the flight exposure, and the change in the I-V characteristics of solar cell (Si NRS/BSF type) A-2, slight change in the output was observed in both of the two cells, and any significant change on the surface of the cells was not observed under a microscope.

(2) Discussion

The output power after the flight test is increased by 2.2% in A-1 and by 3.2% in A-2 in terms of the absolute value. This result suggests that the measuring and evaluating method is not proper, though the cells are not so much deteriorated compared to the ordinary degradation level of solar cell. When the change is examined by each parameter, the results are as follows; 1) the fill factors (FF) are increased in the two cells, 2) the short-circuit current (I_{sc}) is decreased by 4.1% in A-1, and increased by 2.5% in A-2, 3) the open circuit voltage (V_{oc}) is decreased by about 7 mV in A-1, and decreased by about 4 mV in A-2. Especially, those changes in the short-circuit current (I_{sc}) are beyond the range of error. The values of fill factors before the flight are too small, so we think that there is something wrong in contacting in both of the samples when they are measured. From the changes in I_{sc} and V_{oc} , it is considered that there was something wrong in measuring the cell temperature before the flight test. That is the cells were mounted on aluminum holders using resin, and the cells equipped with the holder were measured on a temperature-regulated block. Therefore, the temperature of the cells are likely to have not been properly controlled.

As described above, it is recognized that the solar cells show no significant deterioration in the flight test, and that there are some problems on the measurement of the cell.

5.5.17.2 Cover glass for solar cells

(1) Evaluation

The change in transmittance of a cover glass, OCLI 0213 AR, OCLI 0213 BRR, OCLI 0213 AR + CC, PPE CMX AR are evaluated.

The transmittance of each exposed samples was reduced by about 1% in the whole range of wavelength. The transmittance of AR model made by The OCLI Company was reduced by about 2% the short wavelength region (about 400 nm - 750 nm). No. 12 cover glass was proved to be AR model, though it was scheduled to be AR + CC model.

(2) Discussion

The reduction in transmittance of all the samples in the whole range of wavelength may be qualitatively the same phenomenon as that of the EB-exposed sample in the ground test. The analysis data by ESCA suggest that the scission of bonds between magnesium and fluorine atoms is caused by the irradiation of EB. The reduction in the transmittance of BRR model (No. 11) which has not MgF_2 membrane, however, can not be explained from only the ESCA data. The reduction in the transmittance in the whole wavelength is about 1% at most, and is included in the range of error. To determine the cause of this reduction, more accurate measuring technique will be required, considering reproducibility error.

The reduction in the transmittance of AR model made by OCLI Company in the short wavelength region (400 nm ~ 750 nm) may be the same phenomenon as that of the UV-exposed sample in the ground test. The analysis data by ESCA show that the scission of bonds between magnesium and fluorine atoms is observed in both of exposed AR models (No. 10 and No. 13). From this result, it is guessed that the reduction in transmittance is caused by the scission of bonds between magnesium and fluorine atoms owing to the irradiation of UV rays. The reduction in the electric properties of the cells adhered these glasses will be small because the reduction in transmittance is slight.

The analysis data by ESCA also show that the adhesion of contaminants (silicon oxide) is observed on all the flight exposed samples. (Si which is not found in the controlled samples, is observed in No. 10, 12, and 13. In the comparison to the controlled-samples, the increase or decrease of Si is not reported in No. 11 because the increase or decrease of other atoms is determined by the use of Si as a reference atom, but Si and O are obviously increased when the data is analyzed regarding C or Na as a reference atom.) The contaminants are likely to affect on the optical properties (transmittance), but any obvious conclusion can not be drawn from the current data.

The decrease of F and the addition of O on the surface of MgF_2 layer of No. 10 and No. 13 are obvious from the analysis data by AES. However, in the AO-exposed sample in the ground test, the intensity of O is lower than that of the sample exposed in the space environment, so that the irradiation of AO can not be considered a factor to add O. In the sample exposed in the space environment, an increase of Si in MgF_2 layer is also observed, which can be caused by the adhesion of the silicon oxide.

In case of BRR (No. 11), only the information on SiO_2 layer in the surface has been obtained from the analysis data by ESCA and AES, and from the data, no significant difference are not observed between the sample exposed in the space environment and the controlled sample.

The analysis data on No. 12 was the same as that on No. 10. Model used in No. 12 was not AR + CC but AR.

5.5.17.3 Interconnector for solar cell

(1) Evaluation

The results of OM observation show that the configuration of the surface of the sample exposed in the space environment is different from that of the non-irradiated sample or that of the AO-exposed sample in the ground simulation test, we dare say that it show a medium form between them.

The result of FE-SEM observation also show the same results as that of OM examination. The surface of the AO-exposed sample showed various configurations as the result that the connector material reacted vigorously with AO, but the surface of the sample exposed in the space environment suggested that the reaction between the connector material and AO was mild, and this is not inconsistent with the data obtained in the ground test.

In all the samples, S as well as Ag, C and O was observed from the data by EPMA analysis, but further information was not obtained.

(2) Discussion

In the OM and the FE-SEM observations, the surface of the AO-exposed sample in the ground test showed complicated configurations, probably as results of oxidation and corrosion by AO. It is supposed that the sample exposed in the space environment had the same reaction in mild conditions.

In the EPMA, the counts are performed from all over the visual field without specifying measuring point, which is proved to be proper judgement as the result of above data. A trace of S, which was not observed in the ground simulation test sample, was observed in the sample exposed in the space environment. Intrinsically, the interconnector material reacts with S in air so easily that it can be sulfurized before and after the flight exposure test. Therefore, a conclusion that the source of S is some contaminant in space can not be drawn.

5.5.17.4 OSR for solar cell

(1) Evaluation

The change in reflectance of OSR OCLI 0213 SSM, and the change in reflectance of PPE CMX SSM are evaluated. In the measurement of optical properties of the samples, 0213 SSM model (No. 17) made by OCLI Company, and CMX SSM model (No. 18) made by PPE Company showed slight change.

The ESCA analysis data show that a trace of Ca and a trace of N exist in No. 17 model, though both of them were not observed in the controlled No. 17 model. While several trace elements are observed in No. 18 model without irradiation, especially the concentration of Si and O is higher due to the adhesion of silicon oxide.

The AES analysis data show that no significant difference is observed between the sample exposed in the space environment and the controlled sample for both No. 17 model and No. 18.

(2) Discussion

The difference in the element detected by ESCA can be attributed to the material used by the different maker. A trace Ca and a trace N detected in No. 17 contaminants.

The change in reflectance must be so small that it is included in the range of error, and in investigating the cause of the change, more accurate evaluation considering reproducibility error of data is needed. Since the samples in the ground test were not evaluated successfully because of some trouble in their shapes, any comments on the basis of the ground test data may be improper, as a whole, the difference is so small that the impact on performance of OSR is small.

5.5.17.5 Summary

In the flight-exposed test, the deterioration of the solar cell was hardly observed, and small changes, which can not affect on the performance of the cell, were observed in the cover glass and the interconnector. Contaminants such as silicon oxide, by which the cell will be caused some trouble in a long term flight exposure, were observed in some of the samples. Some of the samples were prepared improperly, and evaluated incompletely. In the analysis required accuracy, the same sample or the same lot sample as a reference material should have been preserved and measured at the same time with the sample exposed in the space environment. Furthermore, accuracy in measurement is important when difference in test data is small, so that full preparation including jigs for measurement is needed before testing when small difference is forecast. These importance were confirmed as a lesson.

5.5.18 Sputtered MoS₂ film

5.5.18.1 Results of surface analysis

FE-SEM examination shows clearly the big difference in the morphology of surface among RF, RF-H and ECR films. The surface of RF film was rugged before the flight test, and after the flight-exposed test, individual particle on the surface got smaller and rougher than that before the test, as if the surface is eroded. The surface of RF-H film was like radially-grown whiskers. In the sample exposed in the space environment, the UV-exposed sample and the AO-exposed sample, the whiskers were observed to have been thinner. Especially, in the UV-exposed sample, the whiskers were collapsed, and surface was fluffy, probably as the result that the cover glass was pressed against the surface at the UV irradiation. There were substantial small abraded marks on RF-H film, compared to RF film and ECR film, probably as the result that the film was scratched during handling. ECR film, in which individual particle was larger than that in RF film, was like the form that the piled particles were smoothed, so that the film seemed dense.. Although the difference in the surface form among the controlled sample, AO-exposed sample, UV-exposed sample and sample exposed to the space in a low altitude orbit, can not be judged by photographs, but the change in the form of the surface of the exposed, UV-exposed and AO exposed samples are small.

The adhesion of Si + O was observed in all samples exposed to the space in a low altitude orbit. After the sample was exposed to the space or exposed with AO, the concentration of O in the top surface of the sample was increased, and the depth of the layer oxidized by O varied by sample. In RF film exposed with AO, an increase in O was observed to about 100 nm because of the oxidation of Mo. In the sample exposed to the space, the oxidation to the same depth was observed, but the concentration of O was lower. In the UV-exposed sample, an increase of the concentration of O was hardly observed. For RF-H film, relatively much carbon was detected in the controlled sample, while in the AO-exposed sample, UV-exposed sample and space-exposed sample, the concentration of carbon was reduced, and as well, an increase in the concentration of oxygen was observed over the depth of 500 nm that is the limit of etching in the space-exposed sample, AO-exposed sample and Uv-exposed sample. RF-H film has a structure comprised of many pillars and is fluffy, so that it was oxidized to such a deep inside. For ECR film, the sample was least affected by the exposure and irradiation. By the AO-irradiation and space-exposure, the increase in the concentration of O by the oxidation of Mo was observed only to a depth of about 8

nm. An increase in the concentration of O by the UV irradiation was hardly observed. No significant difference was not observed between Near side and Far side.

5.5.18.2 Friction test

(1) Method and conditions for friction test

The test conditions show below.

- Test conditions -

Load : 10 N, Velocity : 10 mm/sec, Stroke : 10 mm, Pressure : 10^{-5} Pa

Pin : SUS440C/7.94mm in diameter, Disk : SUS440C+MoS₂

The test was carried out under a load of 10 N, a sliding speed of 10 mm/sec, and a friction stroke of 10 mm. A SUS440C ball having a diameter of 7.94 mm was used as a friction element. The pressure of the vacuum chamber was kept at 10^{-5} Pa during testing. When the coefficient of friction was exceeded a value of 0.3, the film was judged to have been fractured.

(2) RF skin

The surface of the unexposed sample, the non-irradiated surface shaded by the shielding plate in the AO-irradiated sample, and the non-exposed surface shaded by the shielding plate in the flight-exposed sample showed a skin life of about $1E + 5$ times (about 50000 cycles), while the surface irradiated with AO showed a shorter skin life of about $6E + 4$ times (about 30000 cycles), and the surface exposed to the cosmic environment also showed a shorter skin life of about $8E + 4$ times (about 40000 cycles), though not so shorter as the AO-irradiated surface. It is probable that the dose of AO flux onto the sample exposed to the cosmic environment around the low altitude orbit was less than that of AO flux in the ground control test. No significant change in the skin life was observed between the UV-irradiated and non-UV-irradiated surfaces.

The surface irradiated with AO showed a lower coefficient of friction than the surface of the unexposed sample, especially at the initial stage of the friction testing. The surface exposed to the cosmic environment showed the same results as the AO-irradiated surface. Even though it is taken into consideration that the AO in the cosmic environment around the low altitude orbit would influence on the surface, both the exposed and non-exposed surfaces of the flight sample showed a lower coefficient of friction. This would be attributed to contaminants adhered to the surface during or after the flight-exposing, or this is probably because the contaminants affected the shaded surface through the shielding plate.

No significant difference between the exposed and non-exposed surfaces was observed from the photomicrographs of the friction element (pin) after the friction testing.

(3) RF-H skin

In the ground control test, the surface of the unexposed flight sample and the non-irradiated surface of the AO-irradiated sample showed a skin life of about $1.2E + 4$ times (about 6000 cycles). Only RF-H skin irradiated with AO or UV showed about twice the skin life of $3 - 3.7E + 4$ times (about 15000 cycles). The surface exposed to the cosmic environment also showed the same life level as the surface irradiated with AO or UV, so that AO and UV in the cosmic environment around the low altitude orbit would have an effect on the surface. The non-exposed surfaces of the flight samples in two flight tests, however, showed longer skin lives of about $2E + 4$ times and about $3.5E + 4$ times severally. The longer skin lives may be attributed to the effects of contaminants not only on the exposed surface but also on the non-exposed surface.

The surface irradiated with AO showed a lower coefficient of friction than the unexposed surface. The surface irradiated with UV showed the same coefficient of friction as the unexposed surface in the initial stage of the testing, and after that, showed a lower coefficient of friction of about 0.02. The exposed surface of the flight sample showed a lower coefficient of friction in the latter stage of the testing.

The photomicrographs of the friction element after each friction testing of the unexposed surface of the flight sample, the non-irradiated surface of the AO-irradiated sample, and the non-exposed surface of the flight sample showed that a volume of abraded powder adhered to the gate for the friction element. The effects of the abraded powder on the skin life have not been investigated.

(4) ECR skin

For Near side, the unexposed surface of the flight sample and the non-irradiated surface of the AO-irradiated sample showed a skin life of about $3E + 4$ times (about 15000 cycles), but when those surfaces were irradiated with AO, they showed a skin life of about $1.4E + 4$ times reducing by half. When the surfaces were irradiated with UV, they showed slightly shorter skin lives, but no significant difference between the surfaces with and without UV irradiation was observed by the AES analysis. The difference in the skin lives, therefore, would be within the range of the reproducibility of the data in the friction testing. In the case of the flight sample, the non-exposed surface showed the same level of skin life as the unexposed surface, but the exposed surface showed a slightly longer skin life differently from the AO-irradiated surface which reduced the skin life. The AES analysis showed that the oxidized layer in the ECR skin of the flight sample was the thinnest, and the dose of AO flux, to which the ECR skin was exposed, would be less than that of AO flux in the ground control test. The reduction in the skin life of the AO-irradiated surface, therefore, would be more attributed to contaminants than to AO.

The non-exposed and exposed surfaces of the flight sample as well as the surface of the unexposed flight sample and the surface irradiated with AO showed a lower coefficient of friction up to several thousand times in the initial stage of the friction testing, and after that, they increased the coefficient of friction to a plateau. The

period of time while the lower coefficient of friction was provided was slightly shorter. The non-exposed and exposed surfaces showed a coefficient of friction of about 0.06 at the plateau, where the AO-irradiated surface also showed the same level of the coefficient of friction.

No significant difference between the surfaces was observed from photomicrographs of the friction element after the friction testings.

In addition to the AO irradiation, the UV irradiation and the exposure to the cosmic environment, the differences among the skins (disk samples) would mostly affect the test results.

- (5) The test results in the cosmic environment around the low altitude orbit, as compared to those in the ground control test

As for the exposed surfaces of the flight samples, the abrasion life of the RF skin reduced, while that of the RF-H skin increased. Those were similar to the test results from the AO-irradiated sample in the ground control test. The AES analysis of the exposed surface of the flight sample showed the results similar to those from the AO-irradiated surface in the ground control test, except that contaminants based on Si were detected in the flight-exposed sample, supporting the results in the friction testing. The exposed ECR skin of the flight sample, however, did not show the reduction in abrasion life differently from the AO-irradiated ECR skin. How far the contaminants adhered to the surface of the flight sample had an effect on the friction test results has not been investigated.

As for each skin, the non-irradiated surface of the AO-irradiated sample showed the same level of abrasion life as the unexposed surface of the flight sample, so that the AO hardly had an effect on the MoS₂ skin without travelling around to the shielded surface. It is probable that such factors as AO and UV in the cosmic environment around the low altitude orbit would not affect the shielded MoS₂ skin of the flight sample without travelling around to the bottom of the shielding plate, but the two facts that, first, no significant difference between the non-exposed and exposed surfaces of the flight sample was observed in terms of the coefficients of friction and the abrasion lives of the skins, and, second, the skins in those surfaces showed similar tribological properties suggest that the contaminants had an effect onto the bottom of the shielding plate.

In this friction testing, the data were obtained only from the one testing of the AO-irradiated and UV-irradiated samples, and the one or two testings of the flight-exposed sample, so that the reproducibility of the data must be studied in future.

Table 5.5-1 (1/6) Summary of Evaluation of Individual Materials

No.	Sample name	Evaluation of sample exposed to space environment	Comparison with sample subjected to ground simulation test	Remarks
1	Non-flammable electrical wire	<ul style="list-style-type: none"> Surface analysis → The surface is found to be rough and oxidized. Exposure to the space environment has little effect on coating. If a fire-resistant cable is wound into a coil with a minimum radius of 4, the mechanical strength of its coating does not decrease. The wire keeps resistance to arc tracking. 	<ul style="list-style-type: none"> The sample exposed to the space environment is similar in surface condition to the sample exposed to AO rays, but the surface of the former is a little rougher than the latter. 	EEFU: A sample of the same material was also oxidized, showing the same tendency.
2	Epoxy resin adhesive	<ul style="list-style-type: none"> The shear strength of the adhesive does not decrease when it is exposed to the space environment. <p><Shear strength data (average for two samples)> Controlled sample: 13.9 (MPa) Sample exposed to the space environment: 14.8 (MPa) → The difference between these two values is less than 10%. This is within the acceptable variation range.</p>	<p>Sample exposed to UV rays: 17.4 (MPa) The sample exposed to UV rays has a higher shear strength than the sample exposed to the space environment. ← Temperature reached 53°C near the sample when it was exposed to UV rays, so we assume that high temperatures promoted hardening.</p>	
3	Acrylic resin adhesive tape	<ul style="list-style-type: none"> Exposure to the space environment does not reduce the resistance of the tape to peeling. Aluminum foil Controlled sample: 3.18 (kgf/cm²) Sample exposed to the space environment: 2.95 (kgf/cm²) → 7% decrease. This is within the acceptable range of variations. Thermal control film Controlled sample: 1.22 (kgf/cm²) Sample exposed to the space environment: 1.45 (kgf/cm²) → 19% increase 	<ul style="list-style-type: none"> Aluminum foil exposed to rays on the ground 3.41 (kg/cm²), 7% increase Thermal control film irradiated on the ground 1.54 (kg/cm²), 26% increase <p>The samples exposed to EB, UV, and AO rays on the ground are more adhesive than the sample exposed to the space environment. We assume that high temperatures promoted hardening.</p>	

Table 5.5-1 (2/6) Summary of Evaluation of Individual Materials

No.	Sample name	Evaluation of sample exposed to space environment	Comparison with sample subjected to ground simulation test	Remarks
4	Thermal control film without ITO	<ul style="list-style-type: none"> The amount of α_s increased by about 15%, and that of ϵ decreased by about 4%. The mass of the sample decreased by about 5%. ← We project that this was caused by surface erosion due to exposure to AO rays. 	<ul style="list-style-type: none"> For the sample exposed to AO rays, the amount of α_s increased by about 12%, that of ϵ decreased by about 6%, and the mass decreased by 15%. The samples exposed to EB and UV rays did not change. The sample exposed to AO rays underwent almost the same changes as the sample exposed to the space environment. 	For data on α_s and ϵ , see Table 5.5-2.
5	Thermal control film without ITO	<ul style="list-style-type: none"> There was little change in the mass, surface thermal and optical characteristics, appearance, and surface composition of the sample. Specifically, the mass decreased by 0.5%, the amount of α_s decreased by 0.2%, and that of ϵ increased by 2%. ← We assume that this is because ITO film is resistant to AO rays. 	<ul style="list-style-type: none"> Exposure to UV rays caused the surface thermal and optical characteristics to change significantly. The procedures for exposure and sample handling need to be improved. ⇒ Complex-environment evaluation technology simulating the space environment must be established and sophisticated. 	EFFU: For both EFFUs covered with ITO film and SiO_2 film, the amount of α_s and that of ϵ slightly changed. This is the case with the sample exposed to the space environment.
6	White paint	<ul style="list-style-type: none"> The surface optical characteristics of a substrate do not depend on whether it is made of aluminum or CFRP. 	<ul style="list-style-type: none"> We obtained almost the same results as in the case of a ground simulation test. 	EFFU: The amount of α_s increased by 40 to 50% because UV rays are much greater than ESEM.
		<ul style="list-style-type: none"> Exposure to the space environment caused the amount of α_s to increase by 3%. The amount of ϵ, on the other hand, did not change. The surface was found to be rough and corroded. ← We assume that these changes are due to exposure to AO and UV rays. 	<ul style="list-style-type: none"> We obtained almost the same results as in the case of a ground simulation test. ⇒ This confirms that the ground simulation test was appropriate. 	
7	Black paint	<ul style="list-style-type: none"> The surface optical characteristics of a substrate do not depend on whether it is made of aluminum or CFRP. 	<ul style="list-style-type: none"> We obtained almost the same results as in the case of a ground simulation test. 	The surface characteristics of only S/N97, the sample exposed to the space environment, changed significantly. This is because the sample, contained in another lot, differed in coating condition from other samples.
		<ul style="list-style-type: none"> Exposure to the space environment caused the amount of α_s to increase by 3%. The amount of ϵ, on the other hand, did not change. ← We assume that these changes were caused by surface roughening due to exposure to AO and by carbon black exposure due to urethane resin loss. The chemical composition and condition changed presumably because of exposure to AO and UV rays. 	<ul style="list-style-type: none"> We obtained almost the same results as in the case of a ground simulation test. We obtained almost the same results as in the case of a ground simulation test. ⇒ This confirms that the ground simulation test was appropriate. 	

Table 5.5-1 (3/6) Summary of Evaluation of Individual Materials

No.	Sample name	Evaluation of sample exposed to space environment	Comparison with sample subjected to ground simulation test	Remarks
8 9	Solar cell	<ul style="list-style-type: none"> - Any significant change on the surface of the solar cells was not observed under a microscope. - It is recognized that the solar cells show no significant deterioration in the flight test, and that there are some problems on the measurement of the solar cell. 		
10 11 12 13	Cover glass for solar cell	<ul style="list-style-type: none"> - The transmittance of each exposed samples was reduced by about 1% in the whole range of wavelength. The transmittance of AR model made by The OCLI Company was reduced by about 2% the short wavelength region (about 400 nm - 750 nm). 		
14 15 16	Inter-connector material for solar cell	<ul style="list-style-type: none"> - The results of OM observation show that the configuration of the surface of the sample exposed in the space environment is different from that of the controlled sample or that of the AO-exposed sample in the ground simulation test, we dare say that it shows a medium form between them. 		
17 18	OSR for solar cell	<ul style="list-style-type: none"> - In the measurement of optical properties of the samples, 0213 SSM model (No. 17) made by OCLI Company, and CMX SSM model (No. 18) made by PPE Company showed slight change. - The change in reflectance must be so small that it is included in the range of error, and in investigating the cause of the change, more accurate evaluation considering reproducibility error of data is needed. The difference is so small that the impact on performance of OSR is small. 		

Table 5.5-1 (4/6) Summary of Evaluation of Individual Materials

No.	Sample name	Evaluation of sample exposed to space environment	Comparison with sample subjected to ground simulation test	Remarks
20	Bonded MoS ₂ film (HMB34 film)	<ul style="list-style-type: none"> • Polyamideimide and MoS₂ were found to be oxidized. • The friction characteristics were improved. ← MoS₂ scales appear to prevent oxidation on the surface. 	<ul style="list-style-type: none"> • The evaluation results are the same as in the case of the sample exposed to AO rays. 	EFFU: The surface oxidized and the friction life increased. These changes were reproduced in an ESEM test. Table 5.5-3 shows data on the friction characteristics of HBM34 film.
21	Binder of bonded MoS ₂ film (Polyamideimide A)	<ul style="list-style-type: none"> • A binder alone does not oxidize but disappears. • The friction life decreased extremely, since a decrease in film thickness made the surface rougher. 	<ul style="list-style-type: none"> • The friction life of the sample exposed to AO rays decreased significantly both because the surface became rougher and because film thickness decreased. • The friction life of the samples exposed to EB and UV rays increased. 	
22	Binder of bonded MoS ₂ film (Polyamideimide B)	<ul style="list-style-type: none"> • The results of evaluation of polyamideimide B do not significantly differ from those of evaluation of polyamideimide A. 		
23	Binder of bonded MoS ₂ film (Polyimide)	<ul style="list-style-type: none"> • The wear life decreased significantly. ← We assume that the coefficient of friction decreased because shear strength decreased with decreasing surface strength of film. 	<ul style="list-style-type: none"> • As is the case with the sample exposed to AO rays, the wear life of the sample exposed to the space environment decreased significantly. 	

Table 5.5-1 (5/6) Summary of Evaluation of Individual Materials

No.	Sample name	Evaluation of sample exposed to space environment	Comparison with sample subjected to ground simulation test	Remarks
19	Aluminum-deposited β cloth	<ul style="list-style-type: none"> There was no marked deterioration. (The amount of α_s increased by about 1%. The amount of ϵ and the mass did not change.) 	<ul style="list-style-type: none"> The Teflon layer of the sample exposed to AO rays disappeared at some locations. The deterioration of the sample exposed to the space environment was less severe than that of a sample which underwent a ground simulation test. 	EFFU: The amount of α_s increased by about 20%. The Teflon layer disappeared, so that glass fibers exposed. The level of deterioration is lower for ESEM than for EFFU.
24	Silica FRP	<ul style="list-style-type: none"> Abrasion resistance increased. Exposure to AO rays caused resin on the surface to disappear, so that glass fibers exposed. This led the initial thermal conductivity to lower and glass fibers to melt, thus reducing the rate of recession. 	<ul style="list-style-type: none"> As is the case with the sample exposed to AO rays, abrasion resistance increased. 	
25	Silicone adhesive (RTV-S691)	<ul style="list-style-type: none"> The sample did not deteriorate due to exposure to the space environment. The exposure caused a molecular-level change but did not affect resin performance. We assume that the weight reduction is attributed to gas removal (TML = 0.4%, rate of weight reduction = 0.3%) 	<ul style="list-style-type: none"> These results are similar to those of a ground simulation test. ⇒ This confirms that the procedure for the ground simulation test is appropriate. 	
26	Flexible OSR	<ul style="list-style-type: none"> The chemical structure of the sample did not markedly change. The surface thermal and optical characteristics changed slightly but within acceptable limits. We estimate that the weight reduction is due to contamination. Surface analysis proved that the sample was contaminated with organic oxygen. 	<ul style="list-style-type: none"> The surface thermal and optical characteristics of the sample exposed to the space environment more slightly changed, compared with a sample which underwent a ground simulation test. ⇒ This is because the environmental conditions during flight are more moderate than those on the ground. 	

Table 5.5-1 (6/6) Summary of Evaluation of Individual Materials

No.	Sample name	Evaluation of sample exposed to space environment	Comparison with sample subjected to ground simulation test	Remarks
27	Sputtered MoS ₂ film (RF sputtering method, base cooling)	- As for each skin, the non-irradiated surface of the AO-irradiated sample showed the same level of abrasion life as the unexposed surface of the flight sample, so that the AO hardly had an effect on the MoS ₂ skin without traveling around to the shielded surface. It is probable that such factors as AO and UV in the cosmic environment around the low altitude orbit would not affect the shielded MoS ₂ skin of the flight sample without traveling around to the bottom of the shielding plate, but the two facts that, first, no significant difference between the non-exposed and exposed surfaces of the flight sample was observed in terms of the coefficients of friction and the abrasion lives of the skins, and, second, the skins in those surfaces showed similar tribological properties suggest that the contaminants had an effect onto the bottom of the shielding plate.		
28	Sputtered MoS ₂ film (RF sputtering method, base heating)			
29	Sputtered MoS ₂ film (ECR ion beam sputtering method)			

Table 5.5-2 Measurements of Surface Thermal and Optical Characteristics of Thermal Control Film Containing no ITO

Table 5.5-2 Data on Mass and Surface Optical Characteristics of Thermal Control Film

Sample			Rate of absorption of Sunrays						Rate of vertical infrared ray emissions					Mass				
No.	Material name		S/N	Before exposure	After exposure	Change	Rate of change (%)	Average rate of change (%)	Before exposure	After exposure	Change	Rate of change (%)	Average rate of change (%)	Before exposure	After exposure	Change	Rate of change (%)	Average rate of change (%)
4	Thermal control film (polyimide/Al/Ni)	Sample exposed to the outer space environment	49	0.334	0.382	0.048	14.37	15.18	0.649	0.627	−0.022	−3.39	−3.54	28.383	27.123	−1.260	−4.44	−4.56
			410	0.329	0.383	0.054	16.41		0.652	0.625	−0.027	−4.14		28.820	27.629	−1.191	−4.13	
			411	0.332	0.381	0.049	14.76		0.646	0.626	−0.020	−3.10		28.269	26.825	−1.444	−5.11	
		Sample exposed to AO rays	43	0.335	0.376	0.041	12.24	10.84	0.649	0.611	−0.038	−5.86	−6.15	28.717	24.479	−4.238	−14.76	−15.10
			44	0.339	0.371	0.032	9.44		0.651	0.609	−0.042	−6.45		28.664	24.235	−4.429	−15.45	
		Sample exposed to UV rays	47	0.332	0.330	−0.002	−0.60	−0.90	0.648	0.650	0.002	0.31	0.15	28.634	28.607	−0.027	−0.09	−0.09
			48	0.333	0.329	−0.014	−1.20		0.642	0.642	0.000	0.00		27.834	27.811	−0.023	−0.08	
		Sample exposed to EB rays	41	0.328	0.331	0.003	0.91	0.92	0.653	0.652	−0.001	−0.15	−0.15	28.517	28.520	0.003	0.01	0.02
			42	0.325	0.328	0.003	0.92		0.652	0.651	−0.001	−0.15		28.517	28.525	0.008	0.03	
		5	Thermal control film (polyimide/Al/Ni/ITO)	Sample exposed to the outer space environment	59	0.350	0.349	−0.001	−0.29	−0.19	0.472	0.428	−0.044	−9.32	−1.97	29.488	29.089	−0.399
510	0.350				0.350	0.000	0.00	0.475	0.481		0.006	1.26	29.358	29.351		−0.007	−0.02	
511	0.354				0.353	−0.001	−0.28	0.466	0.476		0.010	2.15	28.785	28.784		−0.001	0.00	
Sample exposed to AO rays	53			0.352	0.349	−0.003	−0.85	−0.71	0.479	0.493	0.014	2.92	2.92	29.378	29.358	−0.020	−0.07	−0.04
	54			0.353	0.351	−0.002	−0.57		0.479	0.493	0.014	2.92		29.260	29.258	−0.002	−0.01	
Sample exposed to UV rays	57			0.356	0.388	0.032	8.99	9.62	0.483	0.403	−0.080	−16.56	−18.68	29.511	29.567	0.056	0.19	0.15
	58			0.351	0.387	0.036	10.26		0.481	0.381	−0.100	−20.79		29.339	29.373	0.034	0.12	
Sample exposed to EB rays	51			0.347	0.349	0.002	0.58	0.29	0.471	0.475	0.004	0.85	0.85	28.833	28.812	−0.021	−0.07	−0.08
	52			0.350	0.350	0.000	0.00		0.469	0.473	0.004	0.85		28.879	28.853	−0.026	−0.09	

Table 5.5-3 Comparison of Friction and Wear Characteristics of HMB34

	Unexposed sample	Sample exposed to the outer space environment
Initial coefficient of friction	0.142	0.162
Coefficient of friction at steady state	0.05-0.06	0.05-0.06
Friction life	1.24×10^6 cycles	1.42×10^6 cycles

Table 5.5-4 Comparison of Friction and Wear Characteristics of Solid Lubricant and Binder

		Initial coefficient of friction	Coefficient of friction at steady state	Friction life
Polyamideimide A	Unexposed sample	0.242	0.115-0.120	6.52×10^5
	Sample exposed to AO rays	0.341	0.118-0.122	2.48×10^5
	Sample exposed to UV rays	0.211	0.115-0.121	7.42×10^5
	Sample exposed to EB rays	0.225	0.115-0.122	7.79×10^5
	Sample exposed to the outer space environment	0.331	0.118-0.124	1.21×10^5
Polyamideimide B	Unexposed sample	0.230	0.115-0.126	5.98×10^5
	Sample exposed to AO rays	0.281	0.120-0.130	2.84×10^5
	Sample exposed to UV rays	0.243	0.115-0.121	6.54×10^5
	Sample exposed to EB rays	0.251	0.115-0.121	7.41×10^5
	Sample exposed to the outer space environment	0.311	0.118-0.133	2.11×10^5
Polyimide	Unexposed sample	0.182	1.092-0.104	5.81×10^5
	Sample exposed to AO rays	0.152	0.099-0.112	1.62×10^5
	Sample exposed to UV rays	0.178	0.092-0.099	3.31×10^5
	Sample exposed to EB rays	0.188	0.092-0.099	4.01×10^5
	Sample exposed to the outer space environment	0.211	0.099-0.117	1.11×10^5

Table 5.5-5 Changes in SiFRP Abrasion Characteristics

	Abrasion depth	Recession depth
Unexposed sample	3.8 mm	1.7 mm
Sample exposed to AO rays	3.4 mm	1.4 mm
Sample exposed to UV rays	3.4 mm	1.3 mm
Sample exposed to EB rays	3.1 mm	1.3 mm
Loaded sample	3.0 mm	1.1 mm

Note 1: An error ranges from -0.4 to $+0.4$ mm.

Note 2: ??? characteristic test

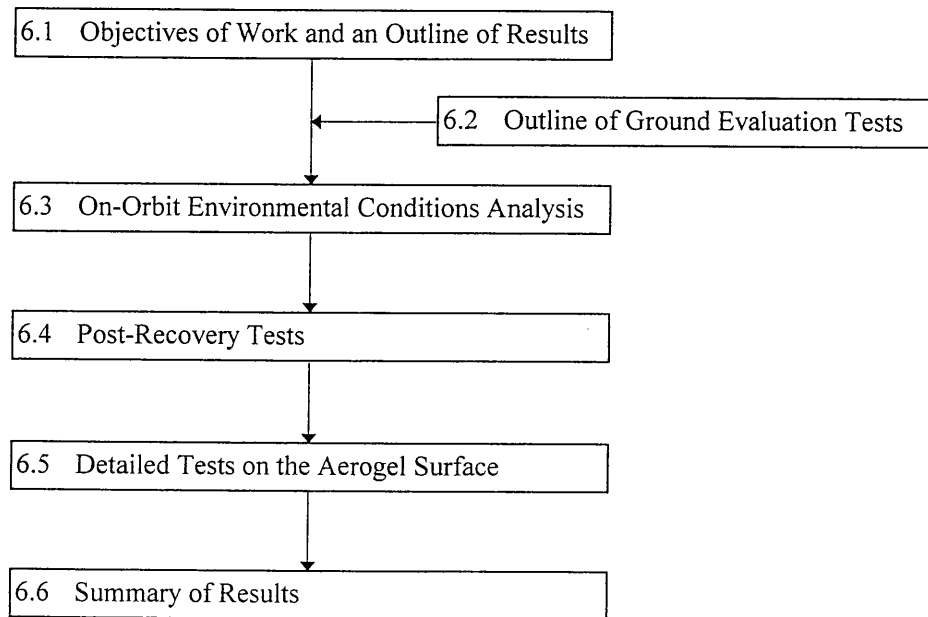
Before and after exposure to rays in a ground comparison test, an abrasion test is performed on a specimen by exposing it to CO₂ laser beams in the air to know a change in its abrasion resistance. For the same purpose, an abrasion test is also performed on a specimen before it is loaded into an MFD and after it is recovered. If the abrasion resistance of a material decreases due to exposure to environmental rays, a design margin for an abrasion resistance decrease is determined through comparison with an unexposed sample.

??? Characteristic Test Conditions

- Equipment used: A 5-kW CO₂ laser owned by the Laser Application Technology Center Co. (ML6050C from Mitsubishi Electric Corp.)
- Site: Laser Application Technology Center Co. in Nagaoka City, Niigata Prefecture
- Conditions for cleaning immediately before testing: Samples were not cleaned.
- Laser output: 875W (equivalent power density: 7.0 MW/cm²)
- Test environment: In the air
- Time of exposure to laser beams: 10 sec

6. Evaluation of Flight Articles of the Cosmic Dust Collectors

Work Flow in Chapter 6



6.1 Objectives of Work and an Outline of Results

6.1.1 Objectives

One objective is to analyze the effects caused on the capturing material of the dust collectors supplied by NASDA for MFD flights and the shape, particle size, composition, etc. of the dust captured. The other objective is to analyze the cosmic dust environment on the MFD orbit by examining the velocity, angle of incidence, etc. of the dust based on the results of the analysis mentioned above and ground tests.

6.1.2 Outline of Results

- (1) Effects produced on the capturing material of the dust collectors
 - With no rupture or the like occurring, the capturing material (aerogel) of the dust collectors was judged to have fully endured use in the flight environment.
- (2) Analysis of the shape, particle size, composition, velocity, angle of incidence, etc. of the dust captured
 - It was considered that no dust with a particle size of more than about 10 μm in diameter had impacted with the dust collectors at a velocity of 1 km/sec or over.
 - A detailed examination indicates the possibility of collision of the following two pieces of debris with the collectors in outer space:

Collector No.	Condition	Diameter	Length (Depth)	Material
PC7	Rod-shaped substance captured in hole	10 μm	1 mm	Silicon, oxygen, carbon
PC10	Substance sticking to crater	30 μm	<10 μm	Carbon

- Since the dust is not considered to have impacted at very high velocities, the debris captured seems to be:
 - debris emitted by the shuttle (STS-85) or
 - debris falling due to air drag (colliding from the direction opposite to the direction of travel).

(3) Dust environment

It is considered that the dust flux value (abundance value) for dust of sizes of several μm in NASA's calculation model (SSP-30425) is about 10 to 20 times as large as the actual value.

- There is a possibility that minute pieces of substance are emitted from the shuttle (or cargo).

6.2 Outline of Ground Evaluation Tests

6.2.1 Objective of Ground Tests

The objective of ground tests is to evaluate the following relations by carrying out a simulated dust irradiation experiment on the dust collector materials selected in the project “JFD Material Exposure Experiment (Design of Material Exposure Experiment Equipment)”:

- (1) Relations between the irradiation speed, angle of incidence, etc. of simulated dust and the effects on the shape, particle size, composition, etc. of simulated dust captured
- (2) Relations between the irradiation speed, particle size, composition, angle of incidence, etc. of simulated dust and the effects caused on the capturing material for dust collectors

6.2.2 Test Specimens

The configurations of ground test specimens are shown in the following figure and table:

- Figure 6.2.2-1: Configurations of Ground Test Specimens
- Table 6.2.2-1: Structures of Ground Test Specimens

6.2.3 Ground Test Conditions

The table below shows ground test conditions:

6.2.3 Results of Ground Tests (Outline)

- (1) A dust collector using silica aerogel (density: 0.03 g/cm³) captured almost all dust colliding at velocities of up to about 1 to 6 km/sec. It is considered possible to capture dust colliding at a maximum velocity of about 12 km/sec.
- (2) Interrelations were observed between the shapes of craters produced in the collector and impact parameters (velocity, particle size, etc.). It is considered possible to estimate dust impact energy, impact velocities, particle sizes, etc. from the shapes, depths, diameters, etc. of the craters.

The figure below shows the shapes of the craters and the items that can be estimated.

- Figure 6.2.3-1: Interrelations Between Crater Parameters and Dust Impact Parameters

Measurement and estimation procedures are described in section 6.4.1. (Figure 6.4.1-2: Aerogel Examination Procedure)

- (3) The simple analysis method based on kinematic theories about meteors qualitatively explains changes in the depth of craters and the size of particles captured. (This section describes the results of IHI's own research.)

The figures and table below show analysis conditions, changes in the depth of craters according to dust impact velocities, and the results of analysis of changes in the particle size of dust captured.

- Table 6.2.3-1: Analysis Conditions in Simple Analysis Method
- Figure 6.2.3-2: Changes in Particle Size of Dust Captured According to Impact Velocities (Comparison of Analytical Results and Experimental Results)
- Figure 6.2.3-3: Crater Depths and Dust Particles Sizes According to Impact Velocities (Comparison of Analytical Results and Experimental Results)

6.3 On-Orbit Environmental Conditions Analysis

6.3.1 Analysis Based on Space Station Design Standard Model of NASA

The frequency of dust impact with the MFD dust collector was analyzed using the space station design standard model of NASA (SSP-30425). The table below shows preconditions for calculations and the results of the analysis.

- Table 6.3.1-1: On-Orbit Dust Environment Prediction and Analysis

Dust impact velocities are as follows:

- (1) Space debris: approximately 1 to 16 km/s
- (2) Meteoroids: approximately 1 to 80 km/s

The diameter of dust particles that can impact with collectors in MFD missions is as follows:

- Shuttle orbit during MFD missions: 1 to 50 μm

6.3.2 Estimations Based on Other Flight Experiments

The figure below shows an example of capture results in a dust capturing experiment using aerogel.

- Table 6.3.2-1: On-Orbit Dust Capturing Experiments

Since the direction of collectors and the orbital altitude differ in the individual missions shown in the table above, these values cannot be used as they are in estimating the number of impact particles in the MFD/ESEM. In the case of EuReCa, in particular, it is considered that because of the high orbital altitude, the decrease in dust due to air drag was smaller, resulting in a larger number of dust particles per collector per day than in other missions.

Based on the results of missions on low orbits (in the neighborhood of 300 km), the number of impact dust particles in the MFD/ESEM mission is estimated at 0 to 1.

6.3.3 Consideration

Results based on NASA's calculation model (section 6.3.1) indicates the possibility of collision of dust particles 10 μm or larger in diameter that can have direct correspondence with ground tests. According to the NASA calculation model, there can also be collision of a significant number (20 or so) of smaller dust particles.

There is, however, a difference between this figure and an estimated value (not more than 1 as mentioned in section 6.3.2) based on the measurement results in other flights.

The volume of dust on orbits has not so far been measured a sufficient number of times, and it is considered that large errors are involved in the NASA models at low altitudes. It is expected, therefore, that the calculated frequency of collision is different from the actual frequency.

For example, it is known that when calculated values based on the NASA models are compared with measured values with respect to dust particles about 10 cm or larger in diameter, the difference between them increases substantially at altitudes less than 300 km.

- Figure 6.3.3-1: Difference Between Measured and Model Values of Volume of Debris Fluxes 10 cm in Diameter

In the above figure, the actual volume is about one tenth of the model value at altitudes lower than 300 km.

In the meantime, while it is assumed in the NASA calculation model that the particle size distribution of debris does not depend on orbital altitudes (i.e. the volume ratio of particle sizes is constant at any orbital altitude), the orbital decay due to air drag actually becomes larger as the particle size becomes smaller.

It is expected, therefore, that the volume of pieces of debris smaller than 10 cm in diameter is even smaller than the model value.

The figure below shows an example of calculation of the orbital lifetime of particles 1.6 μm in diameter on the earth orbit.

- Figure 6.3.3-2: Example of Research on Orbital Lifetime of Particles on Earth Orbit

6.3.4 Evaluation

(1) Prediction of Dust Collision Frequency

The volume of debris based on the NASA calculation model may be about ten times larger than it actually is. In addition, the orbital lifetime of dust several μm in diameter is considered short. It is considered, therefore, that the value calculated in section 6.3.1 is the upper limit of the frequency of dust collision. Actual values may be one tenth or one twentieth of this upper limit.

(When the cargo side of the shuttle faces the earth, meteoroids are interrupted by the earth, and thus the frequency of dust collision is further reduced by half.)

(2) Prediction of Dust Material

It is estimated from Figure 6.3.3-2 that the orbital lifetime of particles at the altitude of the MFD/ESEM (STS-85) (296 km) is approximately 15 minutes. It is considered, therefore, the volume of debris emitted from shuttles and satellites at the same orbital altitude is small.

As a consequence, the following dust is considered captured by the MFD/ESEM (STS-85):

- a. Meteoroids
- b. Debris whose perigee is near the altitude of the MFD/ESEM (STS-85)
- c. Debris emitted by shuttles or equipment on board
- d. Debris falling to the earth due to air drag

(3) Significance of Measurement

As examined in section 6.3.3, the volume of dust at low altitudes is so uncertain that it may be more than ten times larger than it actually is, and thus the frequency data obtained from measurement in this flight will provide meaningful information.

6.4 Post-Recovery Tests

6.4.1 Examination Procedures

The examination flow is shown in the following figures:

- Figure 6.4.1-1: Dust Collector Examination Procedure
- Figure 6.4.1-2: Aerogel Examination Procedure

The following figures show dust collector positions, etc.:

- Figure 6.4.1-3: MFD/ESEM Mounting Condition
- Figure 6.4.1-4: Direction of Dust Collection Assembly
- Figure 6.4.1-5: Configuration of Dust Collector Unit

6.4.2 Particulars of Tests

6.4.2.1 Method of Testing Effects on Capturing Material for Dust Collectors

Observe the surface condition (including sketches and taking photos), measure dimensions and weight, and compare the results with the corresponding pre-flight figures.

6.4.2.2 Method of Testing Captured Dust

Using a magnifying glass or the like, visually check the collector surface (space side), and record the number, positions, sizes, and shapes of craters. Also observe it from a side under penetrating light, checking the depths, directions, and other details of the craters.

6.4.2.3 Other

Make separate records of traces (damage) on collector holders and mounting plates.

6.4.3 Test Results

6.4.3.1 Effects on Capturing Material for Dust Collectors

Test results are shown in the following figures and table:

- Table 6.4.3.1-1: Results of Tests on Capturing Material for Dust Collectors
- Figure 6.4.3.1-1: Example of Change in Surface Condition of Capturing Material for Dust Collectors
- Figure 6.4.3.1-2: Results of Measurement of Dimensions of Capturing Material for Dust Collectors
- Figure 6.4.3.1-3: Results of Measurement of Weight of Capturing Material for Dust Collectors

The above results can be summarized as follows:

- Surface condition: Scarcely any change (Figure 6.4.3.1-1), except that the surface adhesiveness is lost after the flight
- Dimensions: Slightly smaller (approximately 1 mm: Figure 6.4.3.1-2) after the flight
- Weight: No significant change (Figure 6.4.3.1-3)

6.4.3.2 Inspection of Captured Dust

No craters of sizes that could be confirmed using a magnifying glass were detected (about 100 μm or larger in diameter).

6.4.4 Consideration of Test Results

6.4.4.1 Effects on Capturing Material for Dust Collectors

(1) Detection of Surface Adhesiveness

The loss of surface adhesiveness indicates that the $\text{Si}(\text{CH}_3)_3$ component of the aerogel is lost.

Assumed changes in the surfaces are shown in the figure below.

- Figure 6.4.4.1-1: Assumption of Changes in Aerogel Surface

It is assumed from the loss of the $\text{Si}(\text{CH}_3)_3$ component that there is a deterioration in the hydrophobic property. It is considered, therefore, that high humidity must be avoided when handling the material after flights.

(2) Changes in Dimensions

Since slight reductions occur in dimensions, it is necessary to take these changes into consideration when fixing (mounting) aerogel in the JEM, etc. as well as in the MFD.

(3) General

There was no aerogel breakage or the like, and little change was observed in the surface condition after the flight. It is expected, therefore, that aerogel can fully endure use without being so firmly fixed as in the MFD/ESEM.

6.4.4.2 Inspection of Captured Dust

It is judged that there are no craters of sizes that can be confirmed using a magnifying glass (about 100 μm or larger in diameter).

Based on the results of ground evaluation tests, it is considered that the diameter (D_{trk}) of craters on the aerogel surface is about eight times as large as the diameter (D_p) of colliding dust particles.

It is considered, therefore, that there was no collision of dust particles 10 μm or larger in diameter (and at impact velocities of 1 km/sec or over) that can have direct correspondence with ground tests.

6.4.5 Summary of Test Results

- No breakage, etc. of the capturing material (aerogel) for dust collectors occurred, and it was judged that the material had fully endured use in the flight environment, except that some changes were observed in surface characteristics, dimensions, etc.
- It was considered that there had been no collision of dust particles 10 μm or larger in diameter and at impact velocities of 1 km/sec or over that can have direct correspondence with ground tests.

6.5 Detailed Tests on the Aerogel Surface

Since no dust that can have direct correspondence with ground tests was detected in section 6.4, more detailed examinations were made of the aerogel surface in order to detect traces of dust collision.

6.5.1 Estimation of Dust Collision Condition and Targets for Detailed Examinations

6.5.1.1 Assumption of Dust Collision Condition

In case of collision of dust, it is estimated based on the results described in section 6.4 that the diameter of dust particles is not larger than about 10 μm or that the impact velocity does not exceed 1 km/sec. The following assumptions can be made about the collision of dust:

- The size of colliding dust particles is estimated at 5 microns to less than 1 micron.
(According to SSP-30425 calculations, the number of colliding dust particles is a total of about 20 for four collectors [see section 6.3.1].)
- There is dust or its evaporation (pieces, sticking substance) on the gold coated surface or just under the gold coating(i.e. at very shallow points in the aerogel).
(According to extrapolation of the results of ground experiments, the diameter of craters is estimated at about 10 μm and the depth at several μm to 500 μm when the diameter of dust particles is 1 μm .)
- When dust collided at very low velocities (tens of meters per second or less), there is a possibility that the dust is sticking to the surface.
- Irrespective of particle size, dust is considered made largely of inorganic substances such as Al, Mg, Fe, Na, Ca, Ti, K, Ni, Mn, and Cr.

6.5.2 Targets for Detailed Examinations

Based on the estimated dust collision condition mentioned in section 6.5.1, the following targets were set for detailed examinations:

- The primary target is to detect dust particles down to 1 μm in diameter or to optically detect craters caused by collision of such dust (about 10 μm in diameter) and substances sticking to the surface.
- Another target is to analyze the components of detected substances in the greatest possible detail.

6.5.3 Consideration of Detailed Examination Procedure

It is necessary to examine the gold coated surface or the part just under the gold coating (i.e. very shallow points in the aerogel). To this end, the entire gold coated surface was examined uniformly from above using a high-powered microscope (magnifying power of 100 to 150, which is equivalent to power of 200 to 500 on the monitor screen).

The detailed examination procedure is shown in the following figures:

- Figure 6.5.3-1: Procedure for Detailed Examination of Exposed Aerogel Surface
- Figure 6.5.3-2: Illumination Method for Aerogel Examination

As a result of trade-off, it was considered appropriate to use a small stage in IHI as facilities to uniformly move the visual field of observation. The table below shows the trade-off of the optical examination method.

- Table 6.5.3-1: Trade-off of the Optical Examination Method
(Refer to Figure 6.5.3-3: Moving Method for Aerogel Examination.)

The figures below show the configuration of the examination equipment and the condition of carrying out the examination.

- Figure 6.5.3-4: Configuration of Examination Equipment
- Figure 6.5.3-5: Condition of Carrying Out Examination

6.5.4 Examination Results

The examinations were conducted using the following as criteria:

(1) Gold coating in holes and concavities:

There must be no gold coating or coating fragments in holes or concavities. (Holes with such coating or fragments are judged as present before the flight.)

(2) Shape of holes and concavities:

As in craters, rims must be seen around holes.

(3) Presence of ejecta:

As in craters, ejecta (scatters caused by collisions) must be seen around holes.

(4) Presence of sticking or captured substance:

There must be sticking or captured substance.

Of the above conditions, (1) was designated an absolute condition, and those which meet either or both of (2) and (3) were chosen as traces of dust collision.

The following table and figures show traces discovered and CCD fiberscope images:

- Table 6.5.4-1: Traces Discovered in Detailed Examination
- Figure 6.5.4-1: External View of PC7A
- Figure 6.5.4-2: Dimensions of PC7A
- Figure 6.5.4-3: External View of PC7B

With regard to the external views of PC7C and PC10D, optical microscopic photos are shown in sections 6.5.5.3 and 6.5.5.4 because their CCD images are unclear.

6.5.5 Analysis and Consideration

6.5.5.1 PC7A

(1) Shape, Particle Diameter, etc.

The figure below shows an optical microscopic photo and an SEM photo of PC7A.

- Figure 6.5.5.1-1: Optical Microscopic Photo and SEM Photo of PC7A

As seen from the above figure, PC7A is not a hole but a state in which needle-shaped (or rod-shaped) material “sticking into” the aerogel.

Since the material is shaped like a rod with a laminated structure, it is considered artificial, not natural, material. In addition, branch-like projections are seen around the hole, and it is considered that the collision with the collector occurred at a very low velocity (<1 km/sec).

(2) Consideration of Impact Velocity

A ground evaluation test was conducted using a nearly spherical body (ellipse) about $10\text{ }\mu\text{m}$ in diameter and at impact velocities 1 km/sec and over. It was considered difficult to estimate the impact velocity, maintaining direct correspondence to the test data.

Therefore, the impact velocity was estimated by the simple analysis method (based on Kitazawa et al. [1998]). (For consistency between the results of analysis and those of the ground test, see section 6.2.3.)

The table below shows the analytical model for simple analysis.

- Table 6.5.5.1-1: Analytical Model

Results of analysis are as follows:

- Minimum velocity (lower limit of impact velocity): 0.6 m/s ($=2.2\text{ [km/h]}$)
- Maximum velocity (upper limit of impact velocity): 31 m/s ($=112\text{ [km/h]}$)

As seen from the above results, the captured substance of PC7A does not indicate the so-called “collision at a very high velocity (about 3 km/sec or over).” It is difficult, therefore, to consider that debris flying on a different orbit than the shuttle collided.

Supposing that the substance collided in space, it is considered that the substance was on the same orbit as the shuttle because its relative velocity in relation to the shuttle is very small.

It should be noted, however, that as seen in section 6.3.3 (Figure 6.3.3-2), the orbital lifetime of dust-sized particles is short on low orbits such as the MFD/ESEM orbit. It is therefore considered that it is not debris emitted from another spacecraft flying on the same orbit. It is assumed that the debris was generated from either of the following sources:

- Debris emitted from the shuttle itself or from other experiment equipment on cargo or a free flyer floated around the shuttle and collided with the collector when, for example, the shuttle changed its position.
- Debris falling due to air drag collided from the direction opposite to the flight direction of the shuttle.

(3) Consideration of Arrival Direction

The figures below show the direction of the hole.

- Figure 6.5.5.1-4: View from Direction Perpendicular to Each Surface
- Figure 6.5.5.1-5: Angle of Impingement (View A in Figure 6.5.1-3)

Judging from the direction of arrival of the hole, it is assumed that the captured substance collided almost perpendicularly from the space side (which is opposite to the exposed material side).

(4) Consideration of Substance

The figure below shows the results of qualitative analysis of EDX and element mapping.

- Figure 6.5.5.1-2: Results of Qualitative Analysis of EDX

Major elements detected were silicon (Si), carbon (C), and oxygen (O).

When its shape is taken into consideration, the substance is assumed to be:

- Si sticking to carbon fiber,
- a fragment of SiC, or
- carbon sticking to SiO₂.

Although the presence of Si was conspicuous in the qualitative analysis, the presence intensity of Si was low in the element mapping. It is considered, therefore, that the source is carbon sticking to SiO₂.

The captured substance is transparent both in the optical microscopic photo (Figure 6.5.5.1-1) and in the CCD image (Figure 6.5.4-1). When this fact is considered together with the results of qualitative analysis, the captured substance is considered to be SiO₂.

In the meantime, a very small amount of gold was detected. It seems that this is gold on the aerogel surface that fell off when the periphery of the crater was being cut off and stuck to the captured substance. The figure below shows the condition of the gold sticking to the captured substance and the condition of deposition to the nearby aerogel (at the root of PC7A).

- Figure 6.5.5.1-3: Comparison of Gold Sticking Conditions

The deposited gold is uniform and fine. The captured substance has gold on a very small part of its surface. The gold detected from the captured substance is considered to have stuck after the substance was captured.

(6) Photo Checking and Process Confirmation

In the case of the MFD dust collector, the surface to be exposed is coated with gold before the collector is assembled. Therefore, if any substance is sticking to aerogel, the substance and the aerogel are together coated with gold.

Meanwhile, if any substance collides with the exposed surface in space, it is expected that the substance will break the gold coating (or will be put on the gold coating).

As shown in the figure below, however, the position of PC7A is on the edge of the gold coating.

- Figure 6.5.5.1-6: Approximate Position of PC7A

It is difficult to judge by only the visual inspection of the “gold coating” whether the captured substance of PC7A collided with the collector on earth or in space.

In the meantime, the SEM photos (Figure 6.5.5.1-1 (4/6) show a thin coating of gold on the aerogel surface, and SEM photo 2 shows how the coating is off and turned up. Since no gold is deposited on the captured substance, the substance is considered to have collided after the deposition of gold.

Further, the processes before and after the flight were checked using enlarged photos (taken by KSC) of the periphery of the point of collision of PC7A before and after the flight. The following figure and table show the results of checking.

- Figure 6.5.5.1-7: Enlarged Photos of Periphery of PC7A Before and After Flight- Table 6.5.5.1-2: Causes of Inclusion of Foreign Substance into Ground Process

As shown in Figure 6.5.5.1-3, PC7A cannot be recognized in the enlarged photos before and after the flight because of insufficient magnifying power and contrast.

In the ground process, however, there seems to be no factor responsible for the inclusion of silicon or carbon fiber at least after the deposition of gold. (In particular, the inclusion of foreign substance is quite unlikely for the period after the flight to the discovery of PC7A, when the collector was placed in a clean-room environment (or in a nitrogen-substituted packaged environment).

Although it cannot be confirmed from the enlarged photos, it seems quite likely that the captured substance of PC7A collided and was captured in space in consideration of the peeling of the gold coating and the process checking.

6.5.5.2 PC7B

As shown in Figure 6.5.4-3, PC7B (and PC7C [section 6.5.5.3]) is spherical with an uneven surface. It is shaped like a “confetto.” This shape is like that of the so-called “brownly particles,” that is, fluffy cosmic dust particles collected in the stratosphere. The figure below shows an example of fluffy particles.

- Figure 6.5.5.2-1: Example of Fluffy Particles Captured in Stratosphere

No fluffy particles of space origin as mentioned above have ever been captured in space. In the EuReCa mission, however, a report was made on particles shaped like that of PC7C, though collision of these particles in space has not been confirmed.

The figure below shows an example of fluffy particles discovered in the aerogel of EuReCa.

- Figure 6.5.5.2-2: Example of Fluffy Particles Discovered in Aerogel of EuReCa

PC7B is similar to fluffy particles in shape, but there is no convexity in its periphery. Since substance did not stick into the aerogel (simply sticking onto the surface), it is not considered that PC7B collided with a collector.

Like PC7C, which will be described in the next section, PC7B is considered to be a fragment (small particle) of aerogel that stuck to the collector during operation.

With regard to optical microscopic photos and material data, no analytical data was obtained because of breakage of surface aerogel.

6.5.5.3 PC7C

The figure below shows optical microscopic photos, SEM photos, and results of EDX analysis of PC7C.

- Figure 6.5.5.3-1: Optical Microscopic Photos and SEM/EDX Photos of PC7C

Although PC7C is similar to fluffy particles in shape, the possibility of “collision of substance” seems to be small because substance did not stick into the aerogel (simply sticking onto the surface).

Since no components other than silicon (Si), oxygen (O) and gold (Au) were detected, it is considered that aerogel particles stuck to the surface. A tiny amount of carbon (C) detected is traceable to carbon coating carried out in SEM observation.

6.5.5.4 PC10D

The figure below shows optical microscopic photos, SEM photos, and results of EDX analysis of PC7D.

- Figure 6.5.5.3-1: Optical Microscopic Photos and SEM/EDX Photos of PC10D

The main component of the residual substance is carbon (C). Weak reaction of silicon and oxygen seems attributable to the fact that the aerogel is covered in the two layers of sticking and gold coating.

A crater-like convexity (with a rim around it) was observed, and there was a trace of scattered ejecta. It is hence considered that the convexity was generated by a collision of substance. It is unlikely, however, that the collision occurred at a high velocity because there was some remainder without being evaporated. Since there was no such element as iron or magnesium, the colliding substance is assumed to be debris, not meteoroid.

Like PC7A, the substance is assumed to have been emitted from the shuttle or is debris that was falling under air drag (colliding from the side opposite to the direction of flight).

6.5.6 Summary of Detailed Examination

A detailed examination was made of the surface of the capturing material (aerogel) for dust collectors with the aim of detecting dust particles of diameters down to about 1 μm , their craters (about 10 μm in diameter), or substance sticking to the surface.

Four traces (pieces of substance) were discovered. Two of them may have collided with the collector in space. However, their impact velocities could hardly be very high. Therefore, if these pieces collided in space at all, it seems proper to assume that they were emitted from the shuttle (STS-85) or were debris falling under air drag and colliding from the side opposite to the direction of flight.

Of the captured pieces, PC7A is considered to be carbonaceous substance sticking to SiO_2 fiber. Since SiO_2 fiber (such as Q-Fiber) was used as a heat insulator in the shuttle, it seems appropriate to examine if there is any relation to the fiber in the shuttle.

6.6 Summary of Results and Future Tasks

6.6.1 Summary of Results

(1) Effects on Capturing Material for Dust Collectors

- No breakage, etc. of the capturing material (aerogel) for dust collectors occurred, and it was judged that the material had fully endured use in the flight environment.

(2) Analysis of the Shape, Particle Size, Composition, Velocity, Angle of Incidence, etc. of the Dust Captured

- It was considered that no dust with a particle size of more than about 10 μm in diameter had impacted with the dust collectors at a velocity of 1 km/sec or over.
- A detailed examination indicates the possibility of collision of the following two pieces of debris with the collectors in outer space:

Collector No.	Condition	Diameter	Length (Depth)	Material
PC7	Rod-shaped substance captured in hole	10 μm	1 mm	Silicon, oxygen, carbon
PC10	Substance sticking to crater	30 μm	<10 μm	Carbon

- Since the dust is not considered to have impacted at very high velocities, the debris captured seems to be:
 - debris emitted by the shuttle (STS-85) or
 - debris falling due to air drag (colliding from the direction opposite to the direction of travel).

(3) Dust Environment

- It is considered that the dust flux value (abundance value) for dust of sizes of several μm in NASA's calculation model (SSP-30425) is about 10 to 20 times as large as the actual value.
- There is a possibility that minute pieces of substance are emitted from the shuttle (or cargo).

6.6.2 Future Tasks

(1) Capturing Material

Based on the results of the ground tests and flight, the effectiveness of aerogel as a dust capturing material has been confirmed. It is considered that the following improvements are required:

- Reduce variations in density and size, and make the uneven surface smoother
- Reduce waste sticking in the manufacturing process

(2) Ground Evaluation Tests

Based on the results of the ground tests, the technology has been established that can effectively capture dust that has so much energy as to affect space materials (10 μm in diameter and 1 km/sec in velocity or over). It is necessary to determine the upper limit of the sensitivity of measurement of dust on or in aerogel in order to compare meteoroid and debris flux data obtained with the use of the collector developed this time with the results of measurement using other materials or to use this collector as a monitor of debris emitted from stations and shuttles.

To be more specific, the following tests are considered necessary:

- Tests at lower velocities (1 km/sec)
- Tests on smaller particles (less than 10 μm in diameter)
- Tests to compare aerogel with aluminum, foil, and other materials
- Collision tests using fiber, blanket, paint, and other materials as dummy dust

(3) Test Method

In addition to improvement of the aerogel surface, the following work is considered necessary in order to use the collector for measurement of smaller dust particles colliding at lower velocities (10 μm or less in diameter and 1 km/sec or less in velocity):

- More detailed pre-flight tests (corresponding to detailed examinations)
- Construction of facilities and systems for storage and analysis of collected samples (to realize consistent analysis in the same testing laboratories)

Table 6.2.2-1 Structures of Ground Test Specimens

Specimen type	Property of dust irradiation surface	Capturing material for dust collector (Aerogel)			Between aerogel layers
		Thickness per sheet	Number of layers	Total thickness	
A	Gold evaporated	20 mm	4 ^{*1}	80 mm ^{*1}	
B	Gold evaporated	20 mm	4 ^{*1}	80 mm ^{*1}	Gold foils (Thickness: 10 μm × 2)

Note: ^{*1}) When it was expected with certainty that irradiated dust would stop on the first layer of aerogel or on the upper surface of the second layer, two layers (40 mm thick) were used.

Table 6.2.3-1 Ground Test Conditions

Item		Set conditions	Reasons for settings
Environment	Degree of vacuum (Torr)	10^{-5} or less	This value is set to minimize the dust abrasion caused by dust when flying in the air.
	Test chamber temperature (°C)	Room temperature	This value is set to ensure a smooth experiment with the existing facilities (plasma gun, two-stage light gas equipment).
Simulated dust	Shape	Almost spherical	Simulated dust as spherical as possible is used for grasping the degrees of deformation and damage caused by the impact at the time of capturing dust.
	Particle size	10 - 400 μm	<ul style="list-style-type: none"> • With MFD, there is a high probability of collision of dust of particle sizes from 1 to 50 μm. • Dust particles need to be of sizes to pass through the first layer of aerogel (50 to 100 μm) for the purpose of evaluation of the effect of the foils on the boundary surface of the type B model. • Practically, it is difficult to obtain simulated dust of particle sizes less than 25 μm.
		1 mm	• This large particle size is adopted to evaluate dependence on particle size.
	Material	Alumina (Al_2O_3)	Alumina is used to simulate discharges from solid rocket motors, which constitute the bulk of artificial dust.
		Olivine [Silica (SiO_2) particles] Glass	Particles that contain silica, a typical component of natural dust, are used.
Impact conditions	Impingement rate (km/sec)	3 - 14 km/sec	The average on-orbit impact velocity is expected to be 10 km/sec, and the maximum velocity to be 16 km/sec. With the existing facilities, however, 14 km/sec is the highest velocity that can be attained.
	Angle of incidence (degrees)	90 degrees	<p>Agreement between the direction of craters (impact holes) is to be checked.</p> <p>The angle of incidence is set at 90 degrees for the following reasons:</p> <ul style="list-style-type: none"> • It is easy to set this angle when making tests. • Craters being vertical, the collector area required for each test can be minimized. A single specimen can therefore be used for several tests. (It is expected that oblique impingement will produce slanted craters, making it difficult to perform irradiation a number of times with a single specimen.
		45 degrees, 20 degrees	For evaluation of dependence on the angle of incidence

Table 6.2.3-2 Analysis Conditions in Simple Analysis Method

Parameters	Sign	Value	Unit	Remark
Diameter of the Projectile	Dp	50×10^6	m	
Density of the Projectile	—	4.3×10^3	kg/m ³	for Al ₂ O ₃
Latent Heat of the Projectile	Q	5.0×10^6	J/kg	
Drag Coefficient of the Projectile	Γ	0.5	—	
Heat-Transfer Coefficient	Λ	0.1, 0.5, 1.0	—	3 cases are calculated.
Density of the Aerogel	ρ	3.0×10^1	kg/m ³	
Tensile Strength of the Aerogel	Ts	4.8×10^2	Pa	
Fracture Toughness of the Aerogel	Kc	2.4×10^2	Pa · m ^{1/2}	
Poisson's Ratio of the Aerogel	ν	0.2	—	
Young's Modulus of the Aerogel	E	1.0×10^7	Pa	

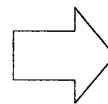
Table 6.3.2-1 Other Dust Capturing Experiments (Based on Tosu [1995] and NASA Home Page)

Flight	Period	Number of days on orbit	Collector area (m ²)	Orbital altitude (km)	Number of craters	Number of craters per day per piece of aerogel (crater/0.01 m ² /day)	Remarks
STS-47	Sep. 12 - 20, 1992	8	0.165 (Effective area)	307	≥4	≥0.03	21 pieces of aerogel on board (Crew included Mr. Mori of Japan.)
STS-57	Jun. 21 - 30, 1993	10	0.165 (Effective area)	467	—	—	21 pieces of aerogel on board
STS-60	Feb. 3 - 11, 1994	8	1.6 (Effective area)	354	≥24	≥0.02	160 pieces of aerogel on board
STS-64	Sep. 9 - 20, 1994	11	0.165 (Effective area)	259	—	—	21 pieces of aerogel on board
STS-68	Sep. 30 - Oct. 11, 1994	11	0.165 (Effective area)	222	—	—	21 pieces of aerogel on board
STS-69	Sep. 7 - 18, 1995	11	0.27 (?)	352	—	—	27 pieces of aerogel on board
STS-72	Jan. 11 - 20, 1996	9	0.165 (Effective area)	463	—	—	21 pieces of aerogel on board (Crew included Mr. Wakata of Japan.)
EuReCa	Aug. 2, 1992 - Jun. 24, 1993	326	0.04 (Effective area)	502	12	0.04	According to Brown et al. [1995]
STS-85 (MFD/ESEM)	Aug. 7 - 19, 1997	12	0.04 (Effective area)	296	[Estimated from other missions: 0 to 1 crater/all collectors]		

Table 6.3.1-1 On-Orbit Dust Environment Prediction and Analysis (MFD dust collectors of NASDA only)

Analysis Conditions

		MFD
Orbital altitude		296 km
Angle of orbital inclination		57 degrees
Dust collector	Area	100 mm × 10 mm × 4
	Face direction	Shuttle flight direction
	Exposure date	August 7, 1997
	Exposure time	56 hours
Shuttle position		Cargo side is space side.
Environment model		Meteorite/Space Lab Environment Model (NASA-SSP 30425)



Results of Analysis

Dust diameter [μm] (Dust mass [gram])	Number of pieces
1 - 5 (10^{-11} - 10^{-9})	24.8
5 - 10 (10^{-9} - 10^{-8})	0.5
10 - 50 (10^{-8} - 10^{-6})	0.1
50 - 100 (10^{-6} - 10^{-5})	—
100 - 500 (10^{-5} - 10^{-3})	—
500 - 1000 (10^{-6} - 10^{-2})	—

Table 6.4.3.1-1 Results of Inspection of capturing Material for Dust collectors

PC (S/N)	Layer number	No.	Condition rank	Special mention about condition			Dimensions (mm)									Weight (g)			Density		
							a			b			c								
				Before flight	After flight	Evaluation	Before flight	After flight	Ratio (after/ before)	Before flight	After flight	Ratio (after/ before)	Before flight	After flight	Ratio (after/ before)	Before flight	After flight	Ratio (after/ before)	Before flight	After flight	Ratio (after/ before)
PC 10 (S/N 001)	1	Gold-1	A		Mesh mark left on surface	No remarkable change is obtained 															

Table 6.5.3-1 Trade-off of the Optical Examination Method

Evaluation Item		NAL-1 (SFU examination table)		NAL-2 (SFU examination table)		IHI		Company N		Company T		NASDA (EFFU examination table)	Remarks
Moving method (See Figure 6.5.3-3)		a. (Movable microscope)		a. (Movable microscope)		b. (Movable mounting stand)		b. (Movable mounting stand)		b. (Movable mounting stand)		a. (Movable microscope)	
Coordinate Measurement	Can coordinate values be specified and reproduced?	△		⊙		○		○		○		⊙ Automatic movement (laser) Manual (color laser)	
	Can entire surface be uniformly surveyed?	△	Manual	⊙	Automatic	○	Manual	△		△		⊙ Automatic scanning range specification	
	Is movable range sufficient (5 cm x 5 cm or over)?	⊙				△		△	25 mm MAX 75 mm (magnifying power of 200 fixed)	△		⊙	
Use of Optical System	Can an optical microscope attached?	⊙		○	(To be rechecked)	⊙		⊙		⊙		×	
	Can a high-powered microscope used?	⊙	Power of up to about 800	⊙		⊙	Power of up to about 1,000	⊙		⊙		⊙ Power of up to 6,500	Both NAL and IHI use substantially the same fiberscopes. Company T uses a similar but more powerful one.
	Can photos and images taken?	⊙		⊙		⊙		⊙		⊙		⊙	
Illumination	Can transmitted illumination be used?	⊙		⊙		○	Small table is used. Illuminated from under, from a slanting direction.	△		⊙		×	See Figure 6.5.3-2.
	Can reflected illumination be used?	⊙		⊙		⊙		⊙		⊙		×	See Figure 6.5.3-2.
Environment, etc.	Can examinations be made without cutting aerogel?	⊙		⊙		⊙		△		⊙		⊙	
	Can clean-room environment be maintained?	△		○		⊙		△		△		△	
	Is environmental vibration level sufficiently low?	△		△		⊙		⊙		⊙		⊙	
	Can work be linked to chemical analysis?	△		△		△		⊙		○		△	
Cost	Examination time and charges	△		○		○		△		△		○	
	Is it scarcely necessary to add or renovate facilities?	○		⊙	However, anti-vibration measures or late-night work is necessary.	○	Improvement of movable table	△		⊙		⊙	
Evaluation		△		○		⊙		△		△		○	
Problems		<ul style="list-style-type: none"> - NAL's approval is required to borrow this. - Large environmental vibrations make it difficult to use high magnifying power. - Since the scope is moved manually, it is difficult to measure coordinates. 		<ul style="list-style-type: none"> - NAL's approval is required to borrow this. - Large environmental vibrations make it difficult to use high magnifying power. 		<ul style="list-style-type: none"> - It is necessary to improve movable table or buy new one. - It is necessary to adjust schedule for use of microscope. 		<ul style="list-style-type: none"> - There is no specialist who can judge craters. 		<ul style="list-style-type: none"> - There is no specialist who can judge craters. 			

Table 6.5.4-1 Traces Discovered in Detailed Examination

Dust Collector No.		PC 7			PC 10
Code		A	B	C	D
Condition		Hole and rod-shaped substance	Sticking substance	Hole (captured substance?)	Hole
Size	Diameter	10 μm	40 μm	10 - 30 μm	10 - 30 μm
	Depth	Approx. 1 mm	—	<10 μm	<10 μm
CCD Image No.		Figure 6.5.4-1, 2	Figure 6.5.4-3	—	—

Table 6.5.5.1-1 Analytical Model

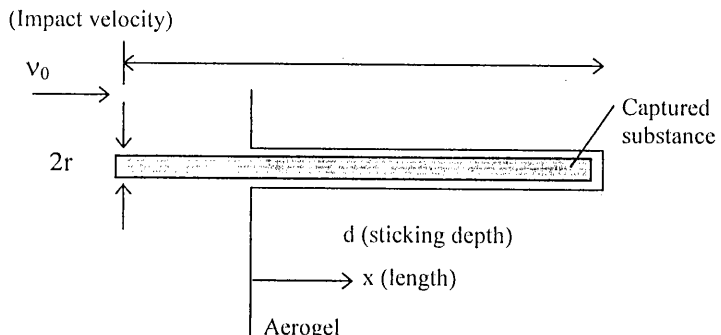
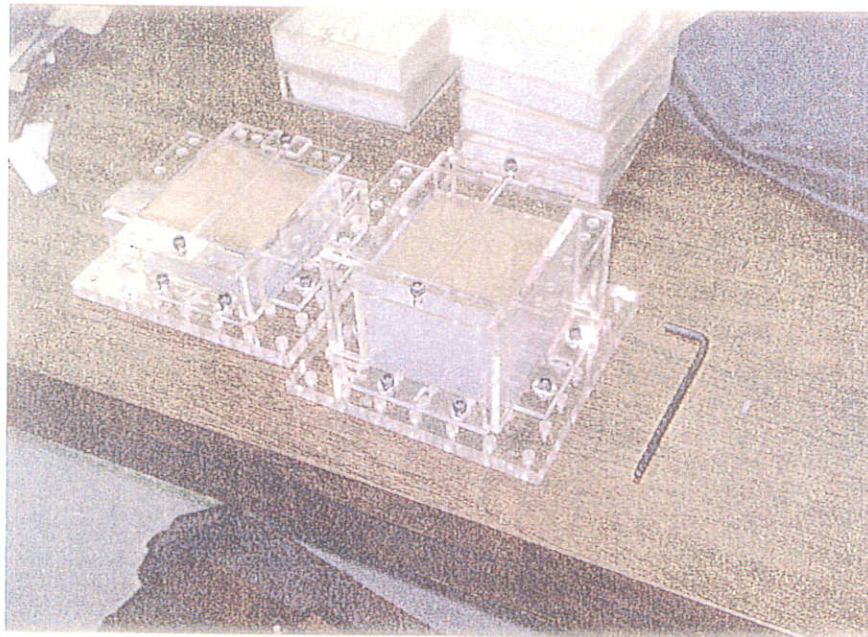
Model drawing	 <p>(Impact velocity)</p> <p>v_0</p> <p>$2r$</p> <p>Captured substance</p> <p>d (sticking depth)</p> <p>x (length)</p> <p>Aerogel</p>	
Analytical approach	Minimum velocity (lower velocity limit)	Maximum velocity (upper velocity limit)
	It is considered that kinetic energy of captured substance was absorbed only by static breakage of aerogel.	Velocity is constant until captured substance comes to a halt (i.e. impact velocity is maintained).
d/l	≈ 1	
T_s (Tensile strength of aerogel)	$5 \times 10^2 \text{ Pa}$	
P_p (Density of impinging substance)	$3 \times 10^3 \text{ kg/m}^3$	

Table 6.5.5.1-2 Causes of Inclusion of Foreign Substance into Ground Process

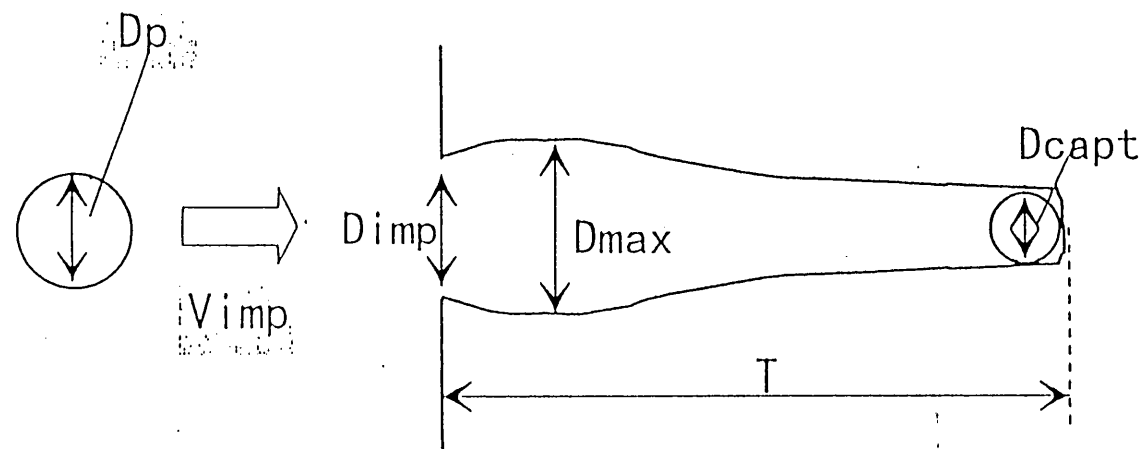
Process			Work	Consideration of Causes of Inclusion of Foreign Substance	Evaluation (degree of likelihood)
Before Flight	HEPL	Manufacture	1. Aerogel is manufactured.	No carbon fiber substance is used in aerogel manufacturing process.	△
		Storage	2. Stored in antistatic plastic case.	Although antistatic storage case contains carbon, it contains no silicon. Material of case is not of fibrous structure.	△
		Transport preparation	3. Put in paper case, which is then put in plastic case. Lid is fastened with tape.	Environment is quite during work.	△
	Transport (HEPL to IHI)		4. Case mentioned in 3 is wrapped up in shock-absorbing material and carried by hand in cardboard case.	Aerogel is put in case. Only plastics and paper are inside the case.	△
	IHI	Storage (clean room)	5. Surface inspection and classification of aerogel conditions. Stored in the same state as in 3 in clean room.	Inclusion of foreign substance is quite unlikely in clean room.	×
		Transport (IHI to Engineering Institute)	6. After 5, aerogel is put in plastic bag and sealed. It is then kept fixed in sealed case (hard plastic case).	Inclusion of foreign substance is quite unlikely in sealed case.	△-×
		Gold coating	7. Carry out gold coating.	Aerogel holder used during gold coating is made of aluminum, and no carbon-containing substance is used.	△-×
		Transport (IHI Engineering Institute to Mizuho)	8. Surface inspection and classification of aerogel conditions. Stored in the same state as in 3 in clean room.	Inclusion of foreign substance is quite unlikely in sealed case.	△-×
		Storage (clean room)	9. Aerogel surface is checked to make sure there is no breakage. Then, aerogel is stored in clean room.	Inclusion of foreign substance is quite unlikely in clean room.	×
		Assembling collector	10. Aerogel surface is checked, aerogel dimensions and weight are measured, and collector is assembled.	Inclusion of foreign substance is quite unlikely because assembly is performed in clean booths in clean room.	△-×
		Transport preparation	11. Lid is applied to collector, which is then put in duralumin case for transport.	Inclusion of foreign substance is quite unlikely because transport preparation is made in clean room.	×
	Transport (IHI to KSC)		12. Carried by hand in the condition mentioned in 11.	There is little likelihood of inclusion of foreign substance in consideration of nitrogen substitution and container transport.	×
	KSC	Storage (clean room)	13. Stored in clean room in the condition mentioned in 11.	There is little likelihood of inclusion of foreign substance in consideration of storage in nitrogen-substituted condition.	×
		Mounting collector	Collector is mounted on MFD, and photos are taken.	Inclusion of foreign substance is quite unlikely because work is performed in clean room.	△-×
		Preparation for launch	Mounting of shuttle on MFD to removal of collector cover.	Inclusion of foreign substance is quite unlikely because work is performed in clean room.	△(?)
		Processing after launch	Attachment of collector cover to removal of MFD from shuttle.	Inclusion of foreign substance is quite unlikely because work is performed in clean room.	△(?)
After Recovery		Removing collector	Collector is removed from MFD, and photos are taken.	Inclusion of foreign substance is quite unlikely because work is performed in clean room.	△-×
		Transport (KSC to IHI)	14. Carried by hand in the condition mentioned in 11.	There is little likelihood of inclusion of foreign substance in consideration of nitrogen substitution and container transport.	×
		Storage (clean room)	15. Stored in clean room in the condition mentioned in 11.	There is little likelihood of inclusion of foreign substance because aerogel is put in nitrogen-substituted container and stored in clean room.	×
	IHI	Disassembly and inspection	16. Collector is disassembled, and aerogel surface is checked.	Inclusion of foreign substance is quite unlikely because work is performed in clean room.	△-×
		Storage (clean room)	17. Lint-free cloth is put under the bottom of aerogel, which is then put in plastic case and stored in clean room.	Inclusion of foreign substance is quite unlikely because aerogel is stored in clean room.	×
		Detailed examination	18. Aerogel surface is examined in detail.	Inclusion of foreign substance is quite unlikely because work is performed in clean room.	△-×



Left: Type B

Right: Type A

Figure 6.2.2-1 Configurations of Ground Test Specimens



Measurement Items of Crater Shape and Available Information

Step	Measurement item	Information available through estimation
1	Diameter (D_{imp}), max. diameter (D_{max})	Dust particle size (D_p)
2	Depth (T) [Characteristics of shape] Diameter of particles captured (D_{capt})	Dust impact velocity (V_{imp})
3	Volume (V)	Dust impact energy (E) Dust mass (D_m)
—	Material of captured particles	Dust material

Figure 6.2.3-1 Interrelations Between Crater Parameters and Irradiation Parameters

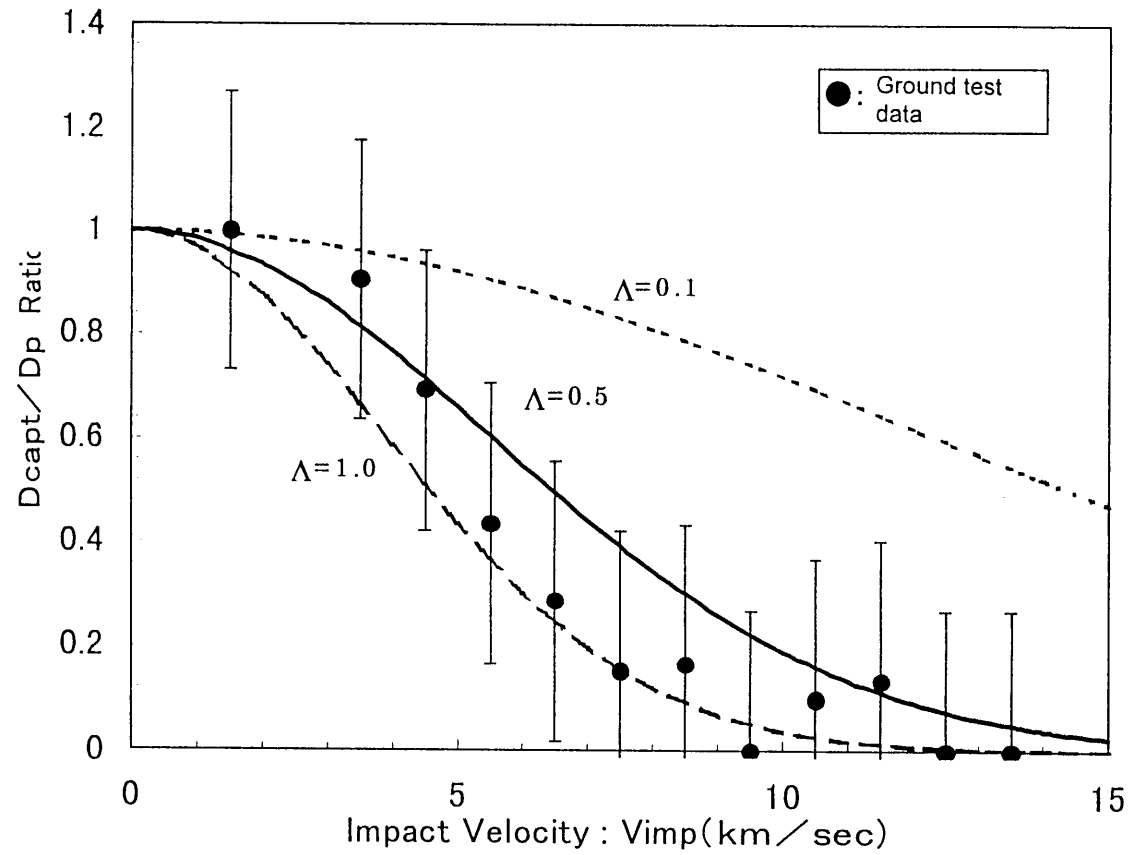


Figure 6.2.3-2 Changes in Particle Size of Dust Captured According to Impact Velocities (Comparison of Analytical Results and Experimental Results) [By Kitazawa et al. (1998)]

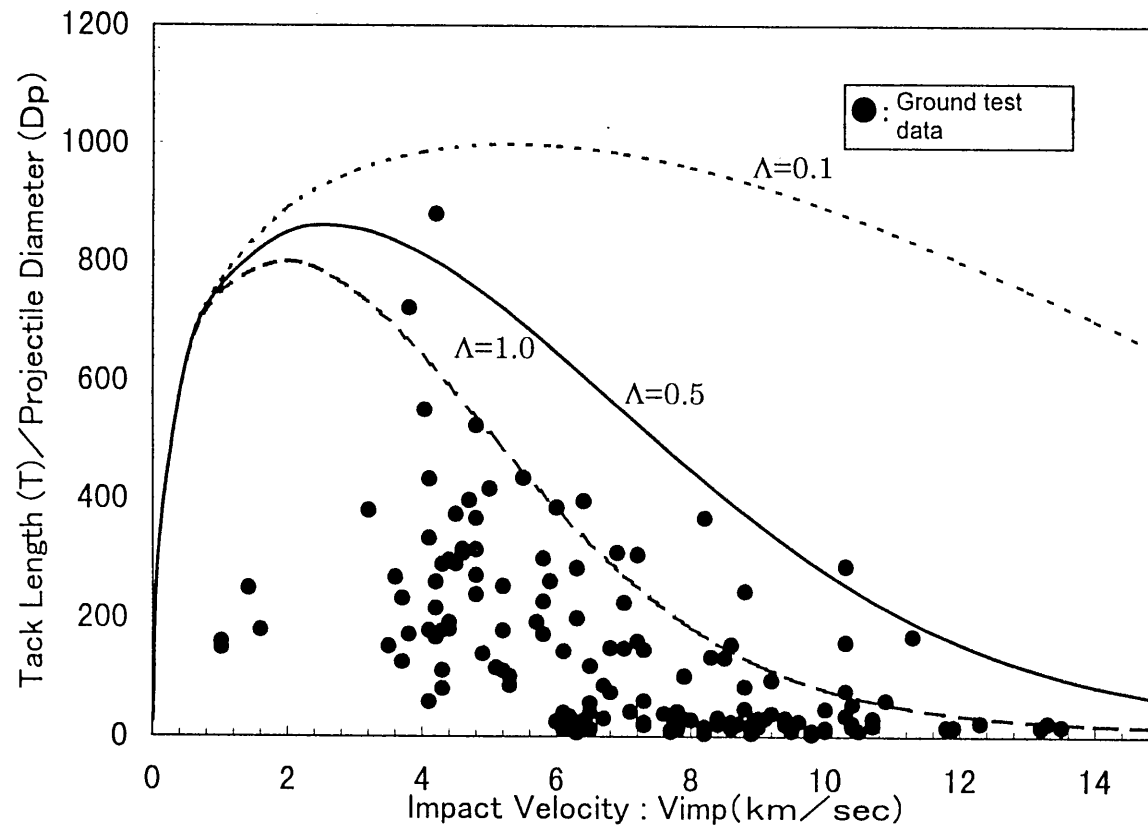


Figure 6.2.3-3 Crater Depths and Dust Particles Sizes According to Impact Velocities (Comparison of Analytical Results and Experimental Results) [By Kitazawa et al. (1998)]

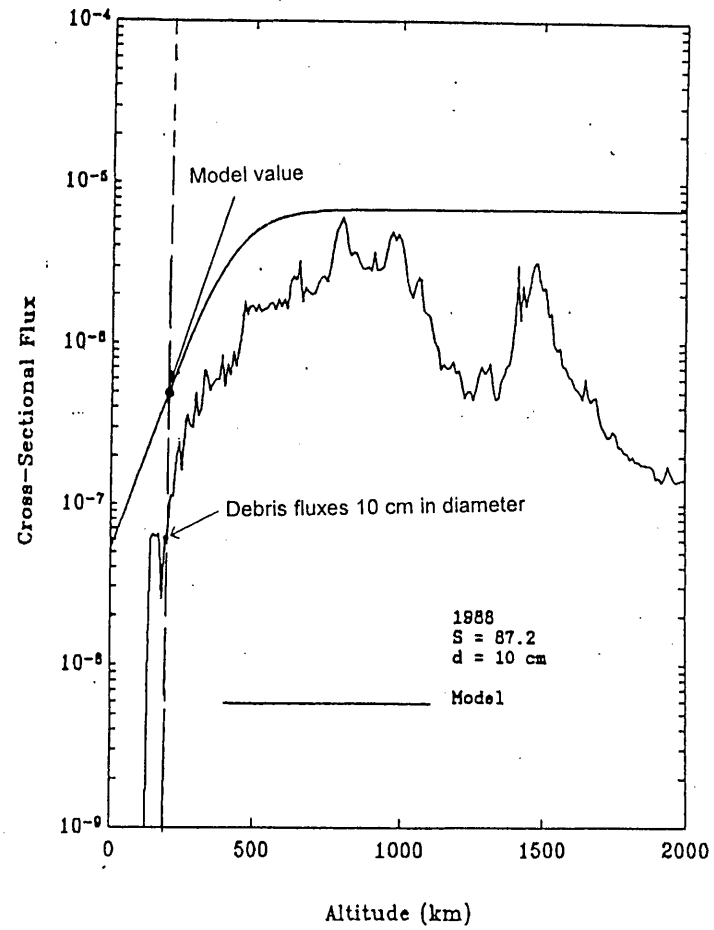
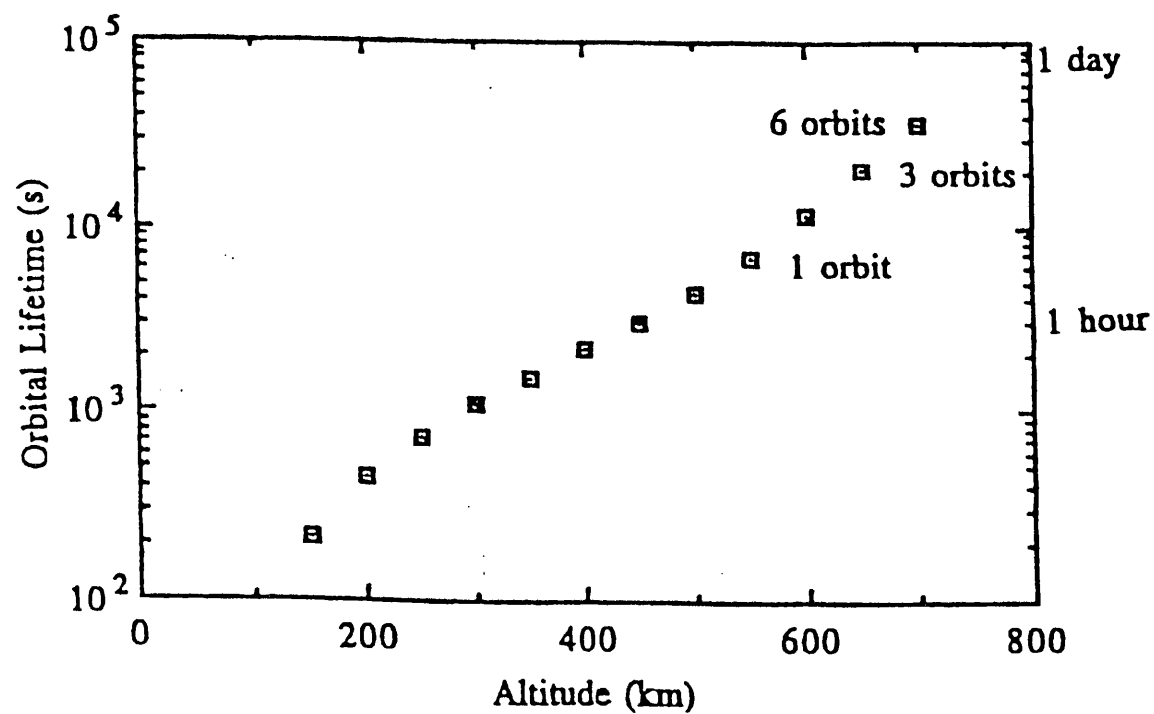


Figure 6.3.3-1 Difference Between Measured and Model Values of Volume of Debris Fluxes 10 cm in Diameter



Circular orbit lifetimes measured as a function of altitude for the atmospheric profile pertaining to MFE exposure epoch for $1.6\text{-}\mu\text{m}$ particles.

(Atmospheric model in 1982 [STS-3]; Calculated for particles $1.6\text{ }\mu\text{m}$ in diameter)

Figure 6.3.3-2 Example of Research on Orbital Lifetime of Particles on Earth Orbit (By McDonnell et al. [1997])

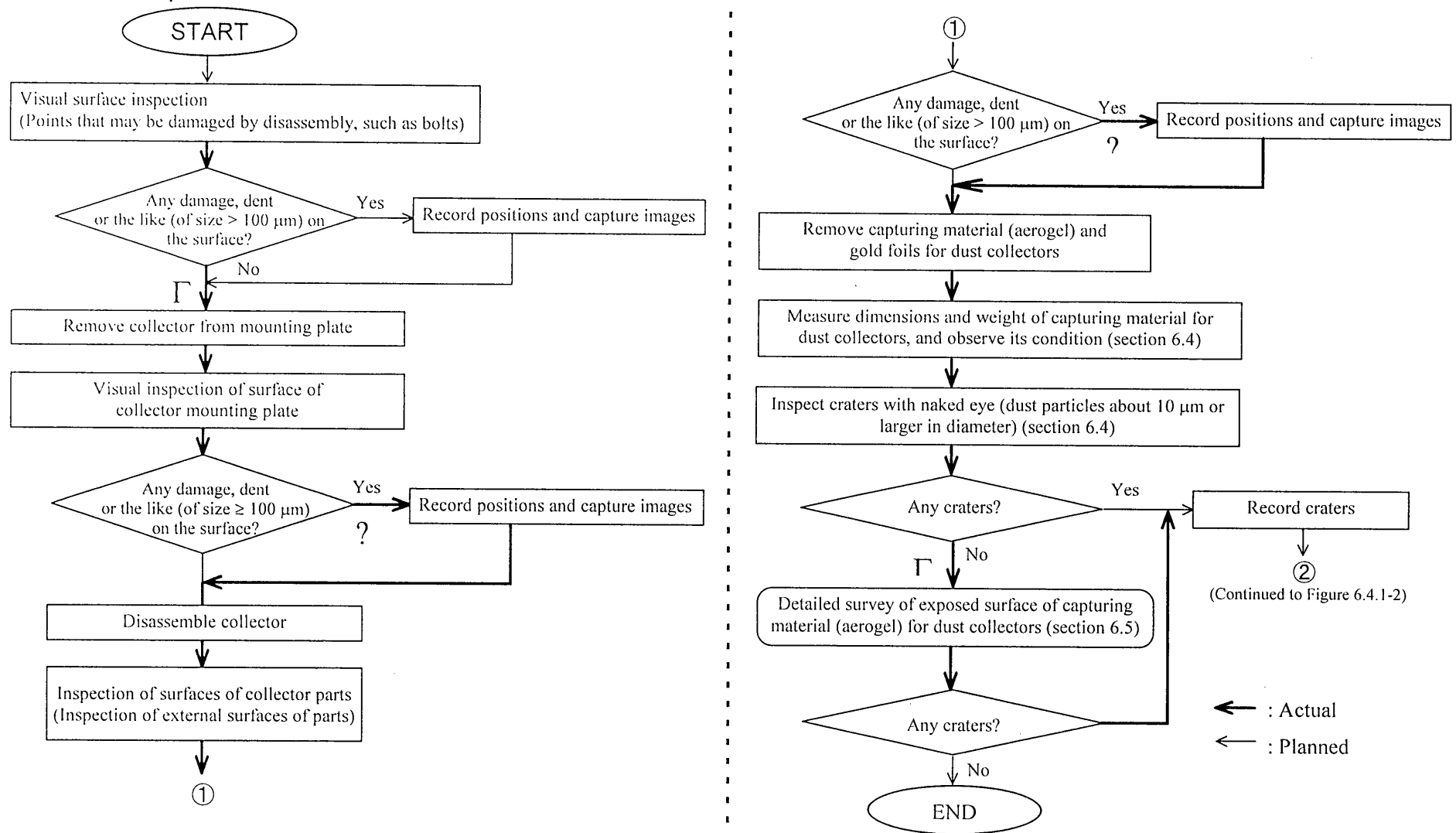


Figure 6.4.1-1 Dust Collector Inspection Procedure

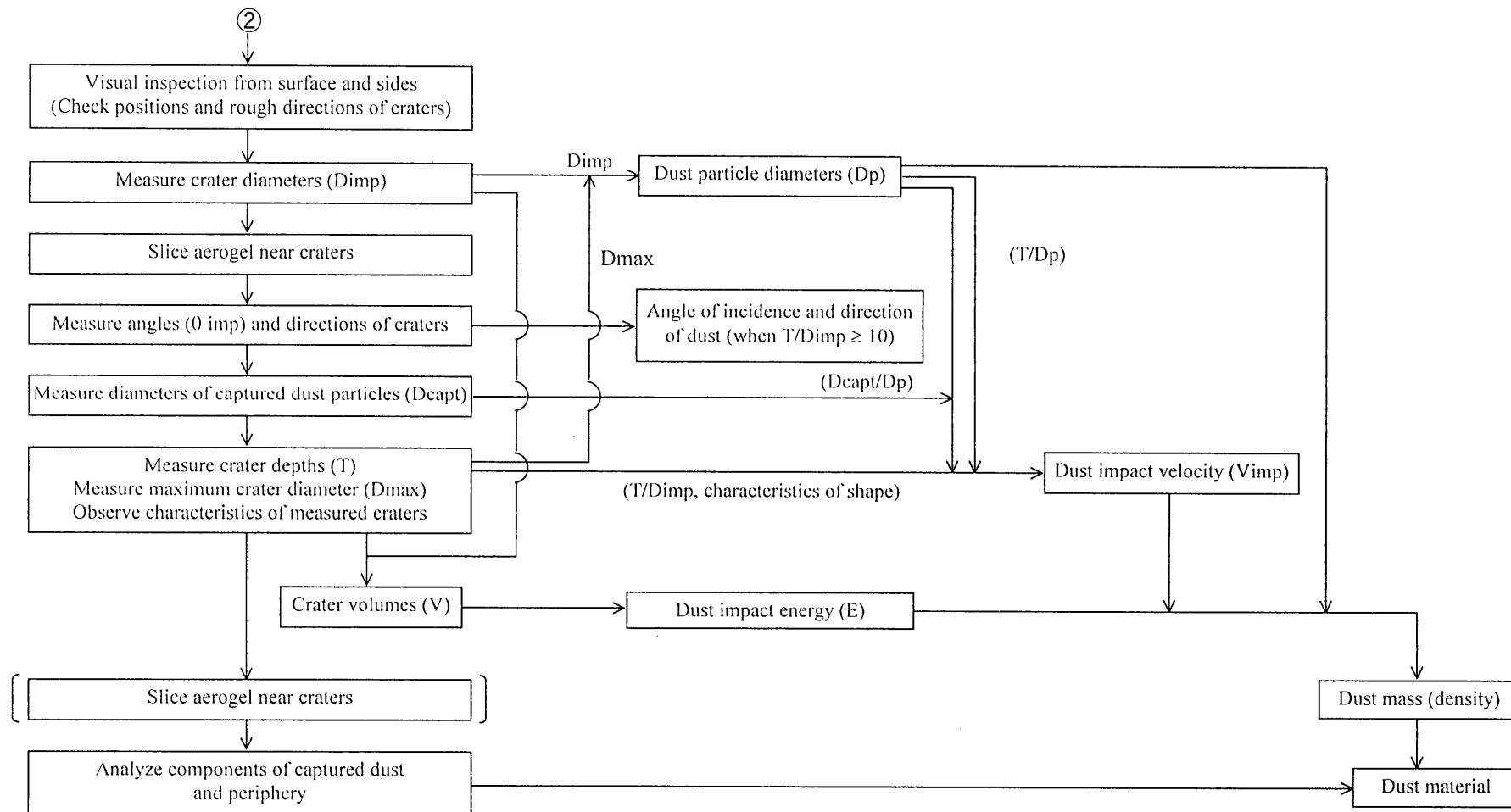
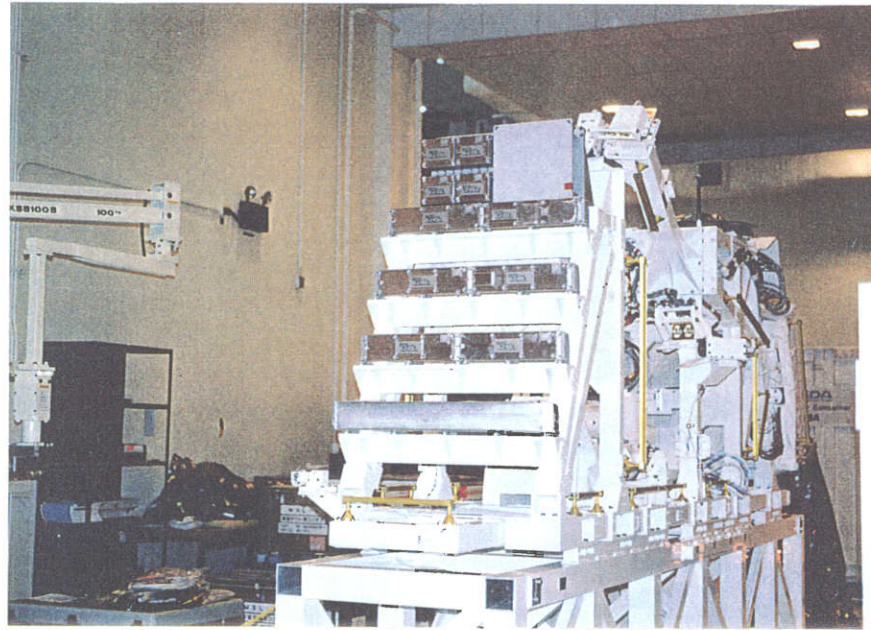


Figure 6.4.1-2 Aerogel Inspection Procedure



(The mounted ESEM is seen in the center of the photo.)

Figure 6.4.1-3 Mounting of MFD/ESEM

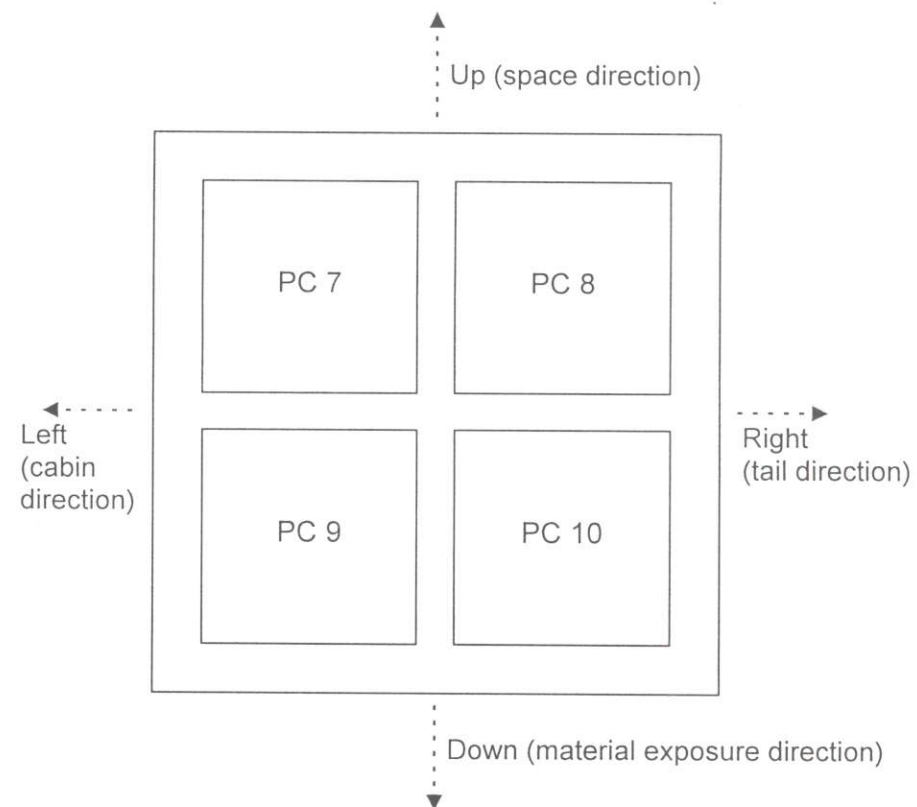
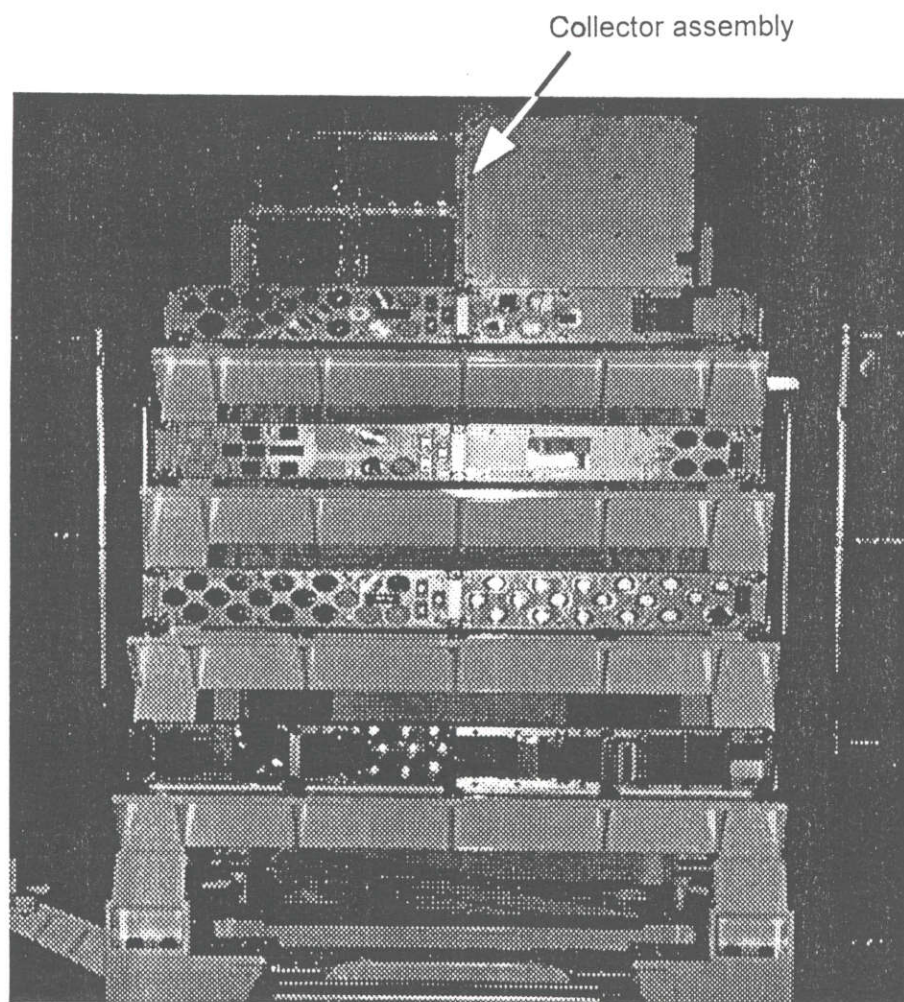
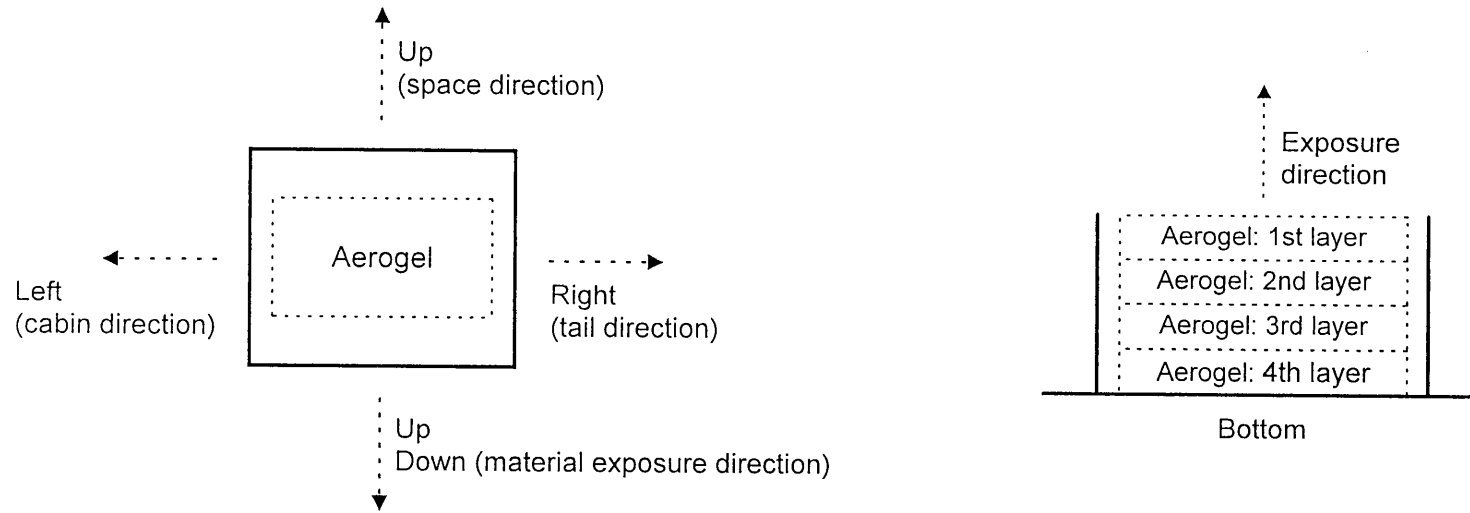
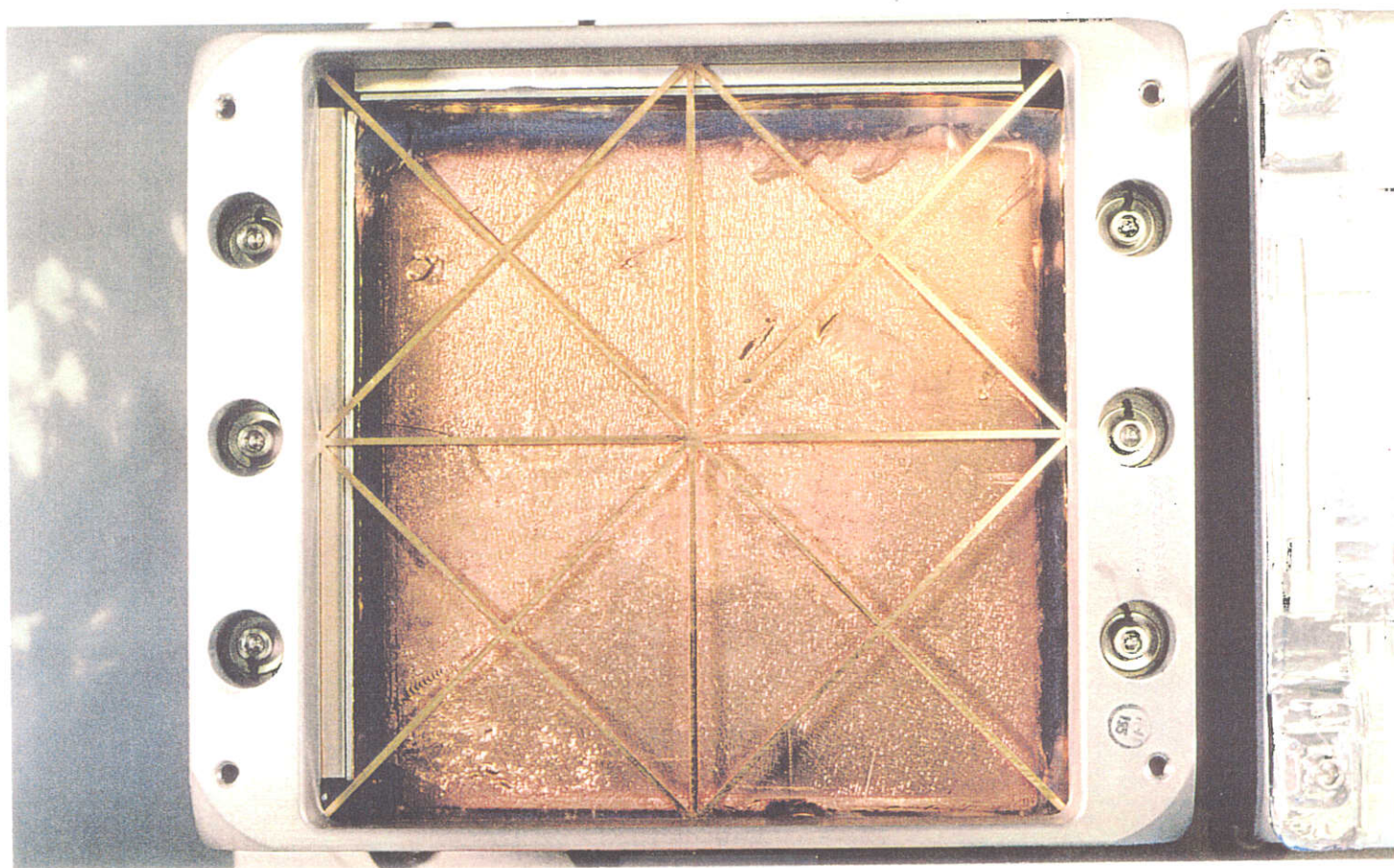


Figure 6.4.1-4 Mounting of Collector Assembly



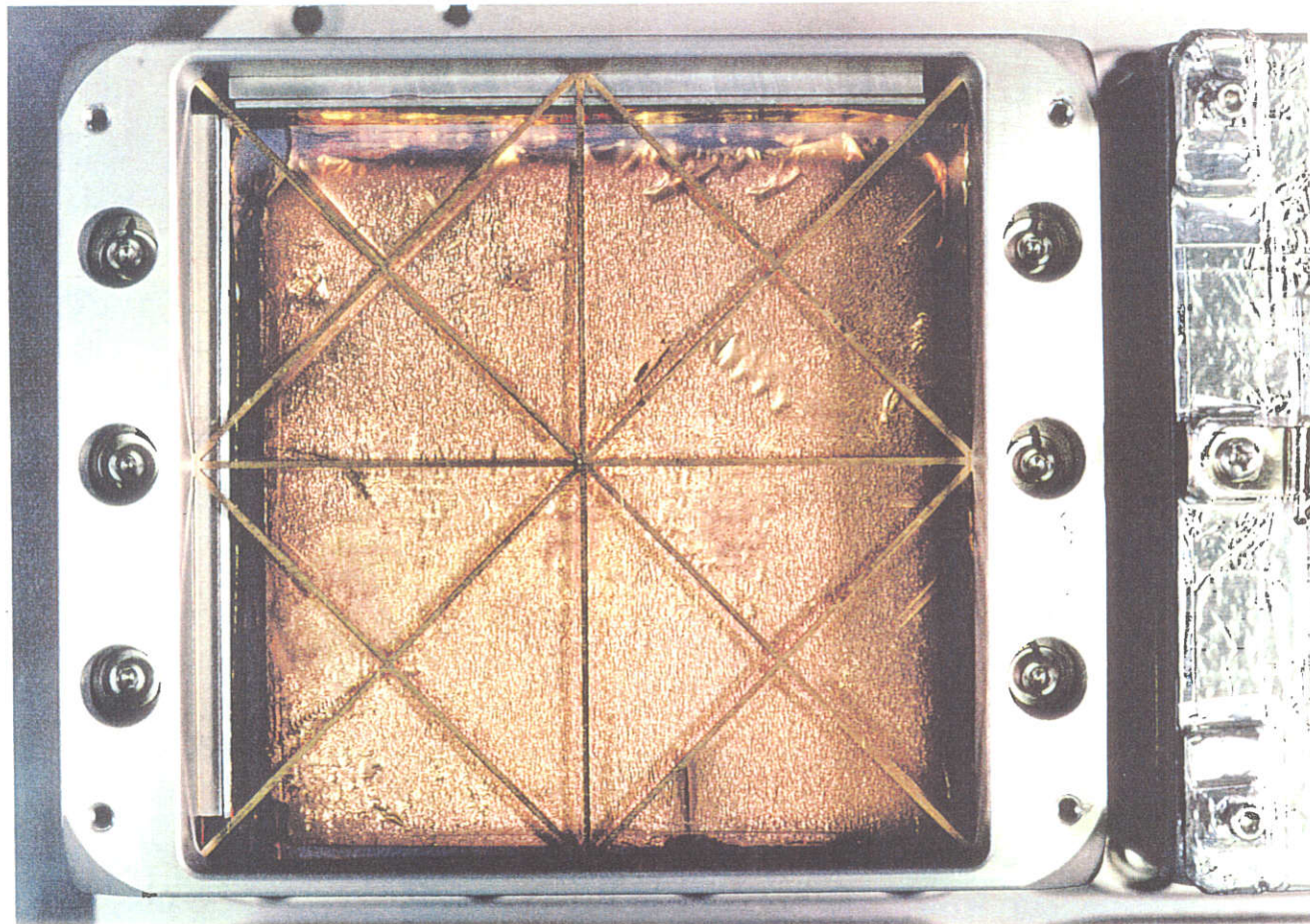
Dimensions of each layer of aerogel:
approx. 10 cm × approx. 10 cm × approx. 2 cm (thickness)

Figure 6.4.1-5 Structure of Dust Collector Unit



Before flight
(KSC)

Figure 6.4.3.1-1 Example of Change in Surface Condition of Capturing Material for Dust Collectors (1/2)



After flight
(KSC)

Figure 6.4.3.1-1 Example of Change in Surface Condition of Capturing Material for Dust Collectors (2/2)

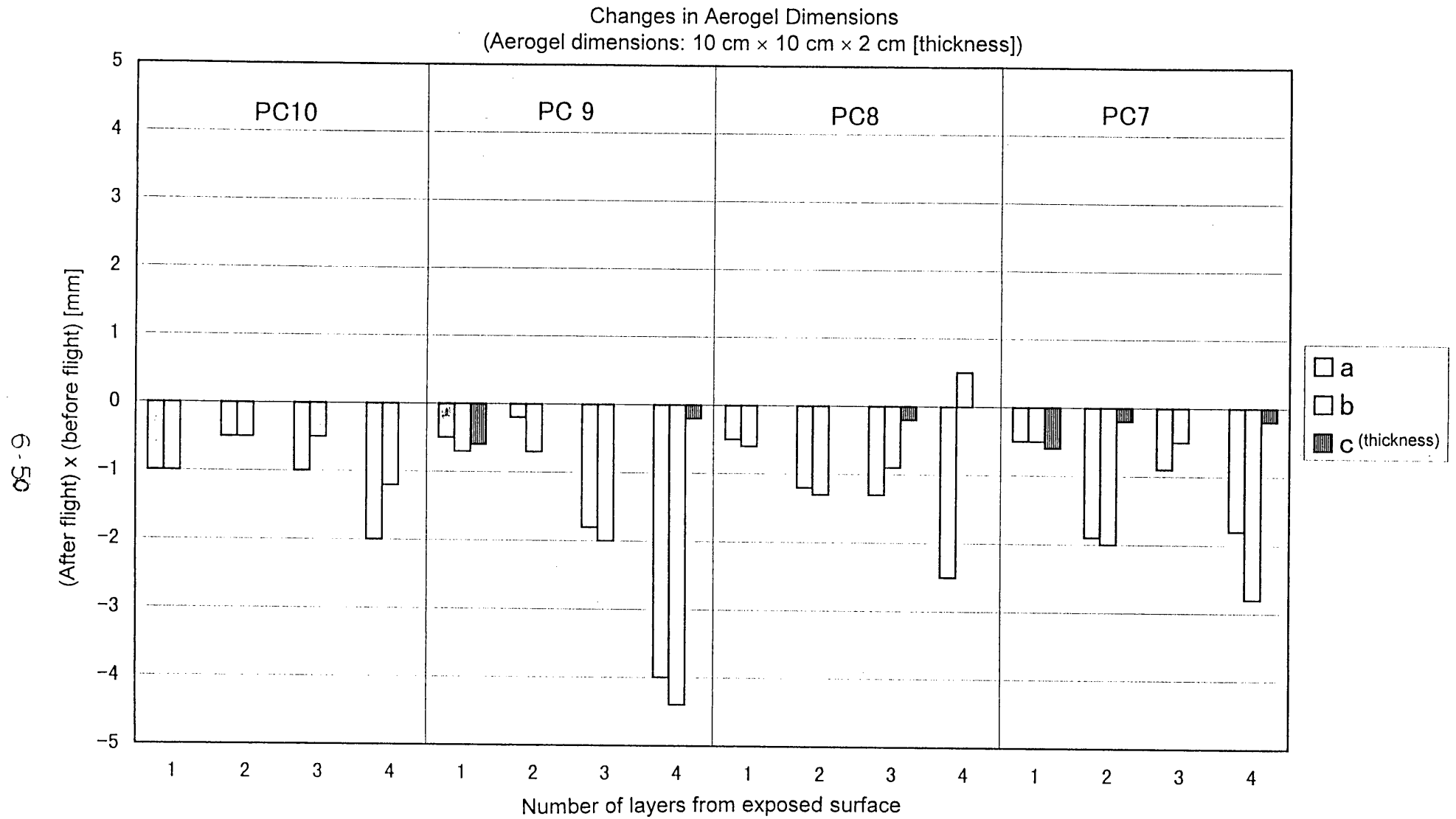


Figure 6.4.3.1-2 Results of Measurement of Dimensions of Capturing Material for Dust Collectors

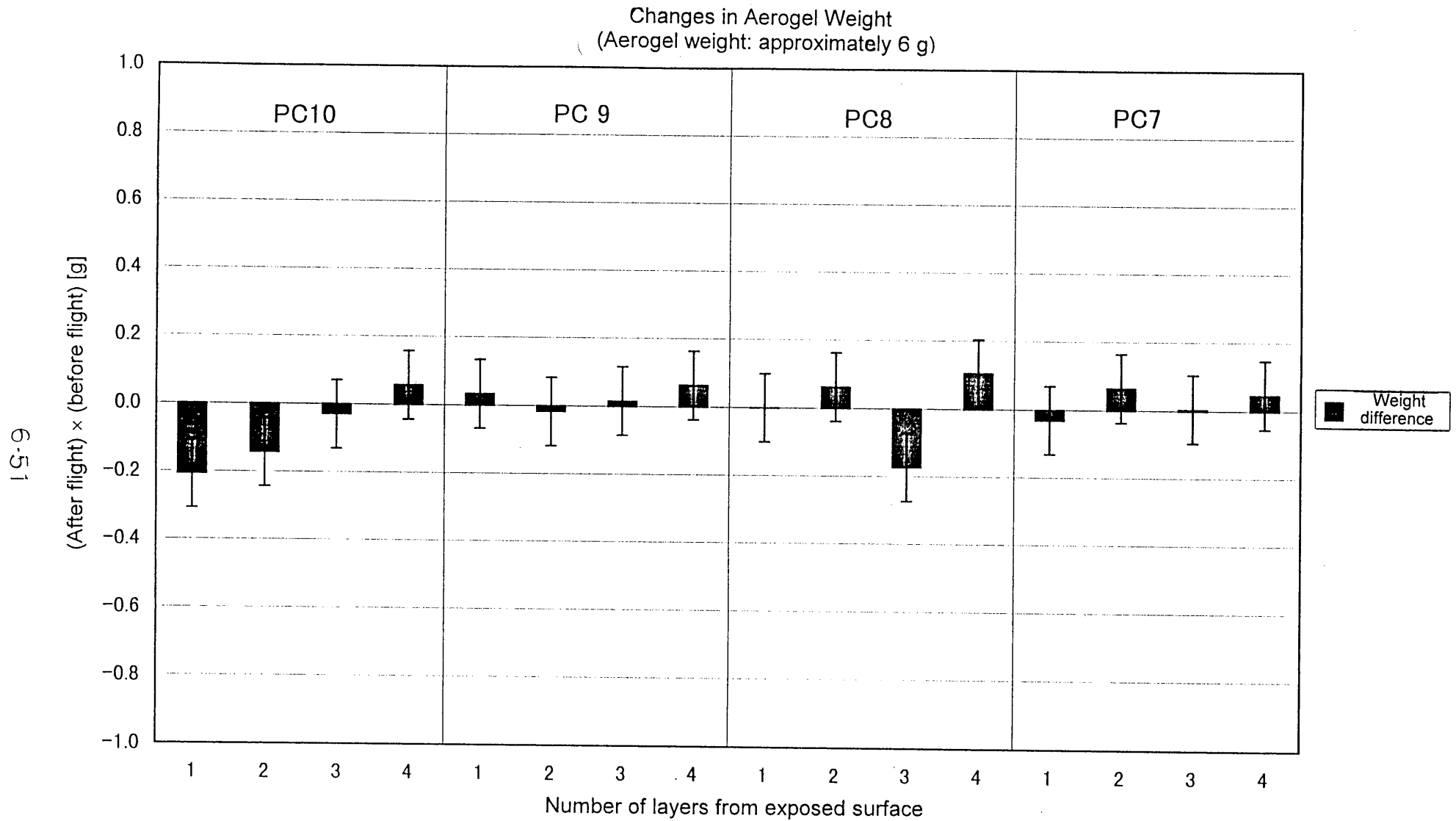
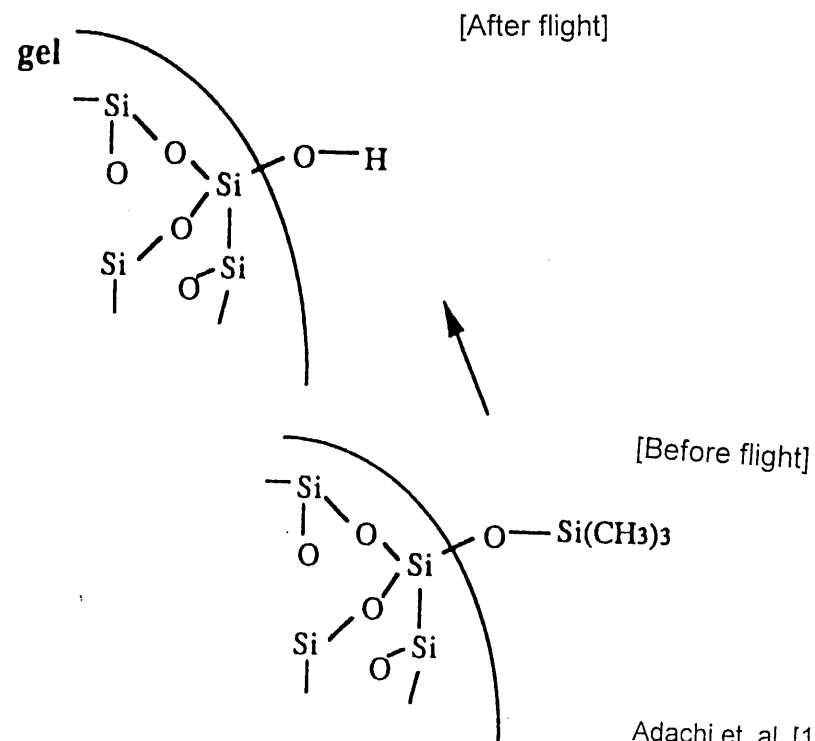


Figure 6.4.3.1-3 Results of Measurement of Weight of Capturing Material for Dust Collectors



Adachi et. al. [1994] used with modification

Figure 6.4.4.1-1 Assumption of Changes in Aerogel Surface

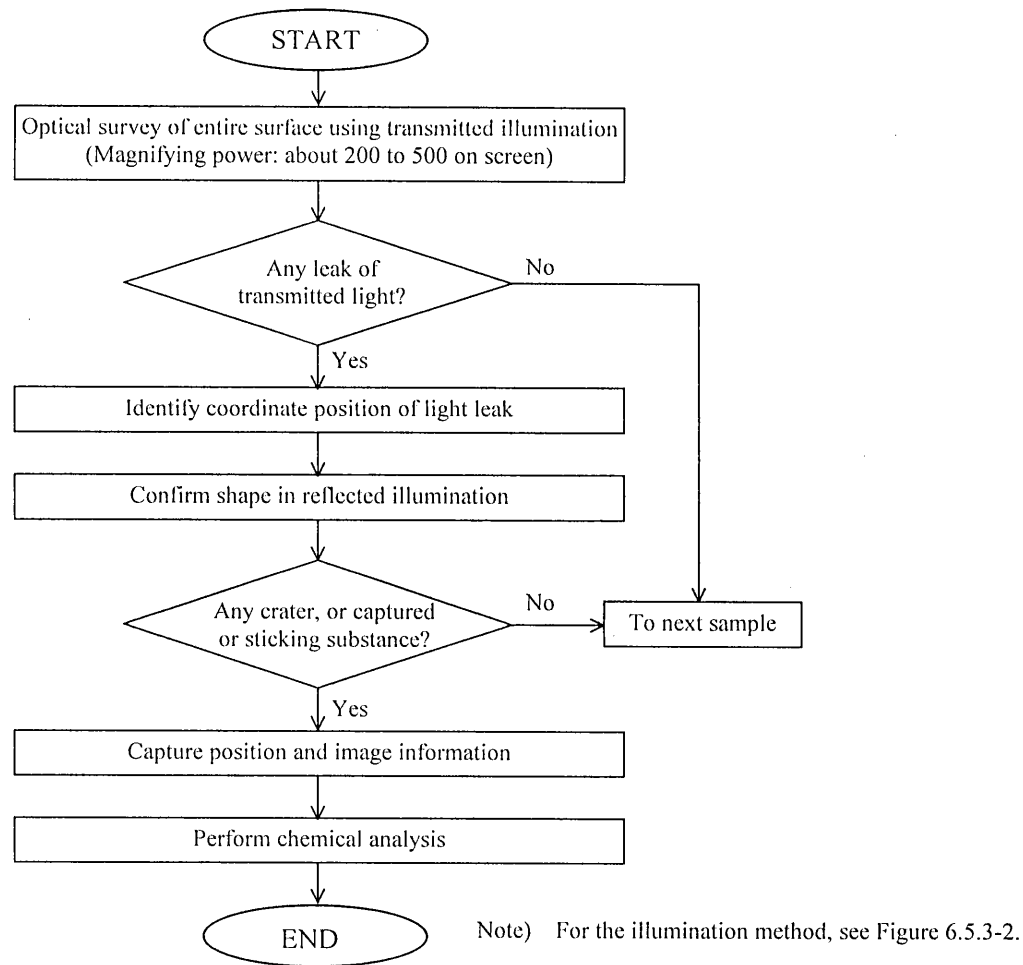
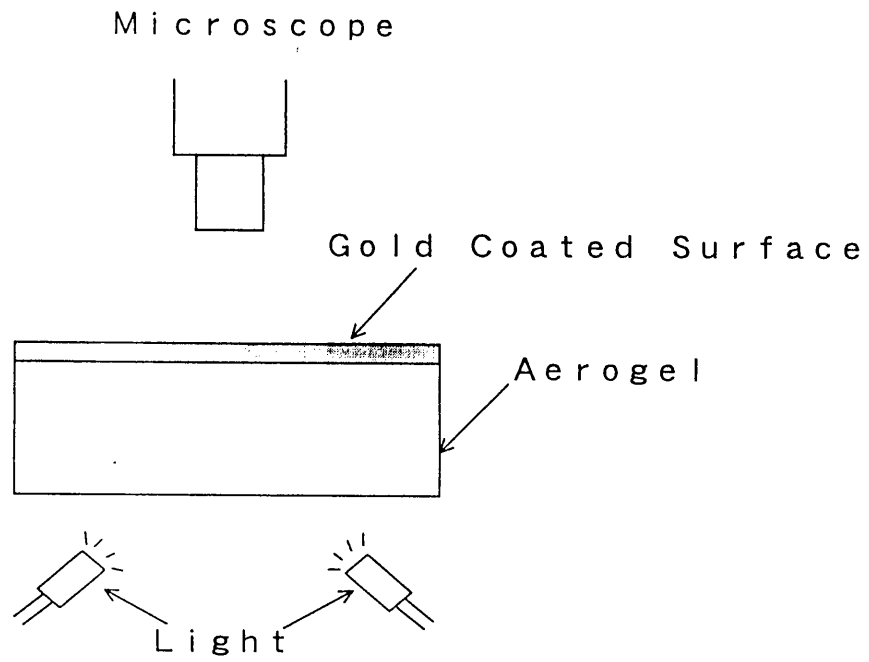
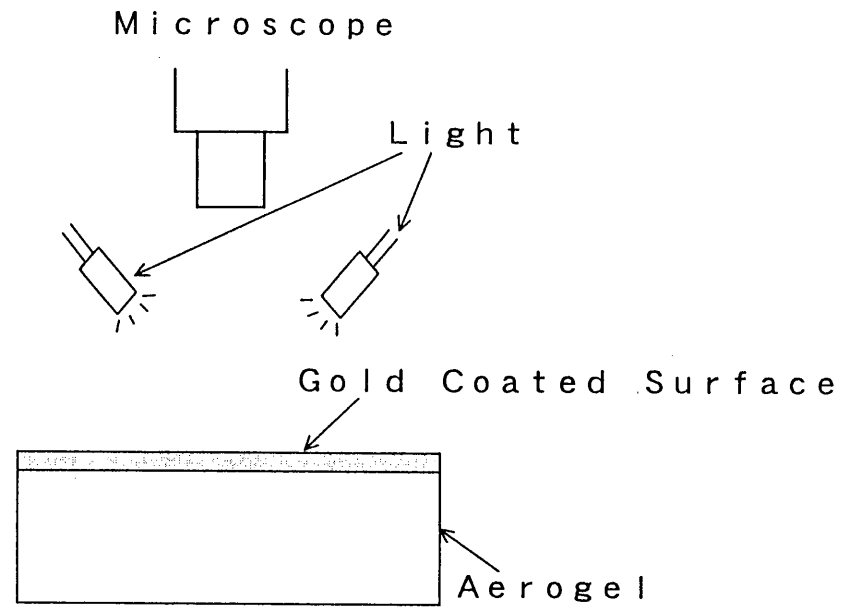


Figure 6.5.3-1 Procedure for Detailed Examination of Exposed Aerogel Surface

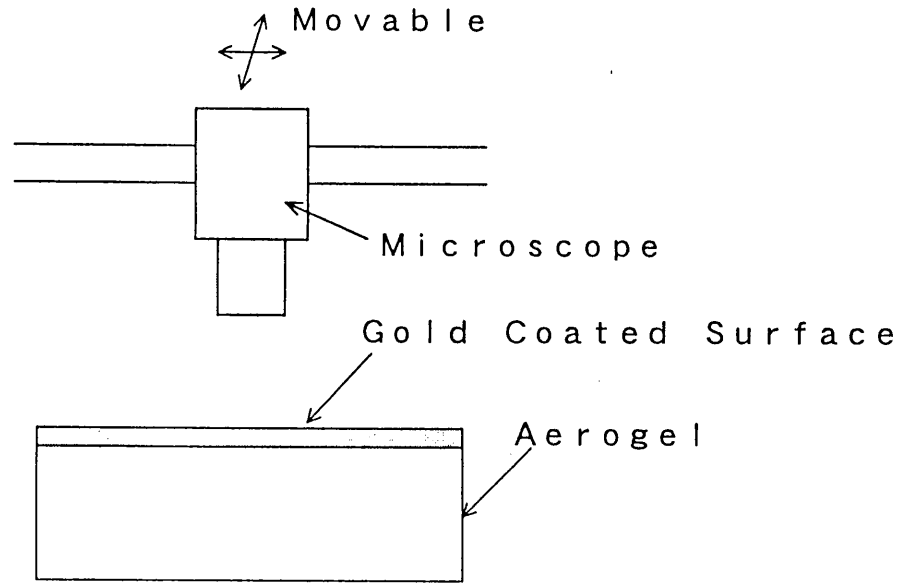


a. Transmitted Illumination

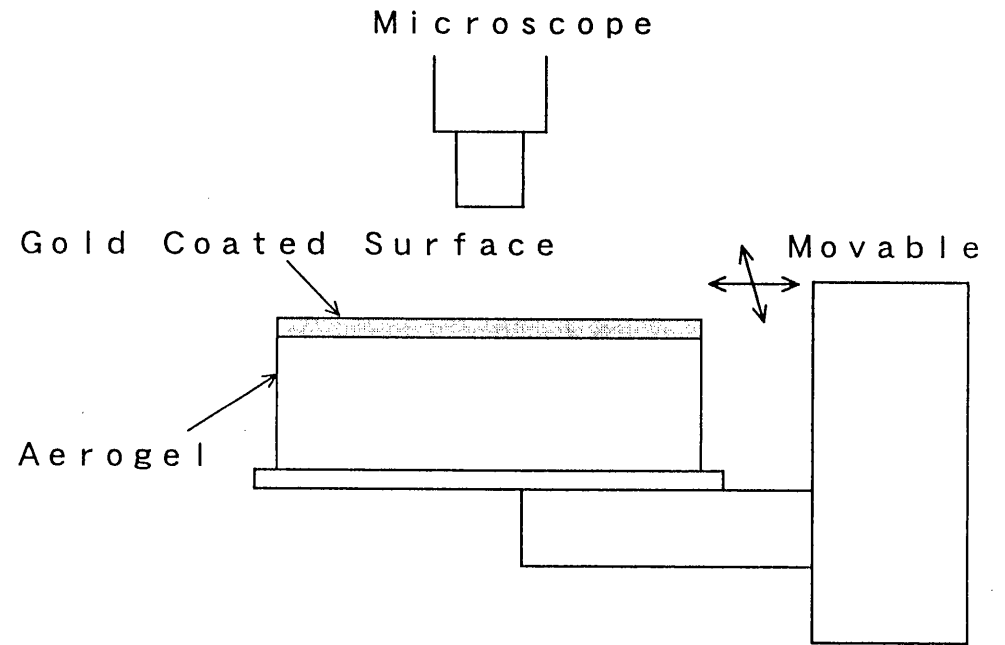


b. Reflected Illumination

Figure 6.5.3-2 Illumination for Aerogel Examination



a. Movable Microscope System



b. Movable Mounting Table System

Figure 6.5.3-3 Moving Method for Aerogel Examination

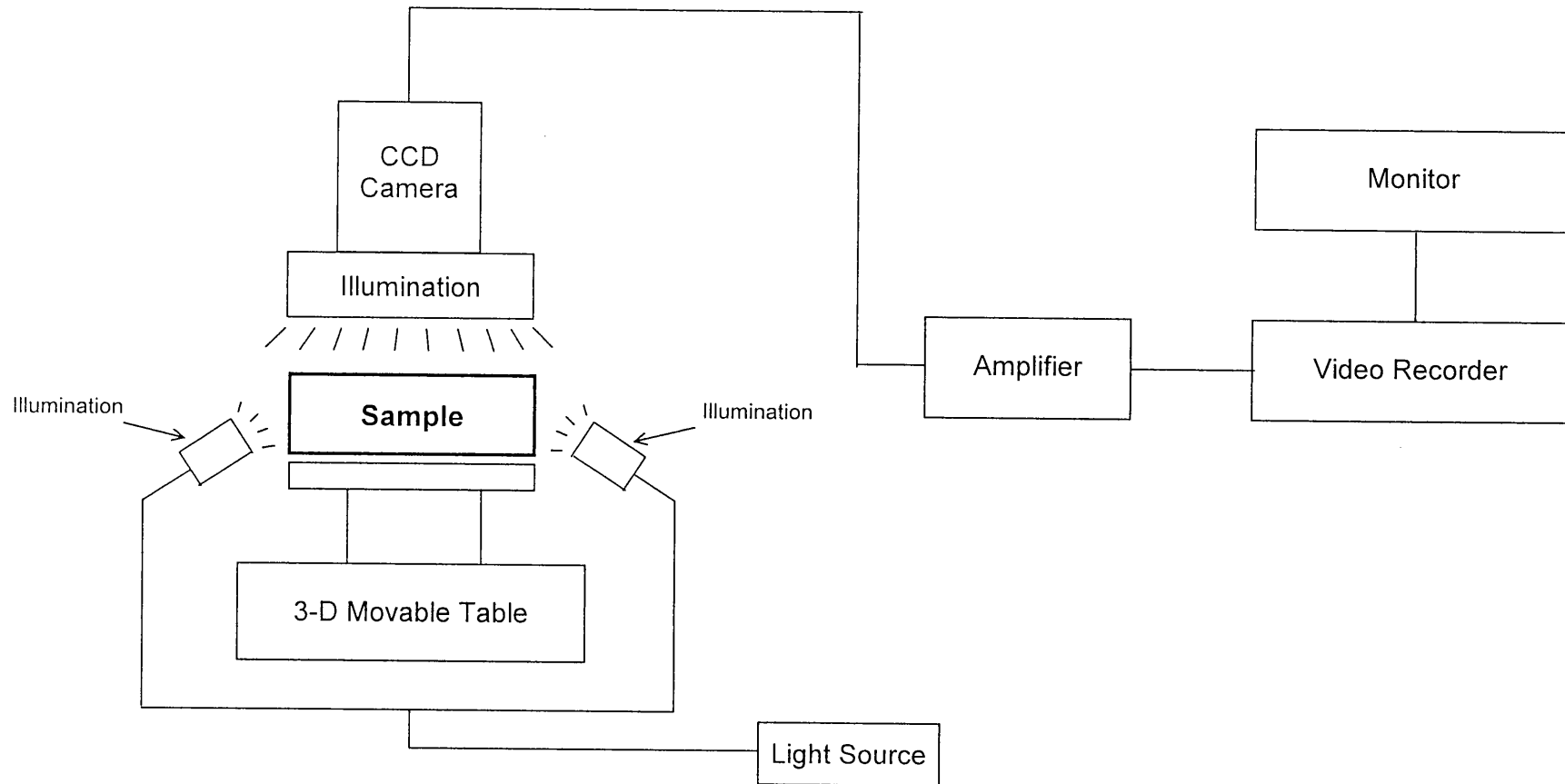


Figure 6.5.3-4 Configuration of Examination Equipment



Figure 6.5.3-5 Condition of Carrying Out Examination

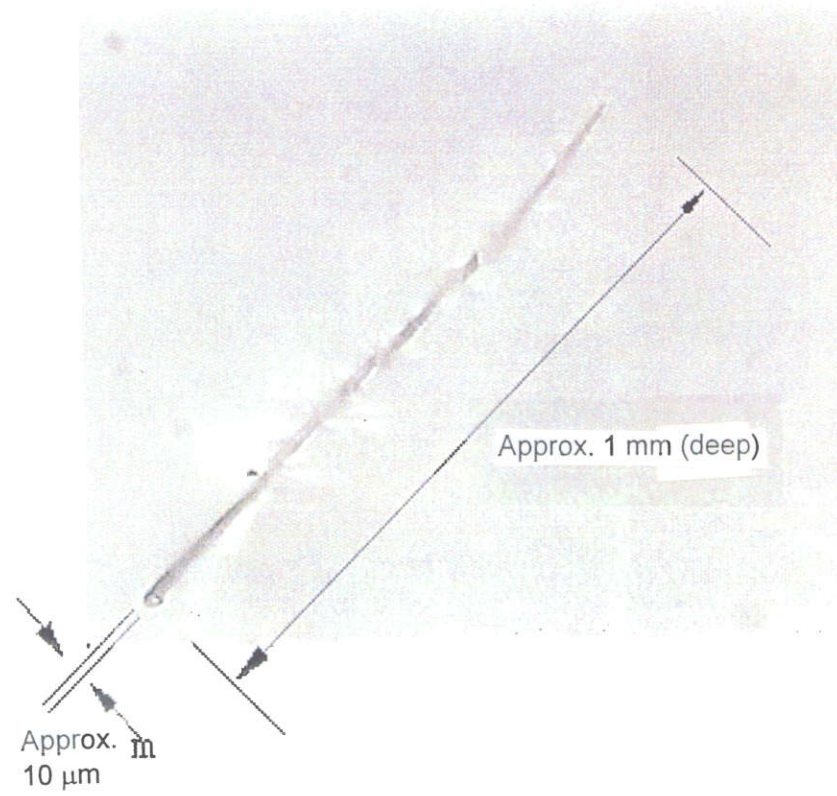


Figure 6.5.4-1 External View of PC7A

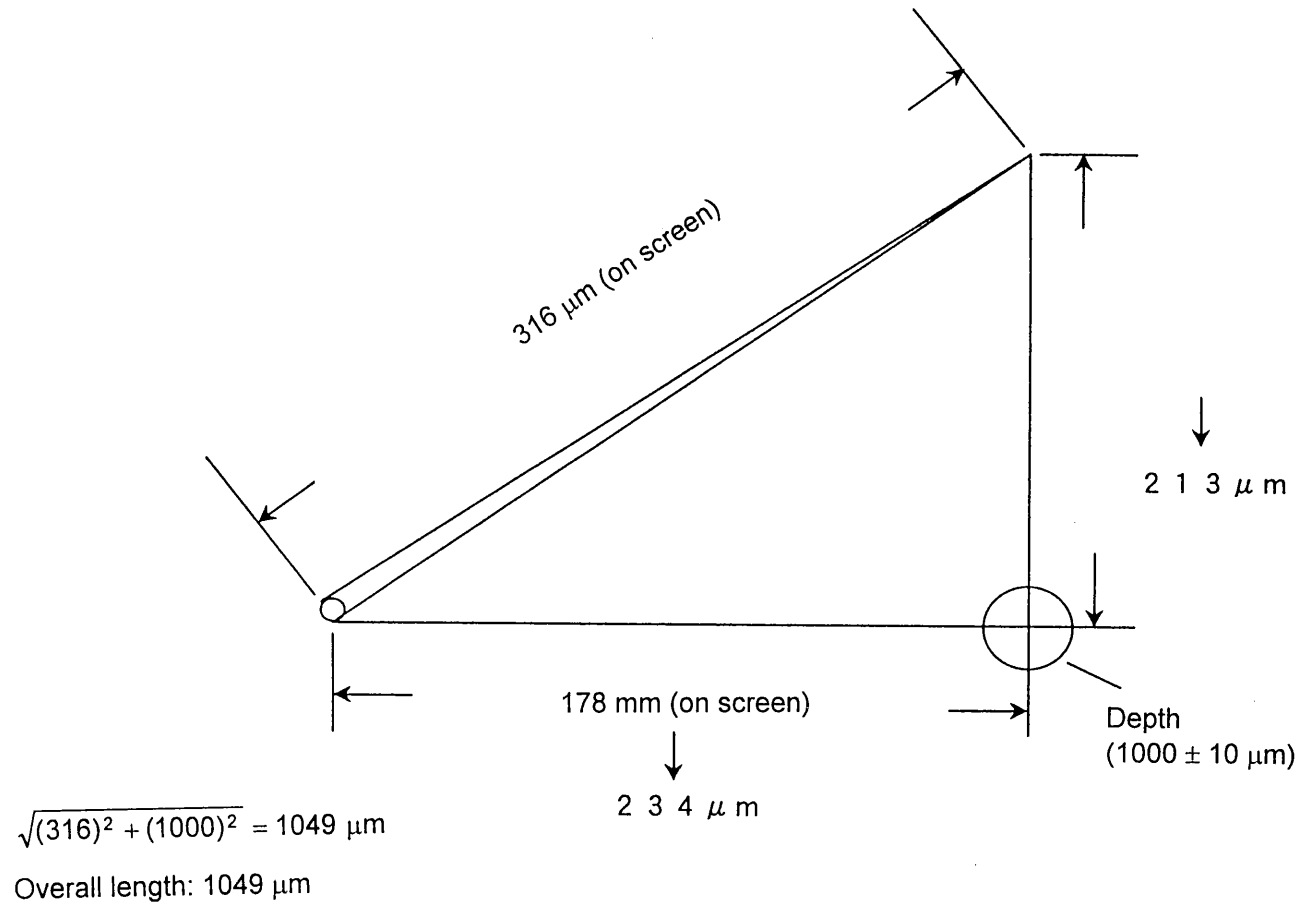
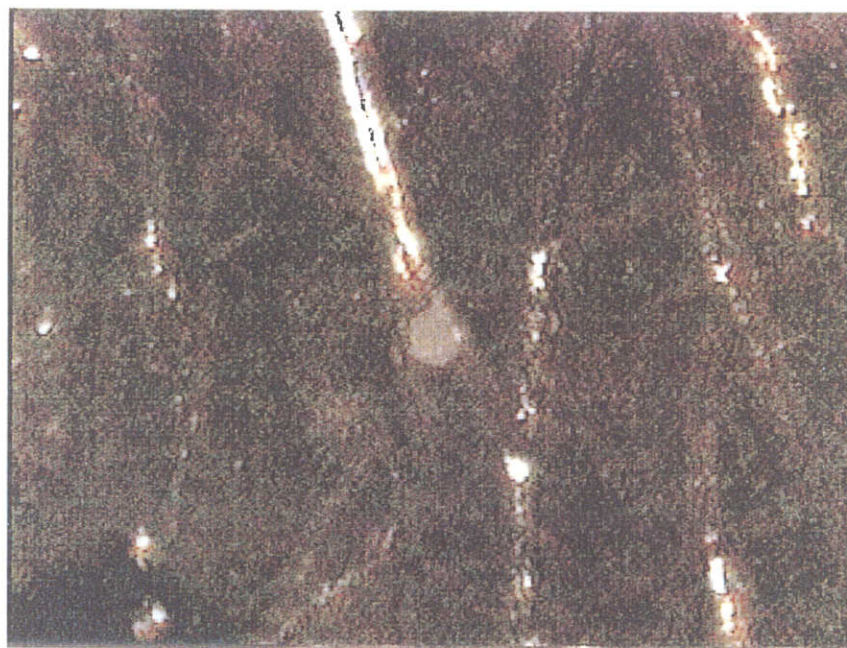
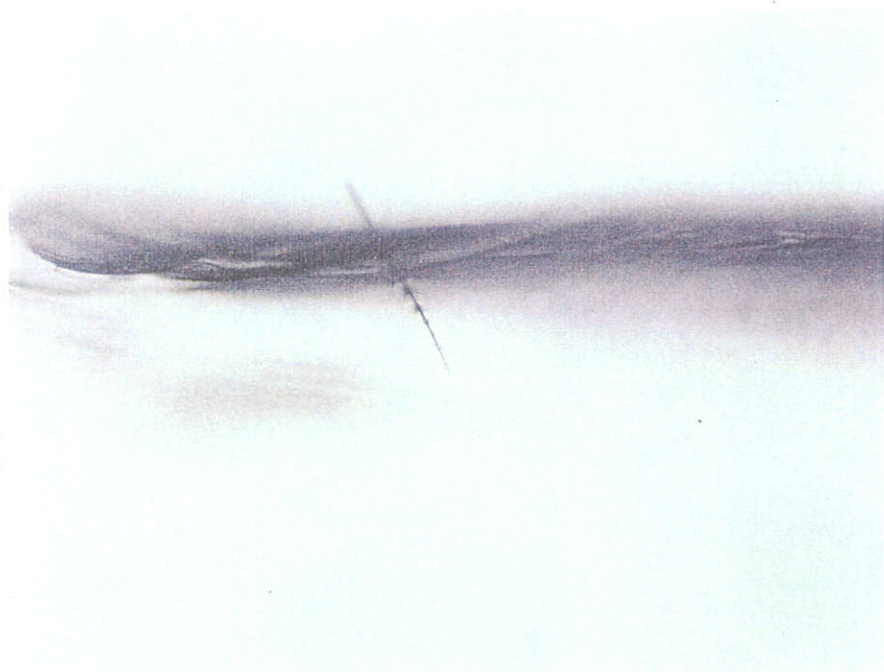


Figure 6.5.4-2 Dimensions of PC7A



0.1mm

Figure 6.5.4-3 External View of PC7B



(Optical Microscopic Photo 1)

500 μ m

[Enlarged Lower Part of Optical Microscopic Photo 1]

(Optical Microscopic Photo 2)

100 μ m

Figure 6.5.5.1-1 Optical Microscopic Photo and SEM Photo of PC7A (1/6).

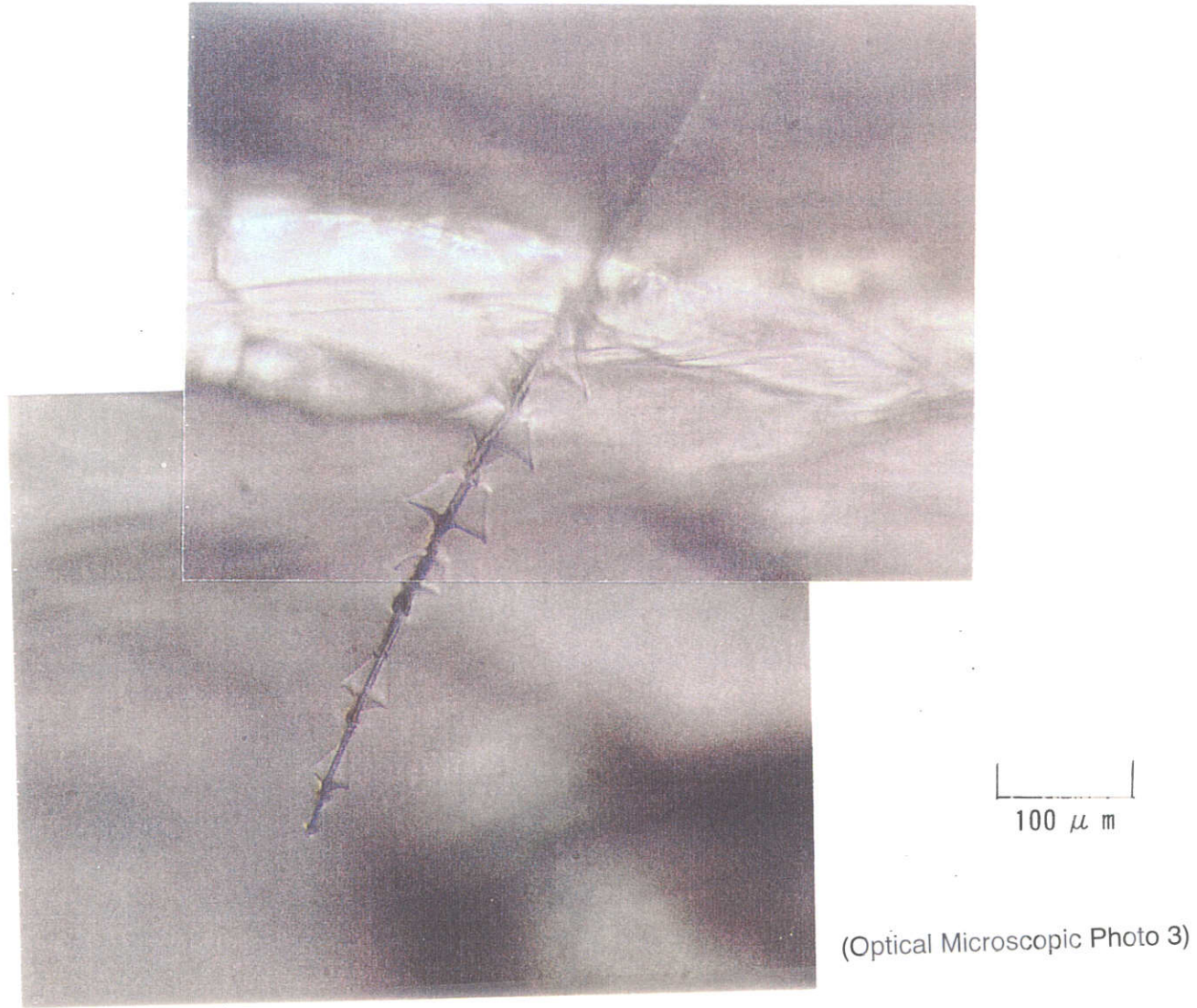
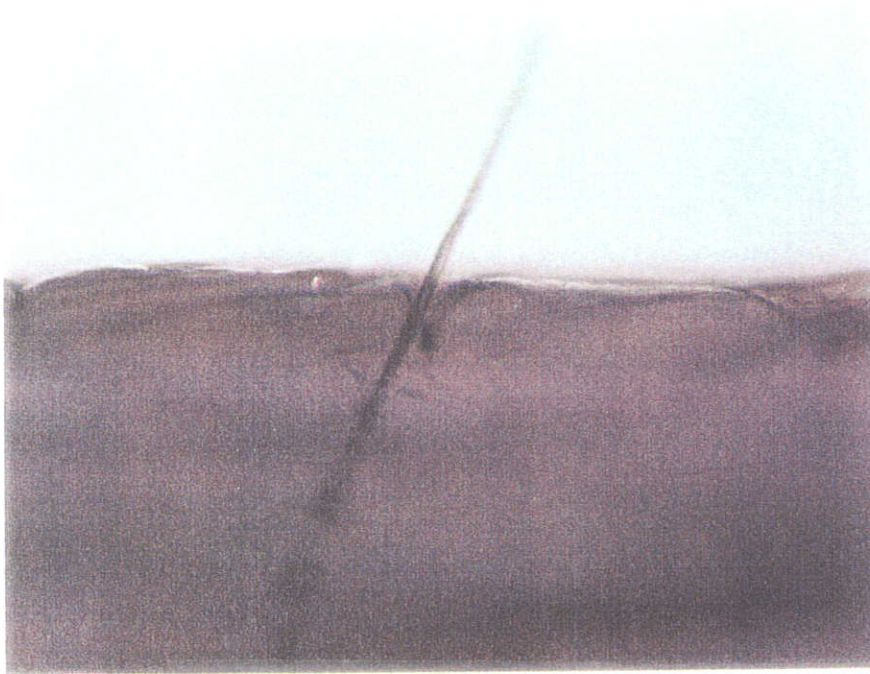
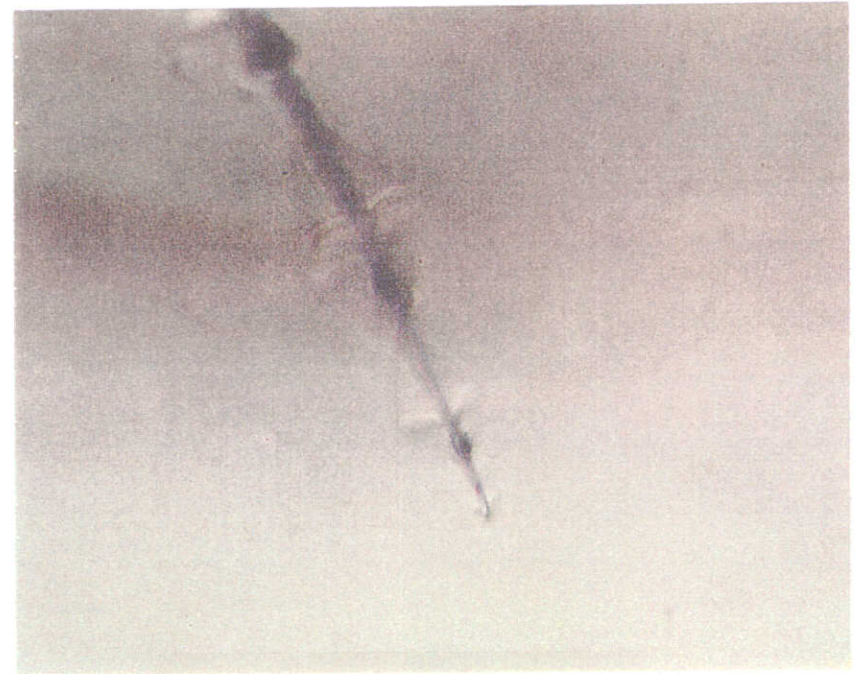


Figure 6.5.5.1-1 Optical Microscopic Photo and SEM Photo of PC7A (2/6)

6-63



(Optical Microscopic Photo 4)


100 μm 

(Optical Microscopic Photo 5)


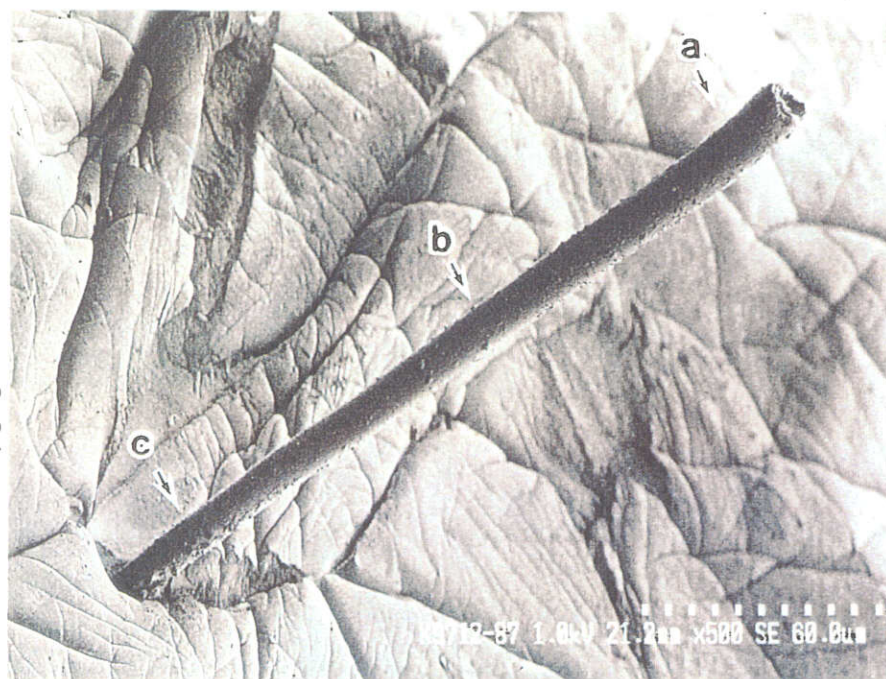
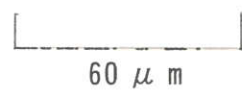

50 μm

Figure 6.5.5.1-1 Optical Microscopic Photo and SEM Photo of PC7A (3/6)



(SEM Photo 1)



(SEM Photo 2)

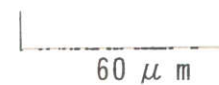


Figure 6.5.5.1-1 Optical Microscopic Photo and SEM Photo of PC7A (4/6)

Observation of End of Embedding - 1

[Embedding has a layered structure and is hollow inside.]

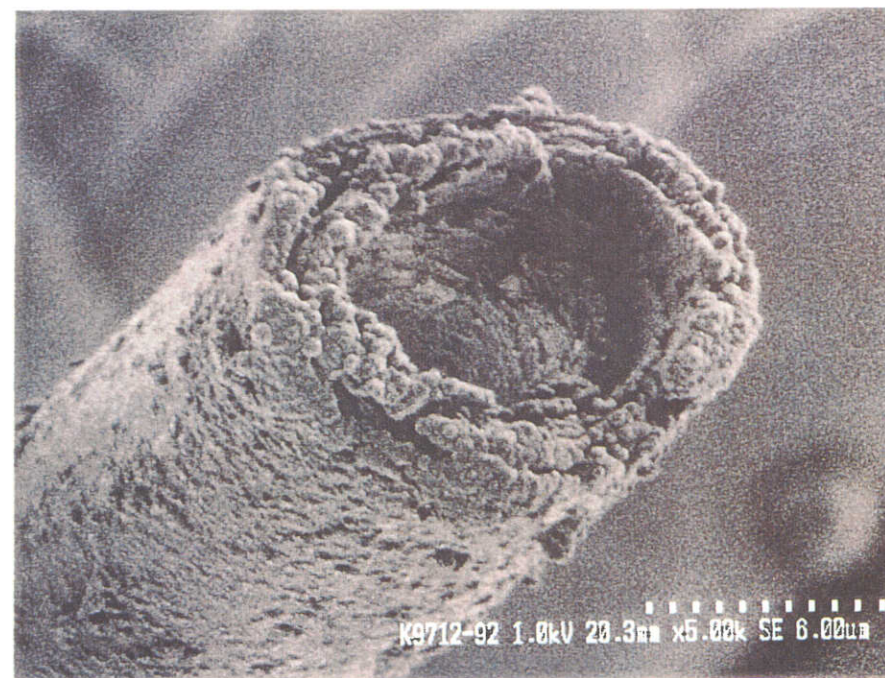


(SEM Photo 3)

6.0 μ m

Observation of End of Embedding - 2

[From arrow direction a in SEM photo 3]

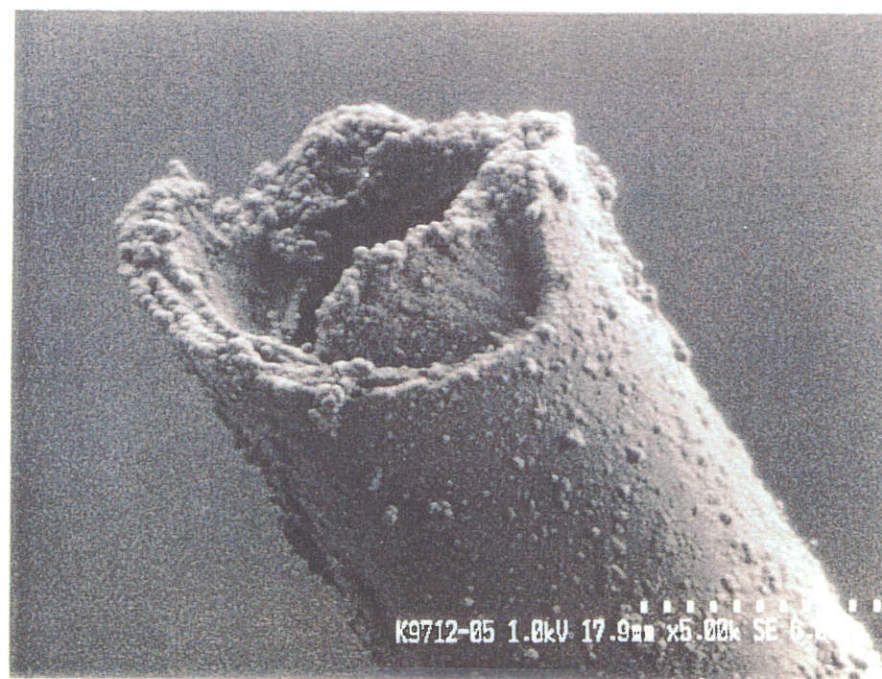


(SEM Photo 4)

6.0 μ m

Figure 6.5.5.1-1 Optical Microscopic Photo and SEM Photo of PC7A (5/6)

Observation of End of Embedding - 3
[From arrow direction b in SEM photo 3]



(SEM Photo 5)



6.0 μ m

Figure 6.5.5.1-1 Optical Microscopic Photo and SEM Photo of PC7A (6/6)

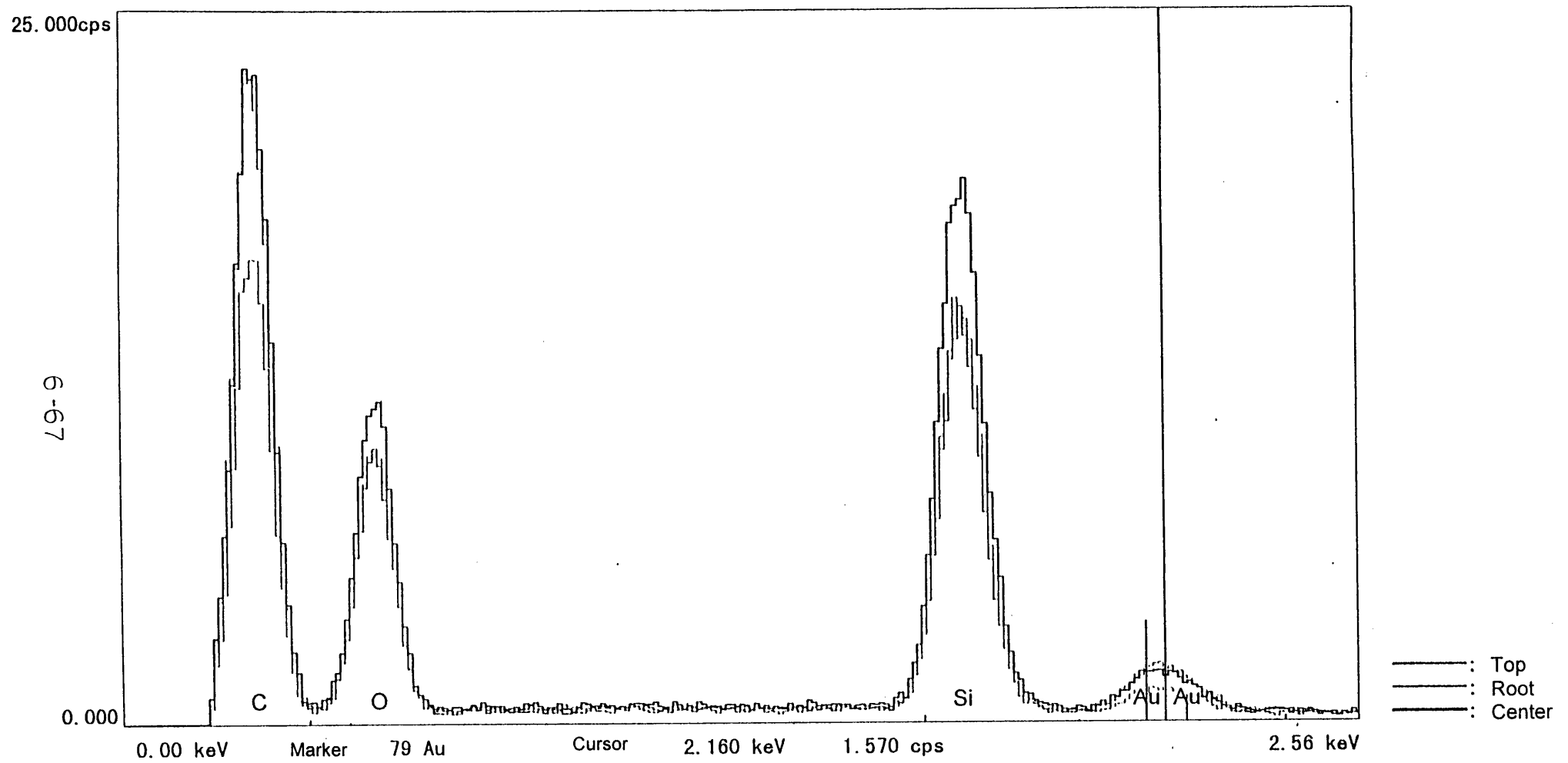
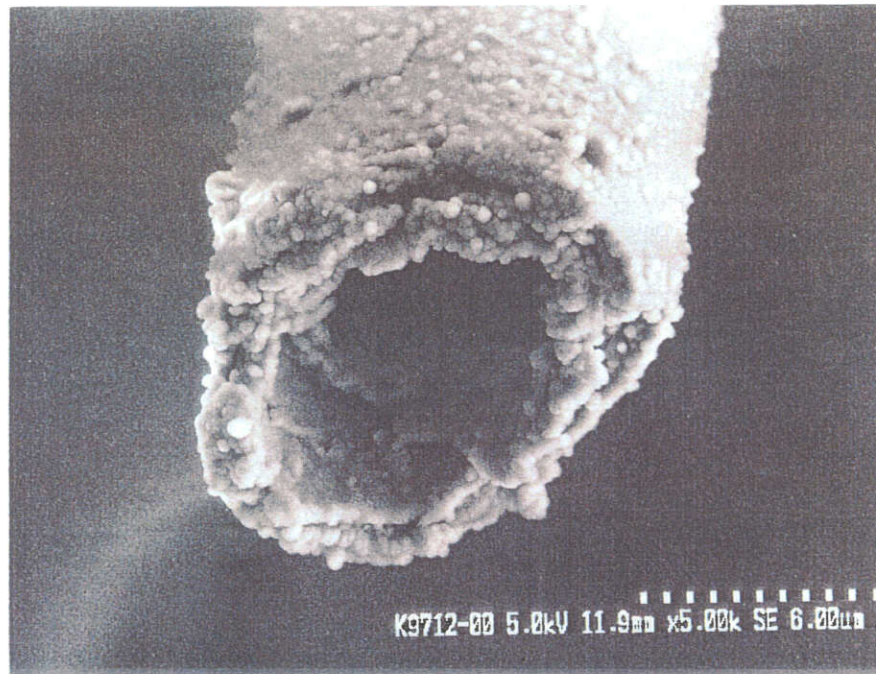


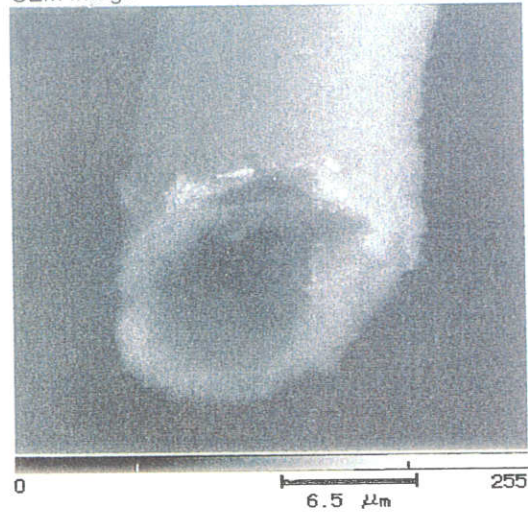
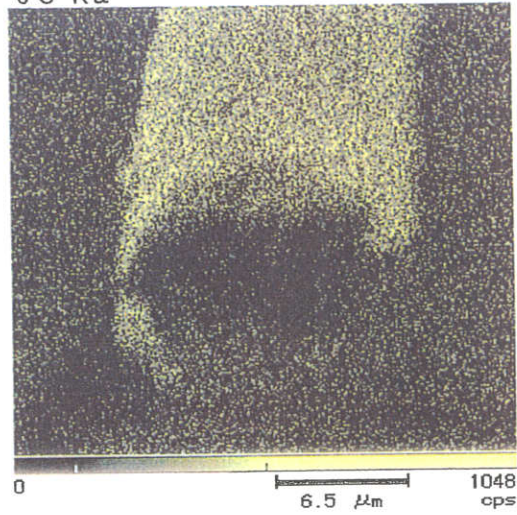
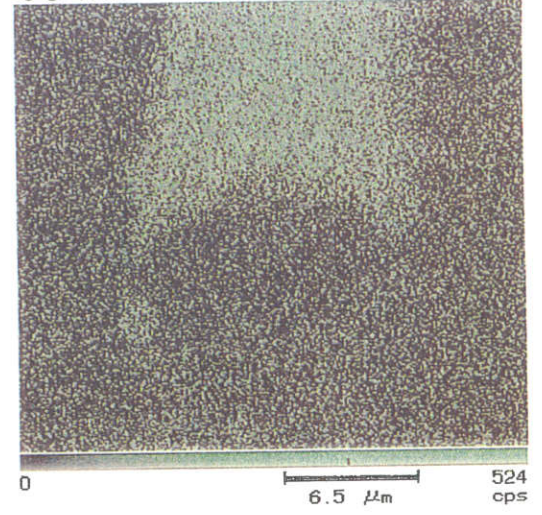
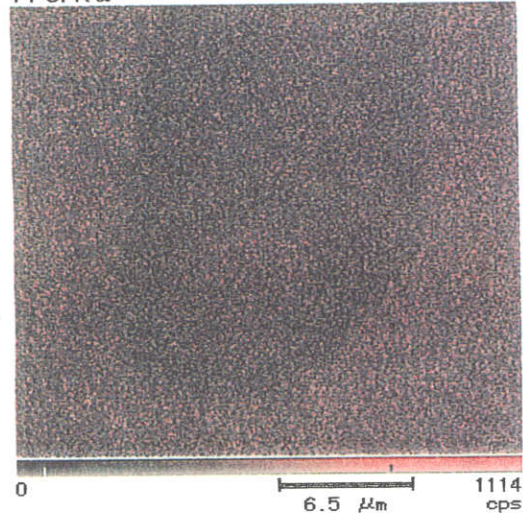
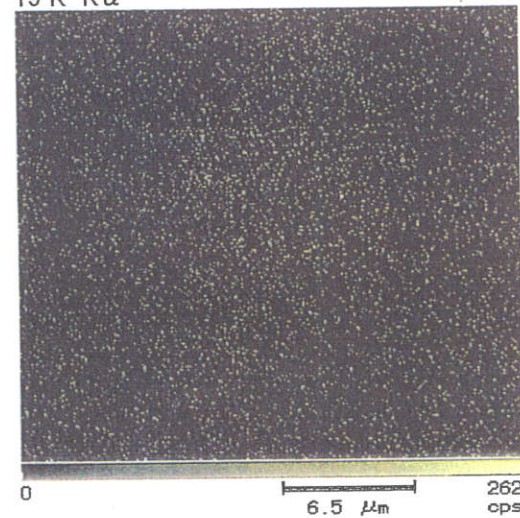
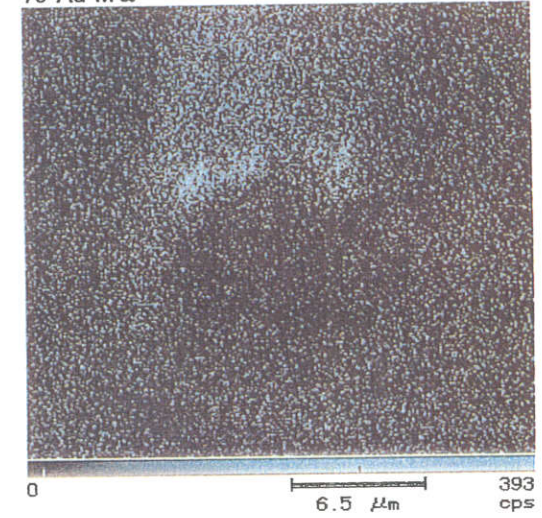
Figure 6.5.5.1-2 Results of Qualitative Analysis of EDX (1/3)



SEM Image of Point of Preparation of Component Map [See (3/3)]

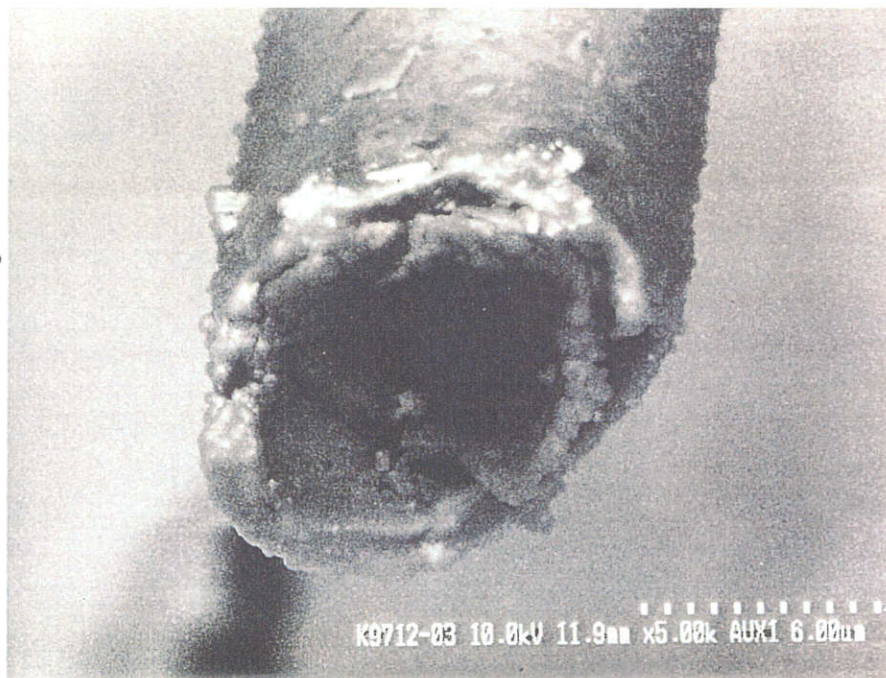
Figure 6.5.5.1-2 Results of Qualitative Analysis of EDX (2/3)

SEM Image

6 C K α 8 O K α 14 Si K α 19 K K α 79 Au M α 

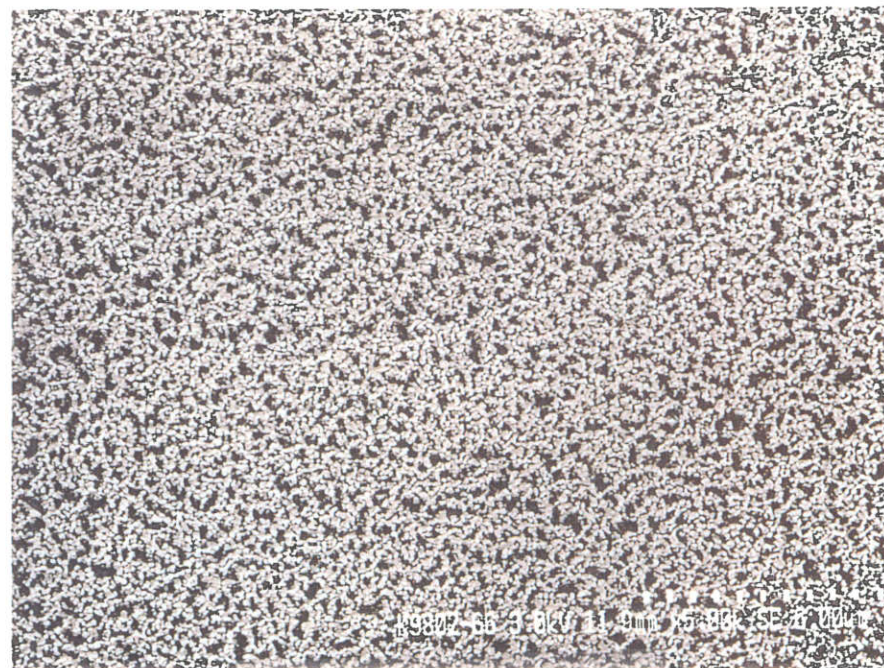
FDX Mapping

Figure 6.5.5.1-2 Results of Qualitative Analysis of EDX (3/3)



(Analyzed Part of PC7A)

Note: Gold (Au) was detected only in the white part.



(Aerogel Surface Near PC7A)

Figure 6.5.5.1-3 Comparison of Gold Sticking Conditions

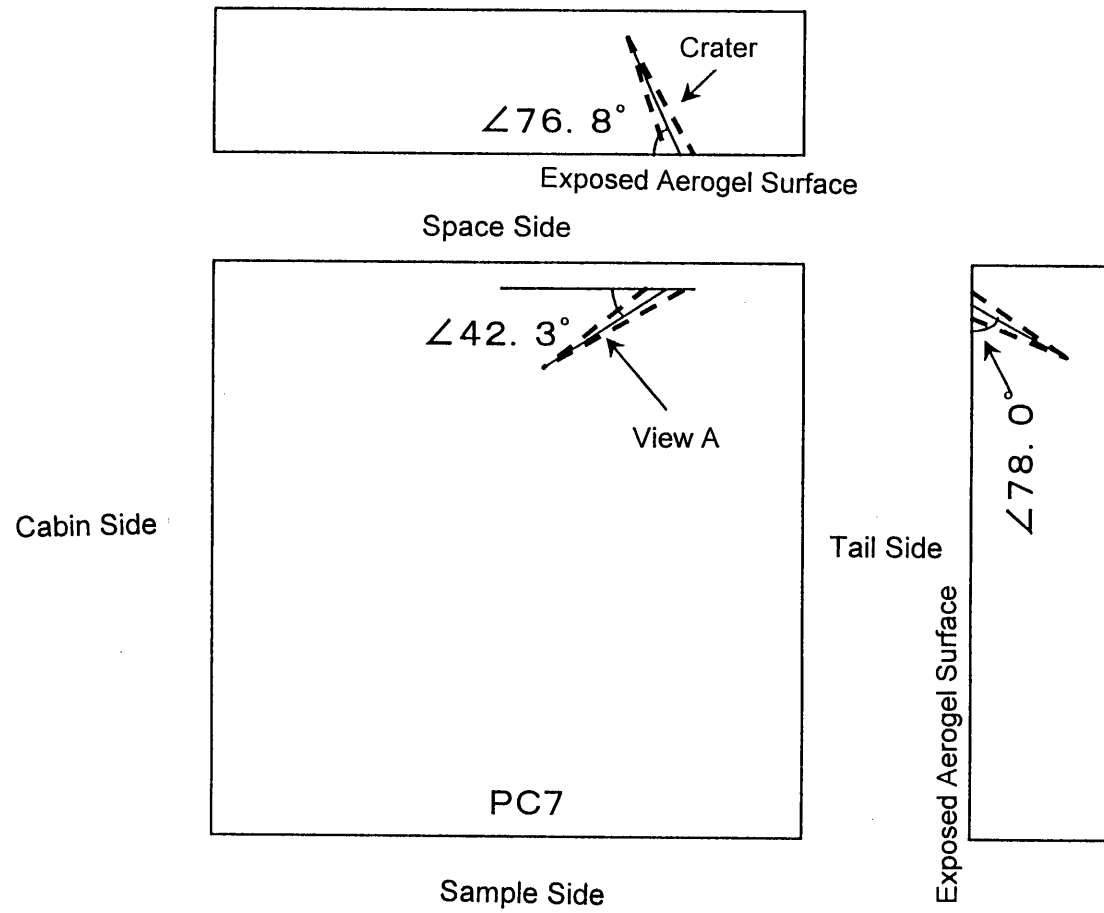


Figure 6.5.5.1-4 All Directions of PC7A

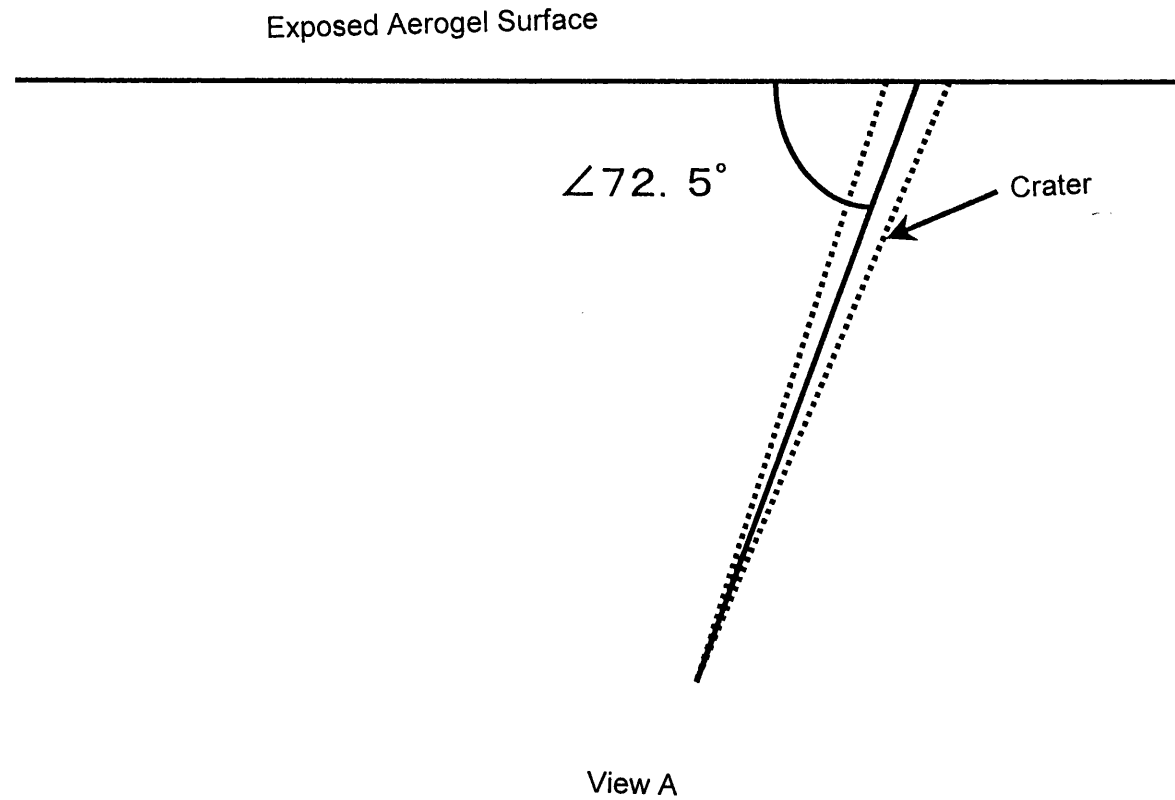


Figure 6.5.5.1-5 Angle of Impingement (View A in Figure 6.5.1-4)

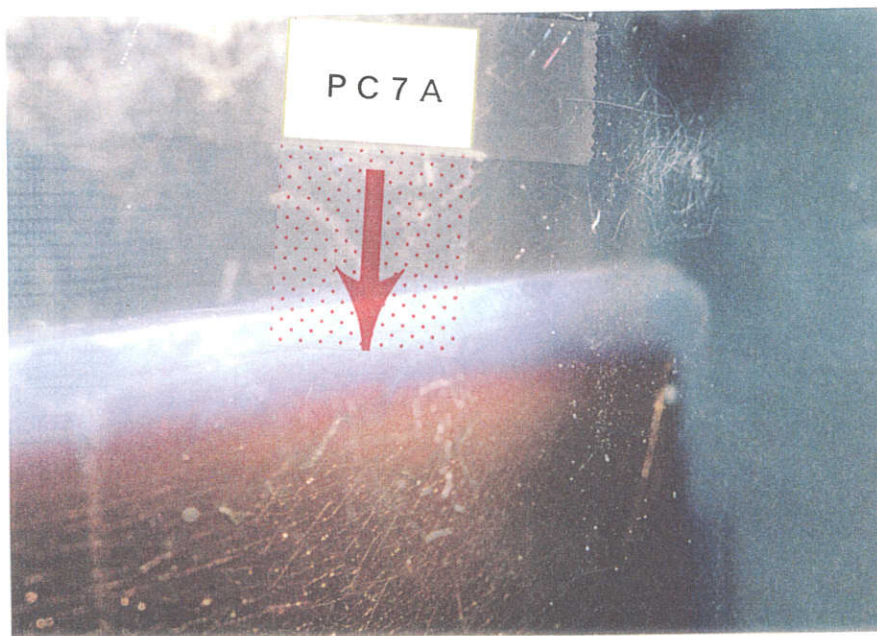
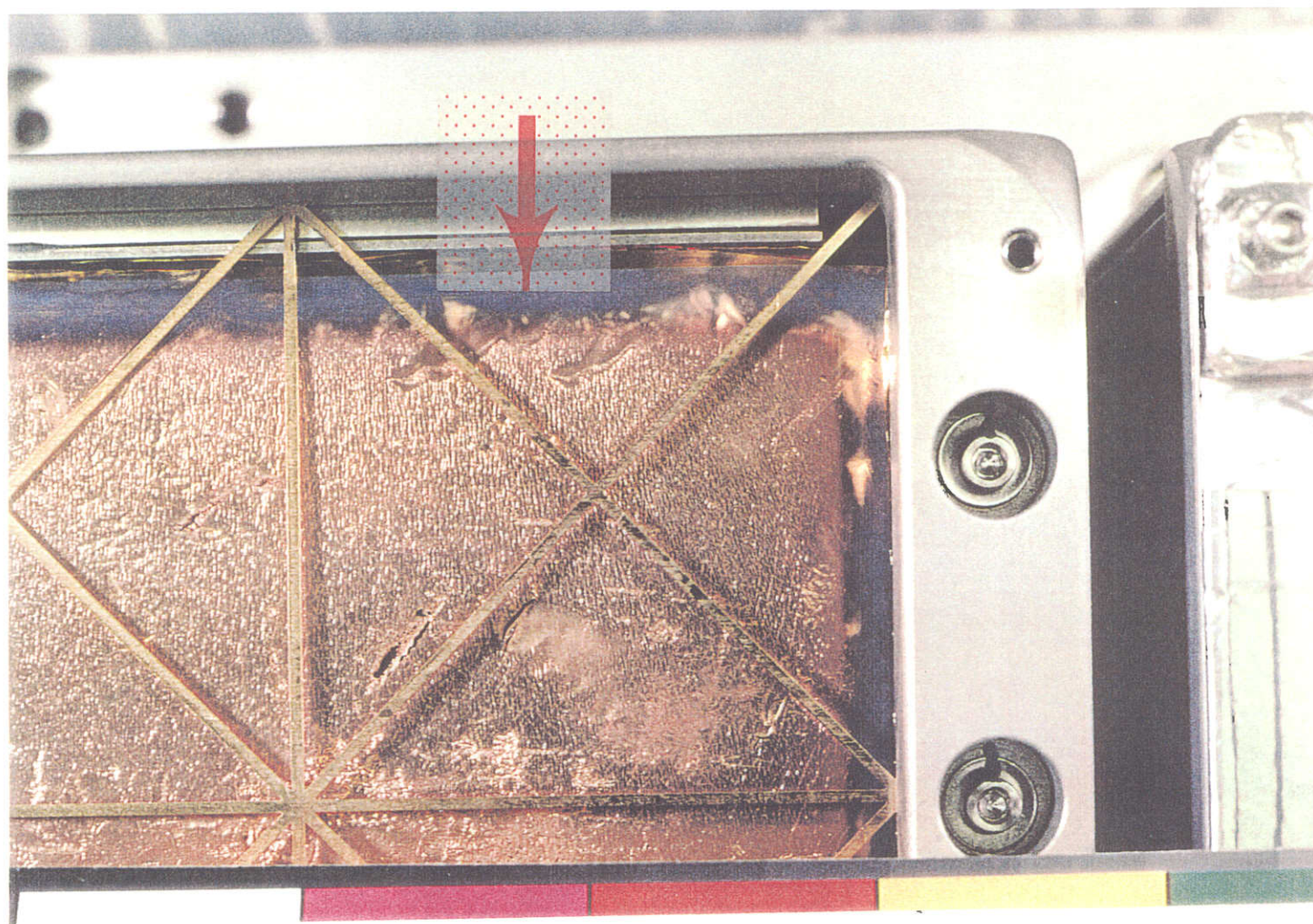


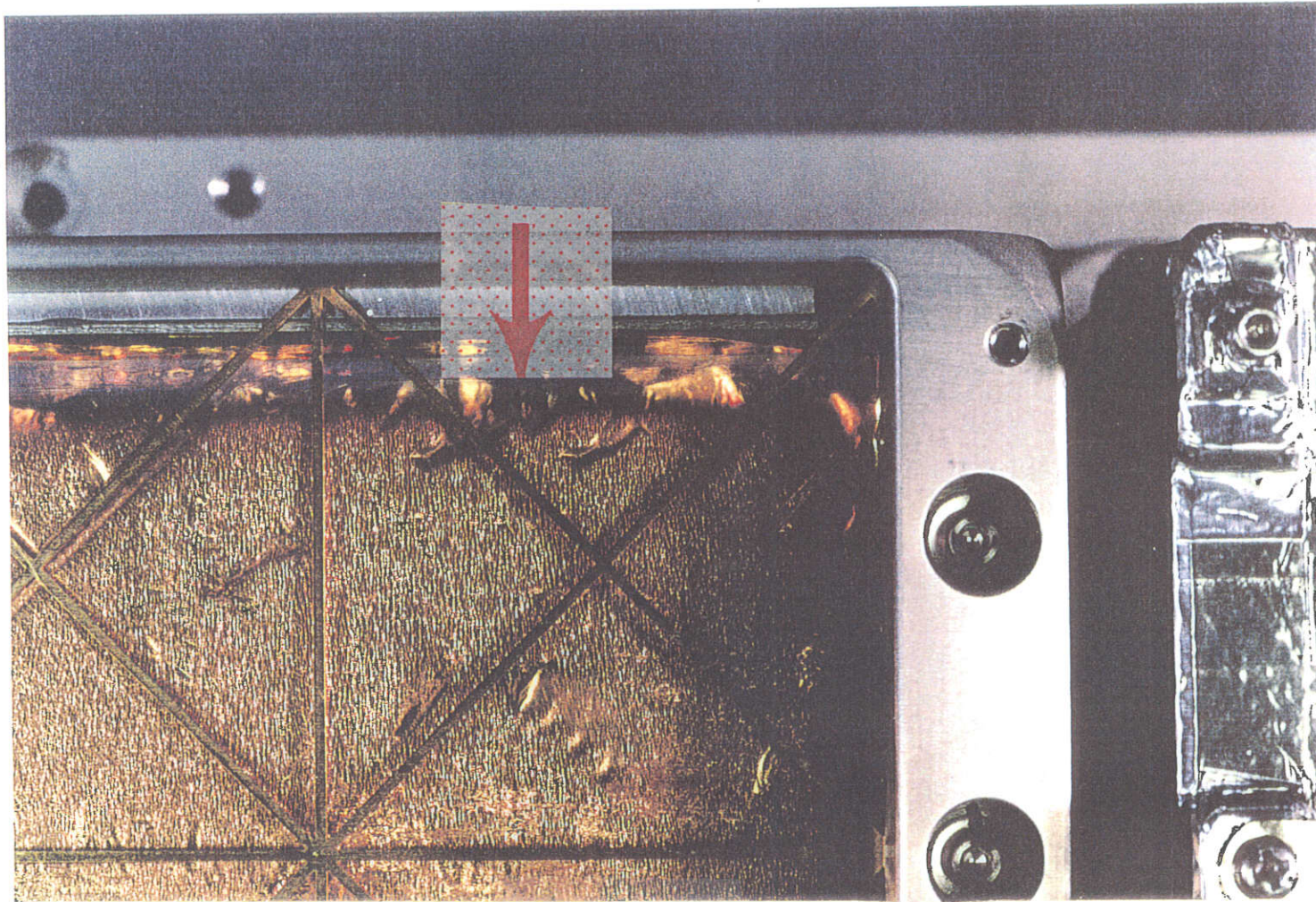
Figure 6.5.5.1-6 Approximate Position of PC7A.



Note)
←: PC7A Position

[Before Flight]

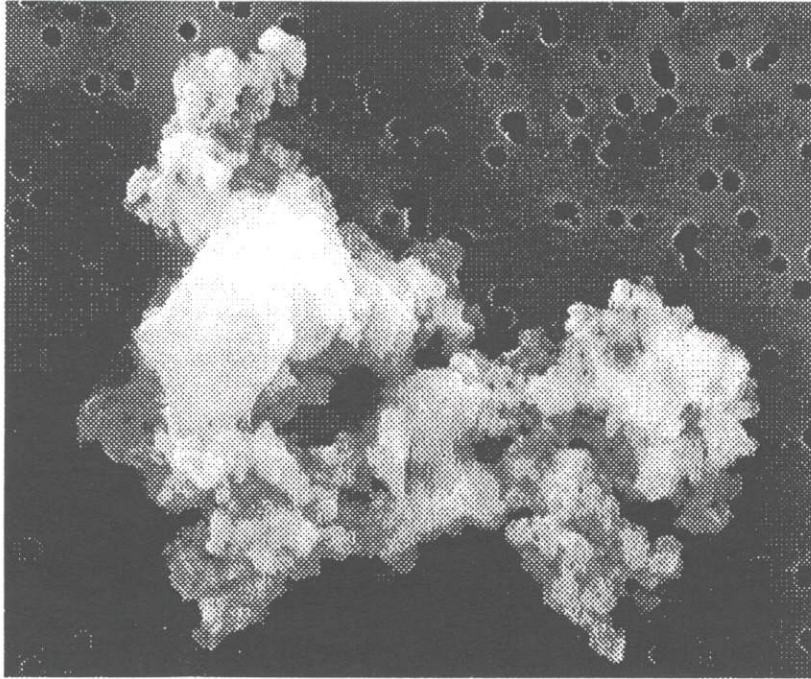
Figure 6.5.5.1-7 Enlarged Photos of Periphery of PC7A Before and After Flight (1/2)



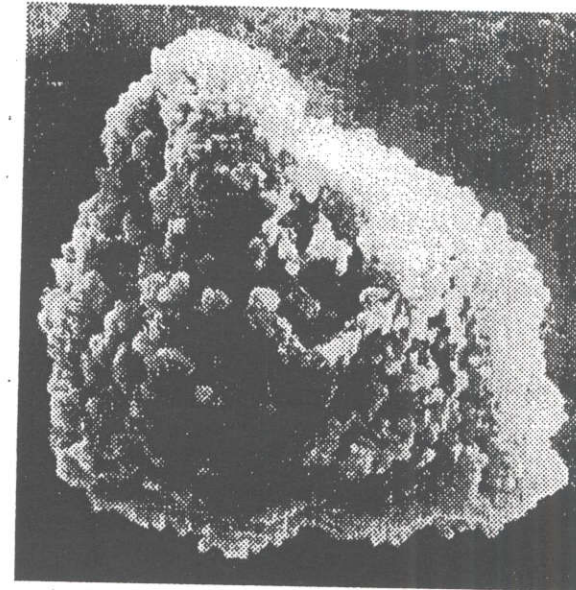
Note)
←: PC7A Position

[After Flight]

Figure 6.5.5.1-7 Enlarged Photos of Periphery of PC7A Before and After Flight (2/2)

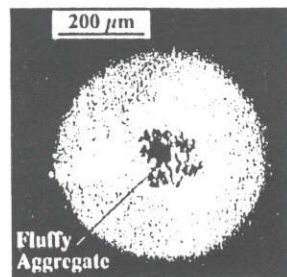


(Photo by NASA)
Si, Ca, etc. are main components.
Size is about 10 μm .



(Cosmic Dust Catalog 12, 71, 1991)
Size is about 20 μm .

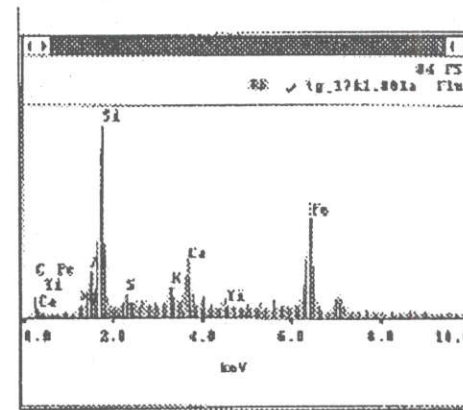
Figure 6.5.5.2-1 Example of Fluffy Particles Captured in Stratosphere



External View



Enlarged

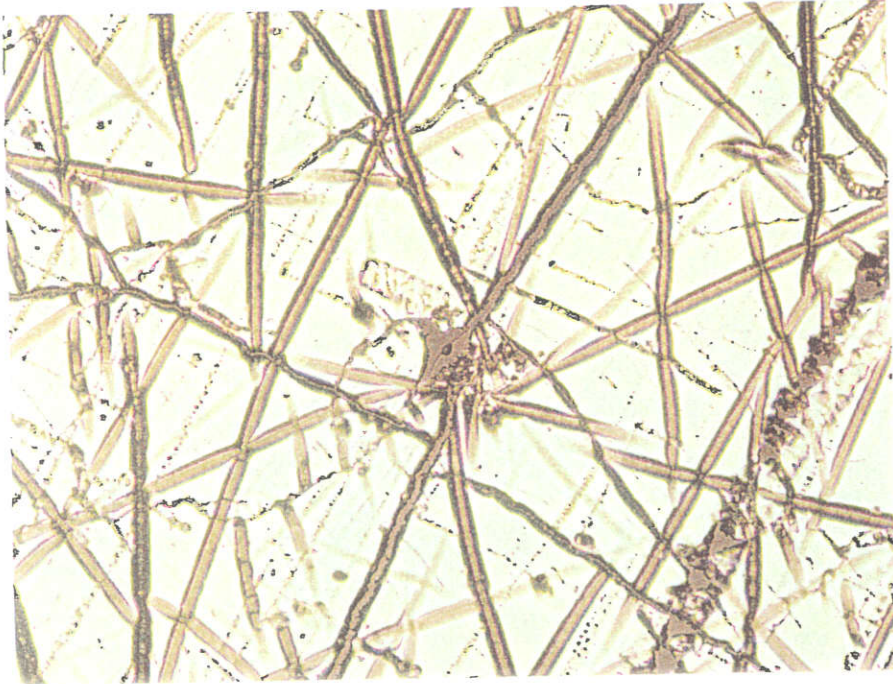


Components

Quoted from [Yano, 1995]

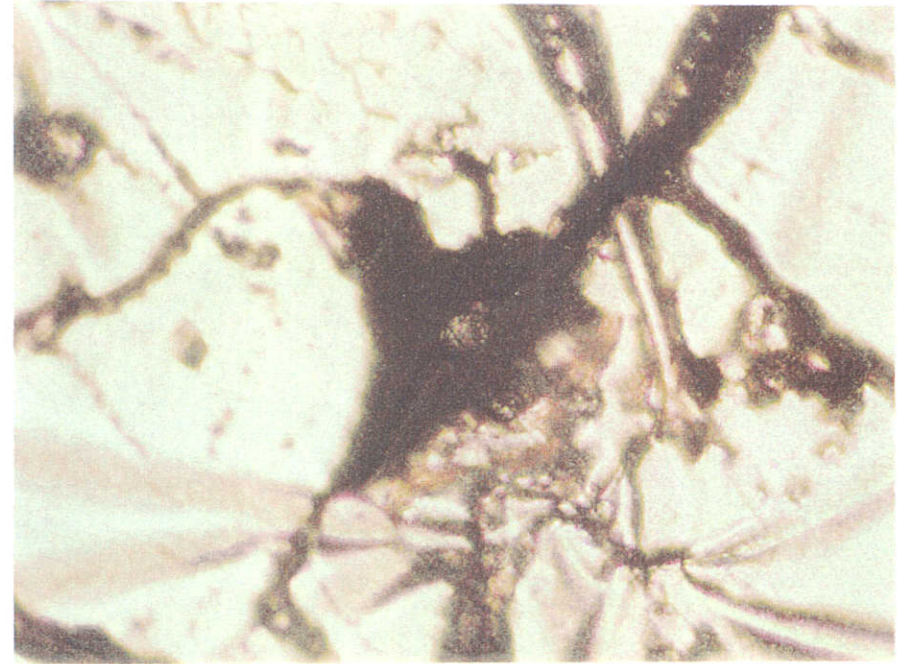
Figure 6.5.5.2-2 Example of Fluffy Particles Discovered in Aerogel of EuReCa

6-78



(Optical Microscopic Photo 1)

100 μ m



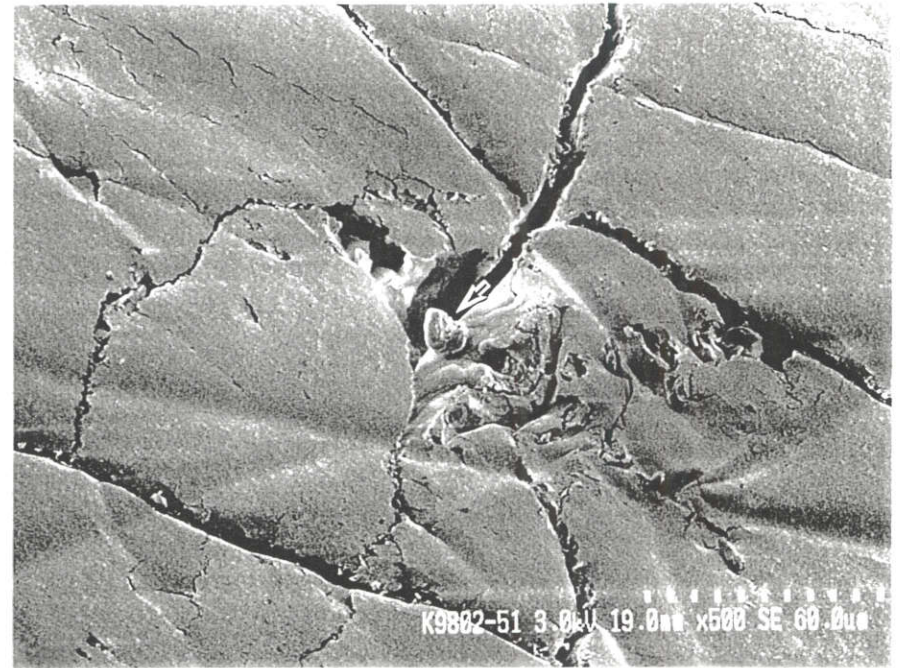
(Optical Microscopic Photo 2)

20 μ m

Figure 6.5.5.3-1 Optical Microscopic Photos and SEM/EDX Photos of PC7C (1/3)

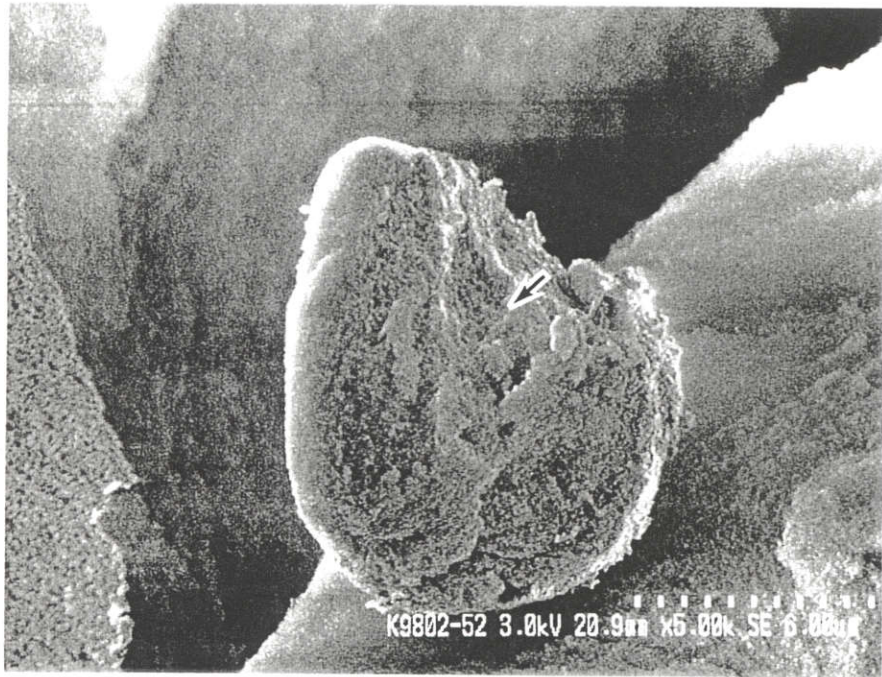


(SEM Photo 1)

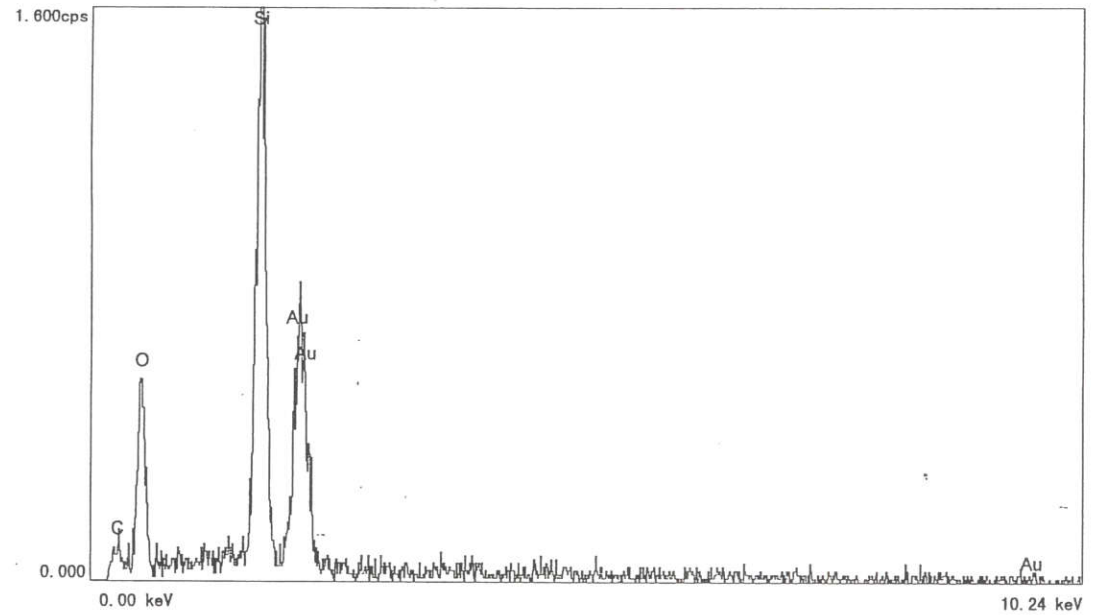


(SEM Photo 2)

Figure 6.5.5.3-1 Optical Microscopic Photos and SEM/EDX Photos of PC7C (2/3)



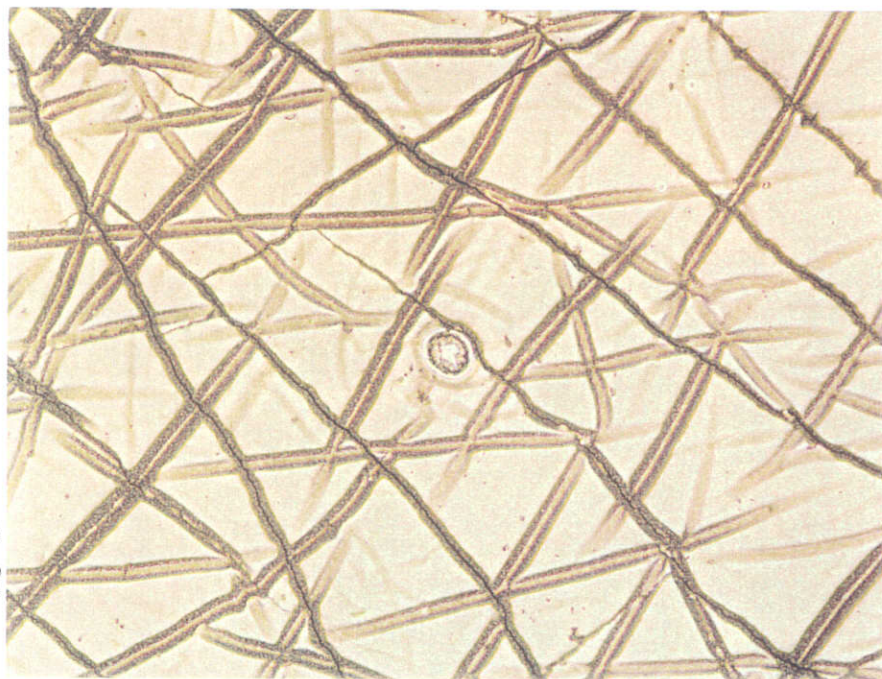
(SEM Photo 1)



(Results of EDX Analysis)

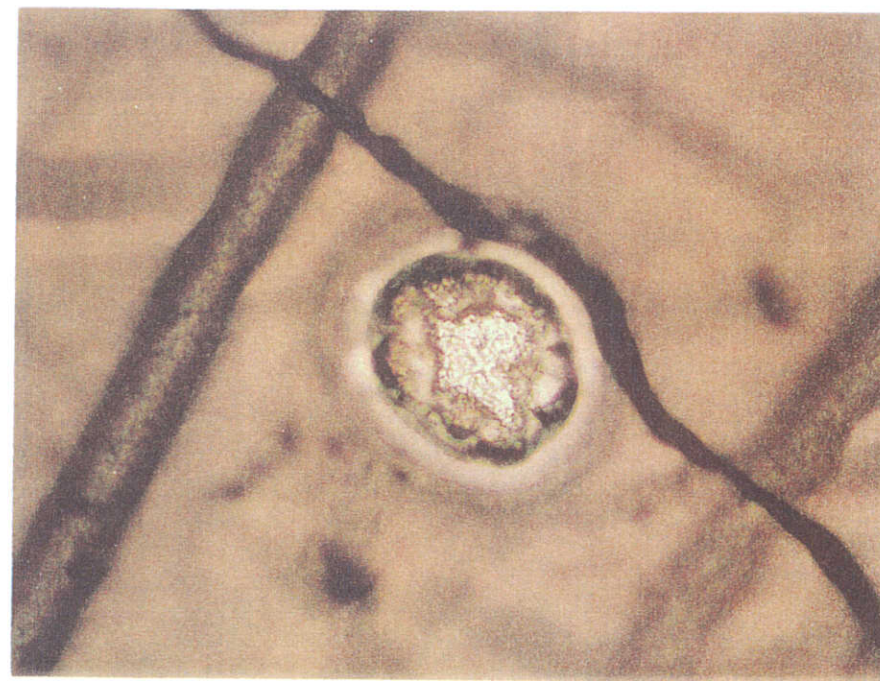
Note: The part pointed by the arrow in SEM photo 3 was analyzed.

Figure 6.5.5.3-1 Optical Microscopic Photos and SEM/EDX Photos of PC7C (3/3)



(Optical Microscopic Photo

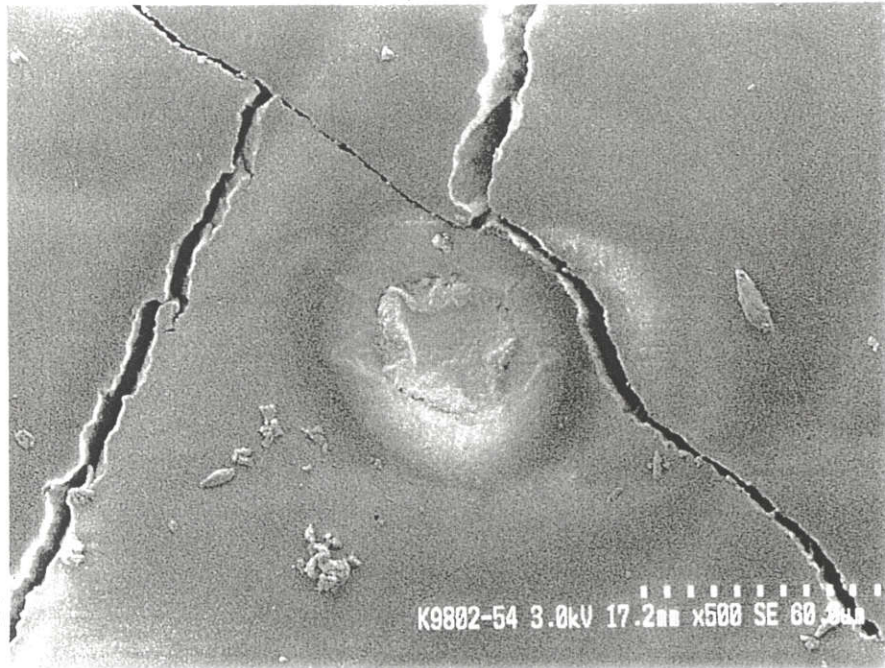
└──┐
100 μ m



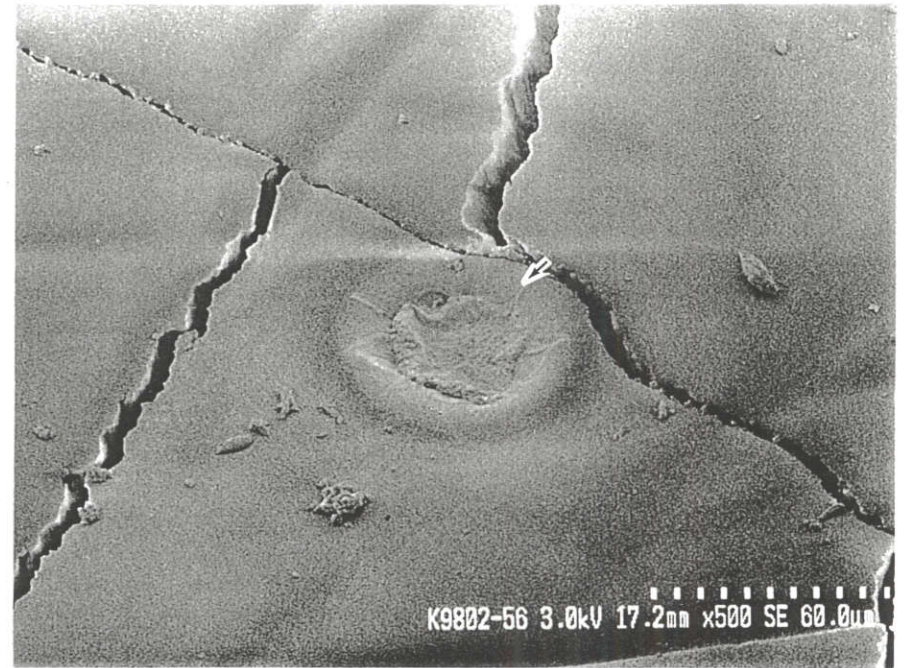
(Optical Microscopic Photo 2)

└──┐
20 μ m

Figure 6.5.5.4-1 Optical Microscopic Photos and SEM/EDX Photos of PC10D (1/3)

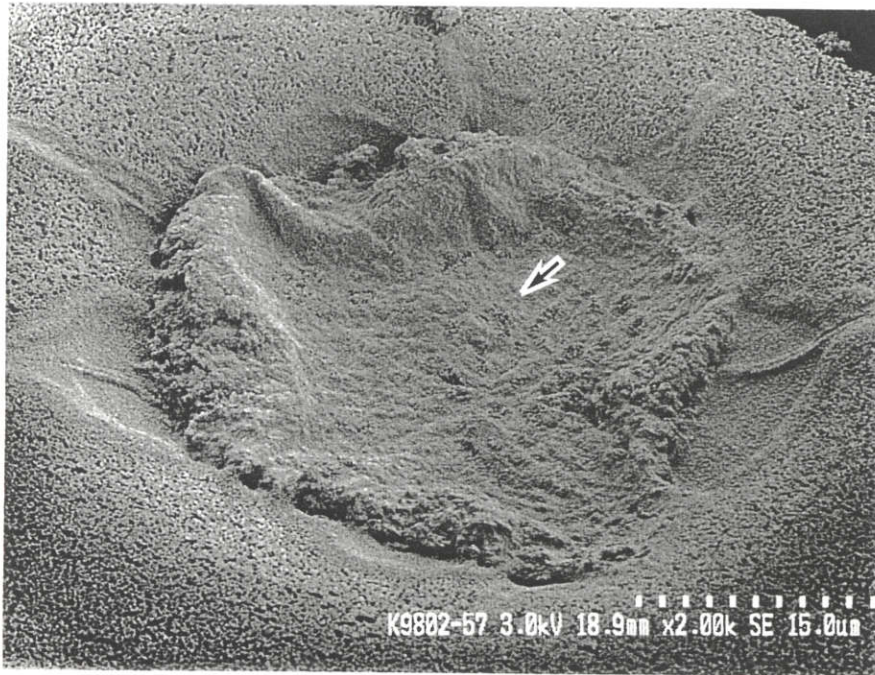


(SEM Photo 1)

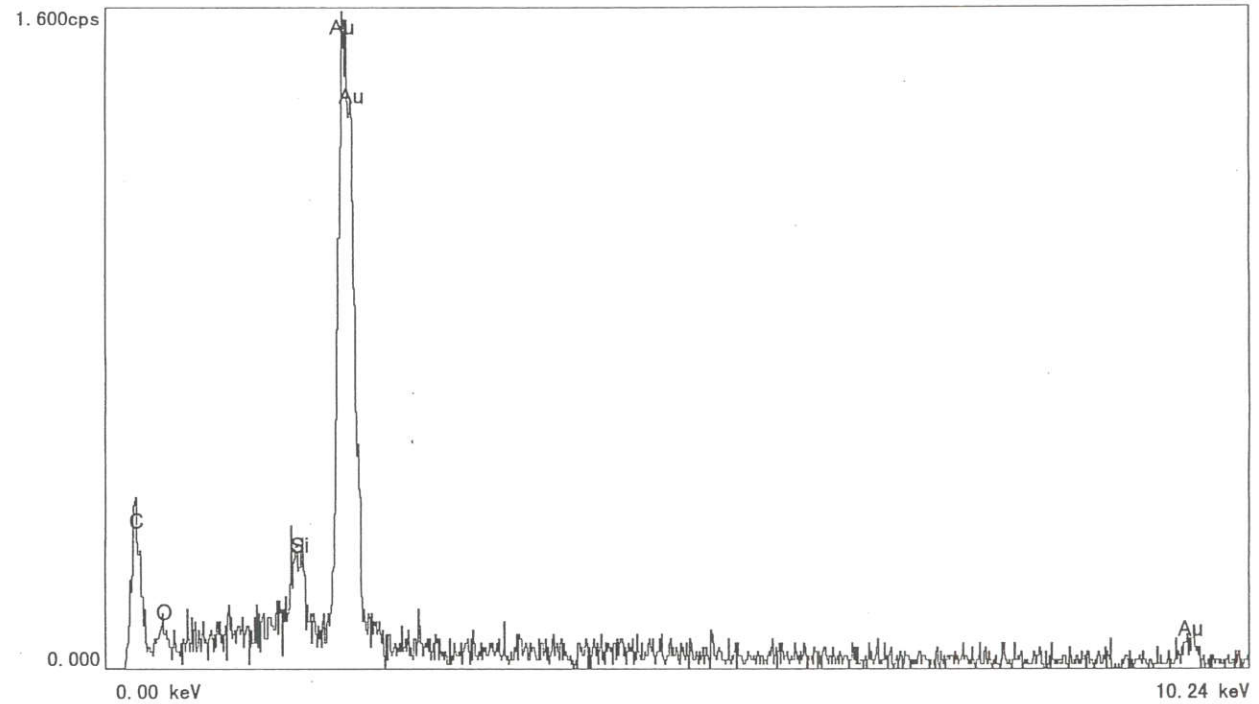


(SEM Photo 2)

Figure 6.5.5.4-1 Optical Microscopic Photos and SEM/EDX Photos of PC10D (2/3)



(SEM Photo 3)



(Results of EDX Analysis)

Note: The part pointed by the arrow in SEM photo 3 was analyzed.

Figure 6.5.5.4-1 Optical Microscopic Photos and SEM/EDX Photos of PC10D (3/3)